

Study of Resource Allocation Schemes for a 2-Hop Network in a Multi-Cell Environment

By

Gerard Jimmy PARAISON

A dissertation submitted in fulfilment of the
requirements for the degree of
Doctor of Philosophy
in
Communications Engineering

Committee in Charge:
Professor Eisuke KUDOH, Thesis Supervisor
Professor Naoshi UESUGI, Thesis Committee
Professor Toshihiro NOMOTO, Thesis Committee

Department of Communications Engineering
Graduate School of Engineering
Tohoku Institute of Technology, Sendai, Japan

March 2015

ABSTRACT

The progress in the electronic industry has led to the development of wireless devices capable of high data processing. The advanced capability of these devices has created data hungry services such as multi-media content, streaming video, real-time applications, online TV, and so on, in wireless mobile networks. These data hungry applications create a high demand for high data transmission rate in mobile wireless networks. Considering the conventional single hop mobile network, increasing the data transmission rate would require an increase in the transmission power.

By reducing the transmission distance between the transmitter and the receiver, multi-hop wireless networks have been proposed to increase the data transmission rate without increasing the transmission power. Multi-hop networks, being a new network architecture, require new resource allocation paradigms.

One of the drawbacks of wireless communication is frequency selectivity. Frequency selectivity can degrade the capacity of a wireless channel. Orthogonal frequency division multiple access (OFDMA), which is a multiple access method based on the orthogonal frequency division multiplexing technique (OFDM), has been used extensively because of its resiliency to frequency selective channels. Furthermore, OFDMA can provide frequency and multi-user diversity in a multi-user environment. Hence, it has been adopted as the basic access scheme by many researchers involved in resource allocation for wireless networks. In addition, in order to provide high data transmission rate in the downlink, OFDMA has been applied as the basic access scheme in multiple resource allocation schemes proposed for two-hop networks.

Though multiple resource allocation schemes have been proposed for two-hop networks, an OFDMA-based allocation scheme which considers the joint allocation of routes and subcarriers for multiple users in an intra-cell and inter-cell interference scenario could not be found in the literature. The optimal solution for such a problem requires an exhaustive search which may not be applicable in a practical environment.

In this dissertation, we study multiple successive and iterative resource allocation algorithms for single cell and multi-cell environments, using OFDMA as the basic access scheme. The proposed successive and iterative schemes take into account the joint allocation of routes and subcarriers in a two-hop network. The performance of the two-hop network when the proposed schemes are applied is compared to that of the conventional single hop network. To approximate the optimal solution of the joint route and subcarrier allocation problem, we propose an evolutionary allocation scheme. With low levels of computational complexity, the evolutionary scheme can provide similar performance compared to the optimal solution.

Acknowledgements

I am thankful for the life, the family, and the friends I am given. I am grateful for the great opportunities, the understanding, the wisdom, the love, and the health I am granted. Thank to Him for the little I have got to know.

I am grateful for the hard work of my favourite Haitian mother Ms Marie S. Paraison. As a single mother of 6 children in a country like Haiti, she can be proud of her achievements. She has taught me by her actions to be passionate and positive. She has lived as if everything was perfect. I am grateful for her sacrifices and her sleepless nights which take me where I am currently. Thank you *manmie* and I love you so much.

Special thanks go to my wife Candace S. Paraison for her continuous support and understanding during those hectic years. She has always been supportive and encouraging. Special thanks go to my family and my friends (in Haiti, France, Canada, and America) who never failed to call me at least twice a week during these studies. Special thanks to a special friend from Uganda, David Otuya Odeke, whose advice was always positive.

In life, you always need someone to push you to excel and to help you discover your capabilities. I am grateful to Professor Eisuke Kudoh who was not only a good adviser to me but also a close friend, with whom I discussed issues which bother me in life. After the March 11th disaster, I thought that it was impossible to submit my first paper for a presentation at an international conference in Singapore. However, with his faith and support, I succeeded in doing it. He would review and comment my papers a thousand times before I submitted them. I would like to thank all the faculty members, especially Professors Naoshi Uesugi and Toshihiro Nomoto for their wise comments and advice.

Being in a country far from home and facing culture shock and language difficulty can be quite challenging sometimes. However, here in Japan, I have been assisted by many kind friends. Some of them have even become my family. I thank all of my friends in Japan, specially my host family Mme Hiroko Otomo which has become my Japanese family, Mme Junko Horie, Mme Misa Muraguchi, Mr. Taniguchi Masaaki, the Ex-President of the University Professor Sawada Yasuji, the office members, the security staff, and the small staff which provided me with a clean environment to study.

Finally, I would like to express my gratitude to Ms Bethany Panian for helping me revising the dissertation. I am thankful to all of my friends that I have met throughout extra-curriculum activities such as badminton, soccer, mini-soccer, Toastmasters, and so on. You have all contributed to my happiness and success in Japan. Those years of studies in Japan have been the most exciting and adventurous years in my life so far. I am looking forward with hope and happiness to the future.

Contents

Abstract	1
Contents	3
List of Figures	6
1 Introduction	9
1.1 Wireless Channel Propagation	9
1.1.1 Orthogonal Frequency Division Multiplexing	11
1.2 Channel Capacity	13
1.2.1 Demand of Increased Channel Capacity	14
1.2.2 Channel Bandwidth Utilization	14
1.3 Mobile Cellular Network	16
1.3.1 Single Hop Network	17
1.3.2 Multi-Hop Network	18
1.3.3 Mobile Relay Network	18
1.3.4 Fixed Relay Network	19
1.4 Resource Allocation in Two-Hop Networks	21
1.5 Allocation Problems in Two-Hop Networks	22
1.5.1 Separate Route and Sub-carrier Allocation	23
1.5.1.1 Route Allocation	23
1.5.1.2 First-Hop and Second-Hop Allocation	24
1.5.1.3 Drawback of This Approach	25
1.5.2 Joint Route and Second-Hop Sub-Carrier Allocation	25
1.5.2.1 Drawback of This Approach	26
1.5.3 Joint Route and Sub-Carrier Allocation	26
1.5.3.1 Time Division Relaying Schemes	27
1.5.3.2 Frequency Division Relaying Schemes	27
1.6 Objective of the Research	29
1.6.1 Single Cell Allocation Problem	29
1.6.2 Multi-Cell Allocation Problem	31
1.6.3 Objective	32
1.7 Thesis Contribution	33
2 Resource Allocation Problem Formulation	34
2.1 Parallel Relaying Transmission	35
2.1.1 Physical Route	35
2.1.2 Logical Route	35
2.1.3 Data Transmission Method	36
2.1.4 Joint Route and Sub-Carrier Allocation	36

2.1.5	Data Modulation in Parallel Relaying	37
2.1.5.1	CP Data Modulation	37
2.1.5.2	WP Data Demodulation and Modulation	39
2.1.5.3	MT Data Demodulation	39
2.2	Single Virtual Cell	40
2.2.1	Numerical expressions	40
2.2.1.1	Logical Route SINR	40
2.2.1.2	System Capacity	42
2.2.2	Sub-Carrier Reuse	43
2.2.3	Single Cell Allocation Problem	43
2.3	Multi-Cell Environment	45
2.3.1	Numerical expressions	45
2.3.1.1	Logical Route SINR	45
2.3.1.2	System Channel Capacity	46
2.3.2	Multi-Cell Allocation Problem	47
2.4	Resource Allocation Problem Complexity	48
3	Successive Allocation Scheme	50
3.1	Single Cell Network	50
3.1.1	Sub-Carrier Reuse Constraints Implementation	51
3.1.2	Single Cell Successive Allocation Scheme	52
3.1.3	Successive Allocation Scheme Complexity	53
3.1.4	Simulation Assumptions and System Model	53
3.1.5	Simulation Performance	57
3.1.5.1	System Throughput	59
3.2	Multi-cell Network	65
3.2.1	Sub-Carrier Reuse Constraints Implementation	65
3.2.2	Multi-Cell Successive Allocation Scheme	66
3.2.3	Simulation Assumptions and System Model	66
3.2.4	Simulation Performance	70
3.3	SAS Performance Comparison With Optimal Scheme	79
3.4	Summary	81
4	Iterative Allocation Scheme	82
4.1	Single Cell Network	82
4.1.1	Drawback of Successive Allocation	82
4.1.2	Sequential Iterative Allocation Scheme (SIS)	83
4.1.3	Random Iterative Allocation Scheme	84
4.1.4	Complexity of SIS and RIS	84
4.1.5	Permutational Iterative Allocation Scheme (PIS)	87
4.1.6	Permutational Allocation Scheme Complexity	88
4.1.7	Permutational Combined Iterative Scheme (PCIS)	88
4.1.8	Permutational Combined Iterative Scheme Complexity .	90
4.1.9	Simulation Assumptions and System Model	90
4.1.10	Simulation Performance	92

4.2	Multi-cell Network	96
4.2.1	Multi-Cell Iterative Allocation Scheme	96
4.2.2	Simulation Assumptions and System Model	96
4.2.3	Simulation Performance	98
4.3	SIS Performance Comparison With Optimal Scheme	105
4.4	Summary	107
5	Evolutionary Allocation Scheme	108
5.1	Evolutionary Algorithm	108
5.2	Single Cell Network	108
5.2.1	Evolutionary Allocation Scheme	109
5.2.1.1	Candidate Validation Method	110
5.2.1.2	Population Creation Method	111
5.2.1.3	Population Evaluation Method	113
5.2.1.4	Archiving Method	113
5.2.1.5	Fitness Assignment and Archiving	115
5.2.1.6	Selection Method	115
5.2.1.7	Reproduction Method	117
5.2.1.8	Mutation Method	117
5.2.1.9	Crossover Method	124
5.2.1.10	Evolutionary Algorithm Core	124
5.2.2	Sub-Carrier Pair Allocation Scheme	124
5.2.3	Simulation Assumptions and System Model	129
5.2.4	Simulation Performance	129
5.3	Multi-cell Network	137
5.3.1	System Model	137
5.3.2	Evolutionary Allocation Scheme	137
5.3.3	Simulation Assumptions and System Model	138
5.3.4	Simulation Performance	140
5.4	EAS Performance Comparison With Optimal Scheme	149
5.5	Summary	153
6	Conclusion	154
6.1	Conclusion	154
6.1.1	Chapter 2	154
6.1.2	Chapter 3	155
6.1.3	Chapter 4	156
6.1.4	Chapter 5	157
6.2	Future Work	157
Glossary		159
Journal Publications and Conferences		160
Bibliography		162

List of Figures

1.1	Multipath wireless channel	10
1.2	Frequency response of a frequency selective channel	11
1.3	Division of channel bandwidth into subchannels	12
1.4	Block diagrams of an OFDM system	12
1.5	Global mobile data traffic forecast	15
1.6	Subdivision of a mobile cellular network	16
1.7	Direct and multi-hop transmission systems	17
1.8	A two-hop mobile relay network	18
1.9	A two-hop fixed relay network	19
1.10	Multi-hop virtual cellular network	20
1.11	Time division relaying	27
1.12	Frequency division relaying	28
1.13	Single virtual cell with sub-carrier reuse	29
2.1	Physical and logical route	36
2.2	Parallel relaying transmission	37
2.3	Data modulation at the CP	38
2.4	Parallel relaying implementation at a WP	39
2.5	Parallel relaying implementation at an MT	40
2.6	Number of combinations to evaluate in the exhaustive search	49
3.1	Initial allocation matrices	52
3.2	Number of combinations for SAS and optimal scheme	54
3.3	Virtual cell layout	54
3.4	Ergodic channel capacity for two MTs	61
3.5	Logical route allocation distribution for $d/d_0 = 0.3$	61
3.6	Logical route allocation distribution for $d/d_0 = 0.7$	62
3.7	Ergodic channel capacity based on the distance ratio	62
3.8	Multi-user ergodic channel capacity	63
3.9	PDF of the channel capacity per MT	63
3.10	Coefficient of variation	64
3.11	Throughput based on normalized transmission power	64
3.12	Second tier architecture	67
3.13	Wrap around structure	67
3.14	First VC layout with six WPs	72
3.15	Single cell and multi-cell Ergodic channel capacity	72
3.16	Probability distribution of MTs located at $d/d_0 \geq 0.7$	73
3.17	Multi-user ergodic channel capacity	73
3.18	Second VC layout with 5 WPs	74
3.19	Third VC layout with 4 WPs	74

3.20 Ergodic channel capacity for $R = 4$, $R = 5$, and $R = 7$ WPs	77
3.21 Ergodic channel capacity based on the distance ratio	77
3.22 Jain's fairness index of the VCN and the SHN	78
3.23 Outage channel capacity per MT	78
3.24 Two WPs VC layout	80
3.25 Comparison with the optimal solution	80
4.1 Interference scenario in successive allocation	83
4.2 Number of logical route candidates to be evaluated	88
4.3 Virtual cell layout	90
4.4 Ergodic channel capacity, SIS and RIS	94
4.5 Ergodic channel capacity, SIS and RIS performance	94
4.6 Ergodic channel capacity, PIS and PCIS	95
4.7 Ergodic channel capacity, SIS and PCIS comparison	95
4.8 SIS and SAS single cell ergodic channel capacity	99
4.9 SIS and SAS multi-cell ergodic channel capacity	102
4.10 Convergence of SIS	102
4.11 Degree of fairness of SIS and SAS	103
4.12 VCN, 1% and 10% outage channel capacity per MT	103
4.13 VCN, 10% outage capacity for 4, 5, and 7 WPs per VC	104
4.14 VCN, degree of fairness for 4, 5, and 7 WPs per VC	104
4.15 Performance of exhaustive, iterative, and successive schemes	106
5.1 Evolutionary Scheme Layout	110
5.2 Ergodic capacity of EAS, modified-SPA, and SIS	133
5.3 Convergence of EAS and SIS	133
5.4 Jain's fairness index	134
5.5 Outage channel capacity per MT	134
5.6 Ergodic channel capacity based on the number of MTs	135
5.7 EAS Ergodic channel capacity different number of WPs	135
5.8 EAS, SIS Ergodic channel capacity based on the number of WPs	136
5.9 EAS, SIS Ergodic channel capacity based on the distance ratio d/d_0	136
5.10 Ergodic channel capacity of EAS and SIS	141
5.11 Outage channel capacity of EAS, and SIS	141
5.12 Jain's fairness index of EAS, and SIS	142
5.13 Ergodic channel capacity based on distance ratio of EAS	142
5.14 Probability for a two hops link to be selected	144
5.15 Outage channel capacity based on distance ratio of EAS	144
5.16 Jain's fairness index based on distance ratio of EAS	145
5.17 Ergodic channel capacity based on the number of WPs	145
5.18 Outage channel capacity based on the number of WPs	146
5.19 Percentage of increased capacity when adding a WP	146
5.20 Ergodic channel capacity based on the number of MTs	147
5.21 Outage channel capacity based on the number of MTs	147
5.22 Jain's fairness index based on the number of MTs	148

5.23 Ergodic channel capacity of EAS, SIS, SAS, and exhaustive scheme	151
5.24 Outage channel capacity of EAS, SIS and exhaustive scheme	151
5.25 Computational complexity of EAS, SIS and exhaustive scheme	152

CHAPTER 1

Introduction

Wireless Communications

A Brief Overview

In the village where I grew up, there is this belief that all babies have to cry on their upcoming to this world. To the villagers, this cry represents a message from the newborn to the audience stating that he/she is well alive and healthy. This belief might not be scientifically proven, however it reveals the fact that, as human beings, communication is a key requirement to our survival.

Communication can be defined as the exchange of information (messages) between at least two entities (a transmitter, and a receiver) through the means of a transport system (medium). In our previous example, the newborn will represent the transmitter, his/her audience the receiver, his/her cry the message, and the air molecules in the space between them would be the media. In most other cases, the transmitter and the receiver are not located in proximity. Hence, the necessity to develop technologies which enable these two entities to communicate reliably.

Throughout the years two main communication technologies have been thoroughly studied and developed: wired communication technology and wireless communication technology. Wireless communication technology differs from wired communication technology by the absence of a wire assuring the transmission between the transmitter and the receiver. While wired communication technology can reliably ensure high data transmission rate between two entities located at intercontinental distances, it remains impractical in many cases, by example in the case of two mobile entities. In this particular scenario, wireless communication technology should be used as it allows the mobility of the entities.

1.1 Wireless Channel Propagation

In wireless mobile communication systems, the transmission of messages happens through the means of wireless channels. A wireless channel is created by the radiation of electromagnetic energy from the antenna of a transmitter

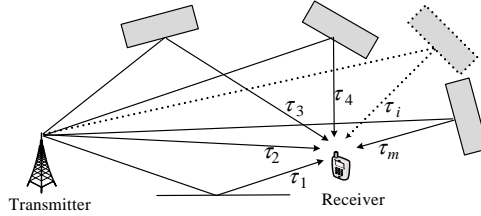


Figure 1.1: Multipath wireless channel

to that of a receiver. This electromagnetic energy constitutes the transport support of the transmitted signal.

A signal transmitted in a wireless channel follows multiple paths before reaching its destination (See Figure 1.1). The creation of these multiple paths is caused by the presence of scatterers and reflectors, such as buildings, moving entities, skyscrapers, hills, etc., in the environment. The occurrence of these multiple paths distorts the transmitted signal in many different ways. The multipath signals can be added constructively or destructively depending on the arrival time of the different propagation paths.

Suppose that $x(t)$ is the equivalent baseband signal expression at time t , the received multipath propagation signal $r(t)$ can be expressed as follows:

$$r(t) = \sqrt{2}\Re \left\{ \sum_i a_i(t) (x(t - \tau_i(t)) e^{j2\pi f_c(t - \tau_i(t))}) \right\} + n(t) \quad (1.1)$$

$$= \sqrt{2}\Re \left\{ \left(\sum_i a_i(t) x(t - \tau_i(t)) e^{-j2\pi f_c \tau_i(t)} \right) e^{j2\pi f_c t} \right\} + n(t), \quad (1.2)$$

where $\Re(z)$, $a_i(t)$, and $\tau_i(t)$ denote respectively the real part of the complex number z , the attenuation factor, and the propagation delay of the i -th path at time t ; f_c represents the carrier frequency of the transmitted signal, and $n(t)$ the additive Gaussian noise at the receiver. From the second part of Equation (1.1), we express the frequency response $H(f_c, t)$ of the channel at time t as:

$$H(f_c, t) = \sum_i a_i(t) e^{-j2\pi f_c \tau_i(t)}. \quad (1.3)$$

Denote the maximum time difference between two propagation paths as $\Delta t_s = \max |\tau_i(t) - \tau_j(t)|$, the frequency response of the channel $H(f_c, t)$ changes significantly when f_c changes by $1/\Delta t_s$.

In wireless communications, Δt_s and $W_c = 1/\Delta t_s$ are usually referenced as delay spread and coherence bandwidth of a channel. The coherence bandwidth W_c determines the rate of change of the channel in the frequency domain. If the coherence bandwidth W_c of a channel is smaller than the signal bandwidth W_s ($W_c \ll W_s$), the channel is said to be frequency selective. Figure 1.2 represents the plot of a frequency selective channel with 5 propagation paths. It can be observed that the magnitude of the frequency response of the

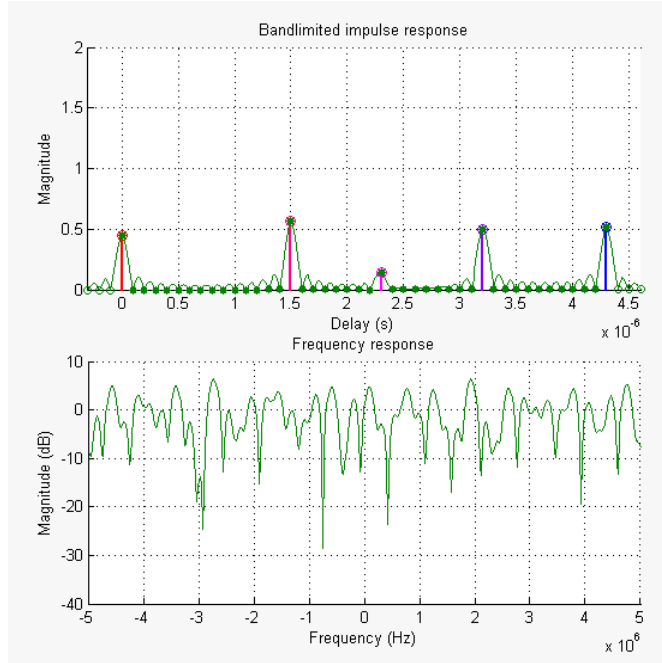


Figure 1.2: Frequency response of a frequency selective channel

channel varies significantly with frequency. Frequency selectivity can cause inter-symbol interference which can degrade considerably the performance of a wireless channel.

1.1.1 Orthogonal Frequency Division Multiplexing

The orthogonal frequency division multiplexing (OFDM) can be implemented to prevent inter-symbol interference and simultaneously provide frequency diversity in a frequency selective channel [1]. OFDM divides the channel bandwidth W_s into N orthogonal narrowband subchannels $\Delta f = W_s/N$ (see Figure 1.3). N is chosen such that Δf is small enough and that the frequency response of the channel is approximately constant for Δf . If the subchannel bandwidth is greater or equal to the coherence bandwidth $\Delta f \geq W_c$, the channel is no longer frequency selective and inter-symbol interference can be eliminated.

An OFDM system can be implemented with low complexity using the fast Fourier transform (FFT) algorithm. In Figure 1.4, we show the block diagrams of an OFDM system using inverse Fast Fourier transform (IFFT) at the transmitter and FFT at the receiver. In the transmitter side the serial input symbol data (X_0, X_1, \dots, X_{N-1}) is converted to parallel symbol streams using a serial-to-parallel converter. The parallel stream is modulated using an IFFT

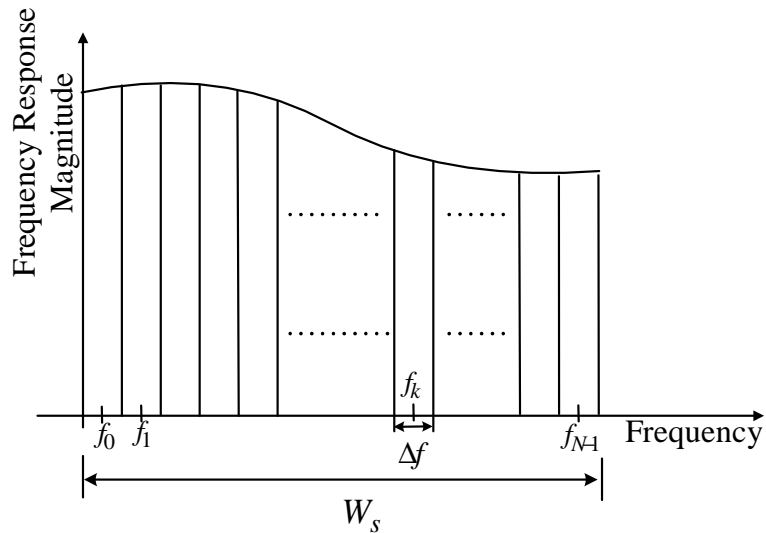


Figure 1.3: Division of channel bandwidth into subchannels

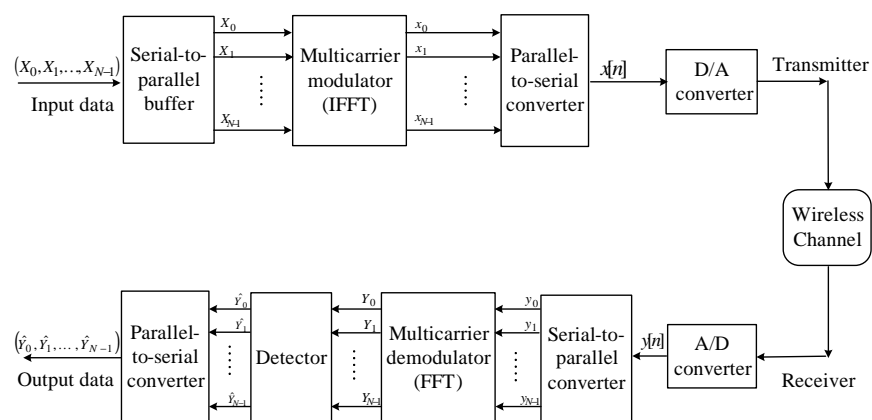


Figure 1.4: Block diagrams of an OFDM system

modulator to produce the OFDM symbols $(x_0, x_1, \dots, x_{N-1})$:

$$x_m = \frac{1}{\sqrt{N}} \sum_{k=0}^{N-1} X_k \exp\left(j2\pi m \frac{k}{N}\right), \quad m = 0, 1, \dots, N-1. \quad (1.4)$$

The obtained parallel OFDM sequence $(x_0, x_1, \dots, x_{N-1})$ is converted back to a serial stream $x[n] = (x_0, x_1, \dots, x_{N-1})$ for further processing before transmission to the wireless channel. At the receiver the sampled received signal $y[n]$ is converted to a parallel stream $(y_0, y_1, \dots, y_{N-1})$ which is fed to a demodulator FFT to produce the demodulated OFDM sequence $(Y_0, Y_1, \dots, Y_{N-1})$:

$$Y_n = \frac{1}{\sqrt{N}} \sum_{k=0}^{N-1} y_k \exp\left(-j2\pi n \frac{k}{N}\right), \quad n = 0, 1, \dots, N-1. \quad (1.5)$$

The demodulated OFDM signal $(Y_0, Y_1, \dots, Y_{N-1})$ is sent to a detector whose output $\hat{Y}_0, \hat{Y}_1, \dots, \hat{Y}_{N-1}$ is converted to a serial data stream. OFDM is widely applied in wireless communication systems to mitigate the effect of frequency selective channel and to provide frequency diversity.

1.2 Channel Capacity

The main objective of a communication system is to be able to transmit a message from a transmitter which can be decoded with a certain degree of accuracy at the receive end. That message is chosen from a set of messages with a specific transmission rate. When designing a wireless communication system, one is interested in knowing the transmission rate that can be used to communicate without error through the specific channel. The capacity of a channel is a measure of the maximum message rate that can be used to communicate through that channel with a probability of error which tends to zero.

Claude Shannon has been the first to propose a formula to measure that information rate in his paper “*A mathematical theory of communication*” [2] for a noisy channel. According to his theory, the maximum rate C with which one can communicate reliably through an additive white Gaussian noise (AWGN) channel can be expressed as [1]:

$$C = \frac{1}{2} \log_2 \left(1 + \frac{S}{N} \right) \quad [\text{bits per Hz}] \quad (1.6)$$

with N and S being respectively the noise power, and the received signal power at the receiver.

In a band-limited and power-limited AWGN channel, the channel capacity is given by:

$$C = W \log_2 \left(1 + \frac{S}{NW} \right) \quad [\text{bits/s}], \quad (1.7)$$

where W denotes the bandwidth of the channel. Dividing Equation (1.7) by the available bandwidth W , the maximum achievable spectral bit rate can be

expressed as :

$$C = \log_2 \left(1 + \frac{S}{NW} \right) \quad [\text{bits/s/Hz}]. \quad (1.8)$$

The ratio $\frac{S}{NW}$ usually referred to as the signal-to-noise power ratio (SNR) is often used when evaluating or designing a wireless communication system.

1.2.1 Demand of Increased Channel Capacity

Mobile cellular networks operate on wireless communication channels. According to the Ericsson Mobility Report, it is expected that mobile subscriptions in mobile cellular networks will reach 9.3 billion by the end of 2018[3]. Based on the same source, mobile subscriptions have grown by around 9 percent each year. This increase of mobile subscribers translates to a high demand for increased capacity in mobile cellular networks. Based on a report submitted in 2012 by Cisco, it is expected an exponential increase in global mobile data traffic is expected in the next few years [4](see Figure 1.5).

The recent advance in complementary metal oxide semiconductor (CMOS) technology has facilitated the development of mobile devices with high processing capabilities. The high processing capabilities of these terminals has boosted the creation of many data hungry applications, such as online TV, real time audio, and video streaming, in mobile cellular networks. These new services which are most of the time IP embedded services, require high speed data transmission [5].

In order to keep pace with the evolution of information and communication technology, the next generation mobile cellular network has to guarantee a high capacity network that can provide a high information transmission rate while ensuring a better quality of service.

1.2.2 Channel Bandwidth Utilization

Let us denote the required information rate of a system by R (bits/s), and the average received energy per bit by $E_b = S/R$, the band-limited and power-limited capacity in Equation (1.7) can be expressed by:

$$C = W \log_2 \left(1 + \frac{E_b}{N} \cdot \frac{R}{W} \right) \quad [\text{bits/s/Hz}]. \quad (1.9)$$

Based on Shannon's theory, reliable communication is possible if

$$R \leq C. \quad (1.10)$$

Let us define the bandwidth utilization λ as the ratio between the information rate R and the available bandwidth W :

$$\lambda = \frac{R}{W}, \quad (1.11)$$

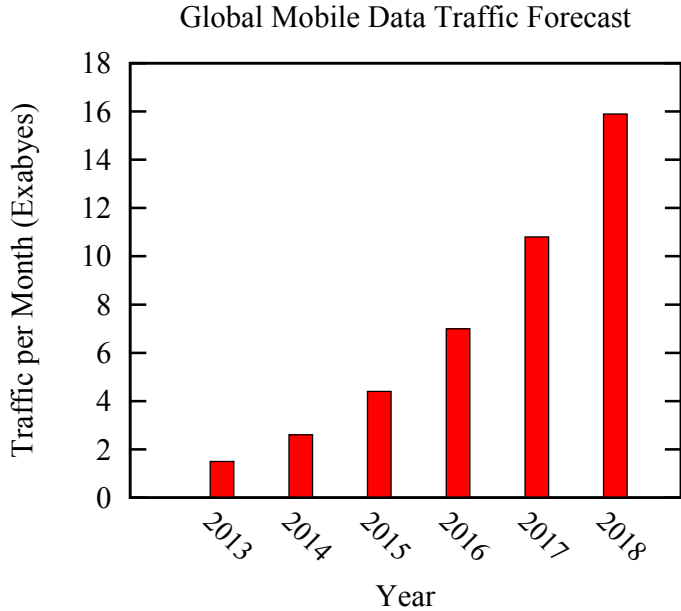


Figure 1.5: Global mobile data traffic forecast

based on Equations (1.7) and (1.10) we can write:

$$\lambda \leq \log_2 \left(1 + \frac{E_b}{N} \cdot \lambda \right). \quad (1.12)$$

Applying a lower bound on E_b/N , we obtain:

$$\frac{E_b}{N} \geq \min \left(\frac{E_b}{N} \right) = \frac{2^\lambda - 1}{\lambda}. \quad (1.13)$$

According to Equation (1.13), for a fixed bandwidth, the augmentation of the bandwidth utilization or information rate requires an exponential increase of the average received energy per bit:

$$\lim_{\lambda \rightarrow \infty} \frac{2^\lambda - 1}{\lambda} = \infty \implies \min \left(\frac{E_b}{N} \right) \rightarrow \infty. \quad (1.14)$$

Hence, in order to accommodate the increased demand of high information rate in mobile wireless networks, it is necessary to increase the received signal power S . In the next section, we discuss a proposed solution adopted by many researchers in the field of wireless communications.

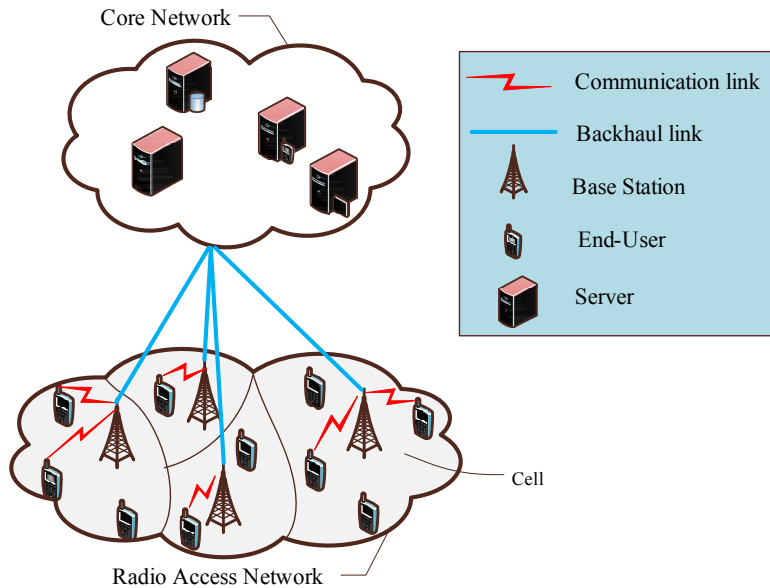


Figure 1.6: Subdivision of a mobile cellular network

1.3 Mobile Cellular Network

A mobile cellular system can be divided into two main parts: the core network and the radio access network (See Figure 1.6). The core network (CN) is responsible for user data management, user authentication, user billing, user services management, etc.. As for the radio access network, it creates and manages the communication links between the users and the CN. Our study focuses on the radio access network.

In general, users are spread through large geographical areas of hundreds of kilometers of radius. At the time of this study, mobile cellular networks operate in the frequency range of 100MHz ~ 6GHz. It is expected that frequencies in the range of 28GHz and 38GHz might be used in the near future [6, 7] in mobile wireless networks. In wireless communications, the attenuation due to free space propagation loss γ in a wireless channel depends on the transmitted signal carrier frequency f_c and is expressed as:

$$\gamma = 20 \log \left(\frac{4\pi f_c d}{c} \right) (\text{dB}). \quad (1.15)$$

where d and c represent respectively the transmission distance and the speed of light. The attenuation path-loss increases with the frequency of the transmitted signal. Frequencies in the range of GHz and hundreds of MHz are used in mobile cellular networks, therefore, the attenuation loss due to path-loss is excessive in mobile cellular networks. The attenuation path-loss limits the transmission distance between the transmitter and the receiver.

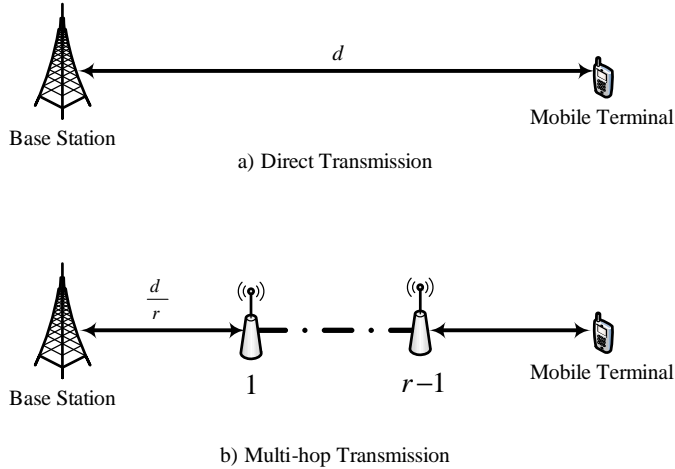


Figure 1.7: Direct and multi-hop transmission systems

1.3.1 Single Hop Network

To limit the attenuation loss due to path-loss and provide radio access to all users in a mobile cellular system, the large geographical area is partitioned into small areas of radius spanning from 100 meters to 5000 meters depending on the environment. A partition is commonly referred to as a cell. In the physical environment, the delimitation of a cell based on geographical partitioning is impractical because of the impairment property of wireless channels. In practice, the received signal strength at the receiver determines the cell boundary.

In the conventional cellular network, a cell is generally represented by the coverage area of a base station (BS) (see Figure 1.6). The BS guarantees the data transmission between the CN and the users located inside the cell. The users communicate directly with the BS. This type of network architecture is referred to as single hop network (SHN) because of the direct route between the users the BS.

Recall that in the previous section, we discussed the fact that high received signal power is necessary to increase the information rate in mobile wireless networks. We consider a SHN where a BS is transmitting at an average transmission power P_{trans} to a mobile terminal (MT) located at a distance d (see Figure 1.7 a)). Suppose that the attenuation path-loss is the only attenuation encountered by the transmitted signal, the average received signal power P_{rec} at the MT can be written as:

$$P_{rec} \simeq P_{trans} \cdot d^{-\alpha}. \quad (1.16)$$

with α being the path-loss exponent. The values of α are in the range $2 < \alpha \leq 4$ depending on the environment. For a large transmission distance d , which is common in the case of SHN, the received signal power at the MT is very

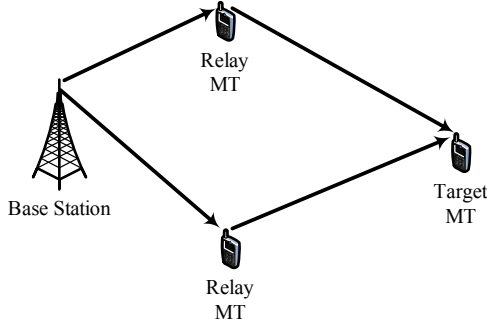


Figure 1.8: A two-hop mobile relay network

weak. Hence, providing a high received signal power for that MT necessitates a significant increase of the transmission power at the BS.

1.3.2 Multi-Hop Network

Instead of transmitting the signal directly from the BS to the MT, we introduce $r - 1$ relay stations which subdivide the large transmission distance d between the BS and the MT into r identical transmission distances (see Figure 1.7(b)). We assume that the available transmit power P_{trans} is equally shared among the r transmitting nodes (counting the BS). In an ideal environment, the received signal power P_{rec} at the MT from the $(r - 1)$ -th relay station can be written as

$$P_{\text{rec}} \simeq \frac{P_{\text{trans}}}{r} \cdot \left(\frac{d}{r}\right)^{-\alpha} = (P_{\text{trans}} \cdot d^{-\alpha}) \cdot r^{\alpha-1}. \quad (1.17)$$

Since $\alpha > 2$, for $r > 1$ the value of $r^{\alpha-1}$ is greater than 1, $r^{\alpha-1} > 1$. Hence, by introducing relay stations between the BS and the MT, the received signal power P_{rec} at the MT can be enhanced by a factor of $r^{\alpha-1}$ without increasing the transmission power.

This type of network which makes use of relay stations to increase the received signal power at the MT is called multi-hop network. Multi-hop networks have been proposed by many researchers [8, 9, 10, 11, 12, 13, 14, 15, 16, 17]. Depending on the mobility of the relay stations, the proposed multi-hop network architecture can be divided into two groups: mobile relay network (MRN) and fixed relay network (FRN).

1.3.3 Mobile Relay Network

In a MRN, the relay stations are considered to be mobile nodes [8, 9, 10, 14, 17]. Most of the MRNs envisage the cooperation of mobile users such as smart-phones to act as relay stations in the transmission between the BS and a targeted MT (See Figure 1.8).

MRNs provide many advantages in the fact that they make use of an existing infrastructure, the MTs. However, the challenges of their application in

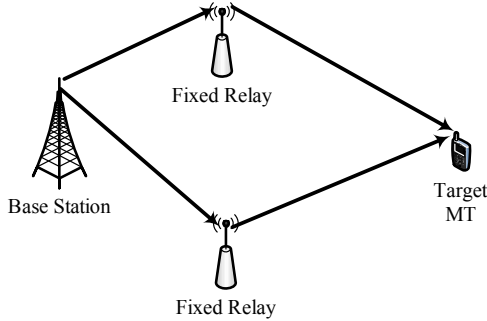


Figure 1.9: A two-hop fixed relay network

mobile cellular networks are nonetheless multi-fold. Some of the main challenges are the users readiness to share their limited power resources and the routing complexity involved with the mobility of the relay MTs.

1.3.4 Fixed Relay Network

Contrary to the MRN, which considers the relay stations to be mobile, the FRN assumes that the relay stations are fixed nodes [15, 16] (see Figure 1.9). The fixed relay nodes can be deployed by the operator or by a third party depending on the business schematic. Compared to the MRN, the FRN can be easily implemented without changing the current business model. On the technical side, its implementation is more straight forward than the MRN. Hence, we decided to choose a FRN as our multi-hop network design.

An example of a FRN is the virtual cellular network (VCN) proposed in [15, 16]. The VCN redefines the concept of cell as a virtual cell (VC). The relay stations are called wireless port (WP). A VC designates a group of WPs where one of the WPs named as central port (CP) acts a gateway to the CN (see Figure 1.10).

The CP is considered to be a WP with advanced capability. Any WP can be chosen as the CP, it is left to the discretion of the operator to configure the desired WP as the CP. The flexibility of choosing the CP by changing the configuration of a WP in the software level facilitates the expansion of the network to support additional loads.

The grouping of WPs to form a VC may not necessarily be fixed. VCs may be constructed using different number of WPs. An MT can connect with any surrounding WPs for transmission or reception. Furthermore, an MT can belong to two distinct VCs depending on the configuration paradigm. The transmission and reception links of an MT can be taken in charge by two neighbouring VCs as illustrated in Figure 1.10. Figure 1.10 illustrates the case of four VCs with different number of WPs. A group of four WPs the VC₁ while only two WPs are used to construct VC₂. MT₁, MT₂, and MT₃ belong simultaneously to VC₁ and VC₄. VC₁ ensures the data transmission in the

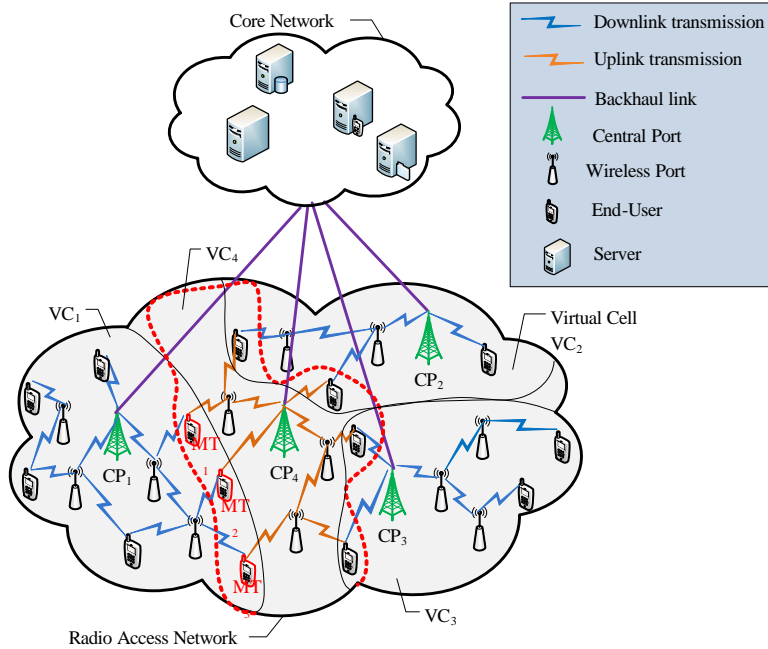


Figure 1.10: Multi-hop virtual cellular network

downlink from the CN to the MT₁, MT₂, and MT₃ through CP₁, while MT₁, MT₂, and MT₃ are connected to VC₄ for data transmission in the uplink to the CN.

It has been shown in [15] that the VCN can reduce the power consumption of the MTs and the WPs. By applying *Maximum Ratio Combining* at the CP in the uplink transmission, the authors of [15] have also shown that for a number of eight WPs the transmission power of an MT can be reduced to less than 1/100 of its value for SHN.

Though our work can be applied to any FRN, for consistency and simplicity we use the nomenclature central port for base station and wireless port for relay stations as defined in the VCN.

Taking into account that a migration step will be necessary to upgrade the current SHN into a multi-hop VCN, a two-hop VCN can be considered as an intermediary design. Hence, we have decided to focus our study on a two-hop VCN.

1.4 Resource Allocation in Two-Hop Networks

Mobile cellular systems operate on a scarce and highly priced resource, the spectrum. Multiple users are competing for this common resource. To satisfy each user in a fair way, optimal resource allocation methods are to be implemented.

In mobile cellular networks, multiple access methods can be considered when allocating resources to multiple mobile users. Time division multiple access (TDMA) subdivides a fixed time-frame into a given number of timeslots. A number of timeslots are allocated to each mobile user. During the assigned timeslots, transmission to or from the allocated MT occupies the entire bandwidth. TDMA constitutes the multiple access method implemented in the second generation (2G) mobile cellular network Global System for Mobile Communications (GSM) [18]. Some TDMA based resource allocation schemes for multi-hop networks are investigated in [19, 20, 21].

Another well known multiple access method assigns a unique sequence code to each user. The transmitting data of each user are coded using the assigned sequence coded and transmitted simultaneously through the entire bandwidth. This access method is commonly referred to as code division multiple access scheme (CDMA). CDMA had first been implemented in mobile cellular networks in the first generation (1G) mobile cellular system IS-95 technology [22]. Its application on multi-hop networks has been investigated in [23, 24, 25].

Orthogonal frequency division multiple access (OFDMA), which is based on the OFDM technique defined in the previous chapter, represents another multiple access method used in mobile cellular networks. OFDMA is resilient to frequency selective channels and can provide multi-user diversity in a multi-user environment. Hence, it has been widely applied in resource allocation schemes in both single hop [26, 27, 28, 29, 30] and multi-hop networks [31, 32, 33, 34]. The Third Generation Partnership Project Long Term Evolution (3 GPP LTE), and WiMAX [35, 36] have implemented OFDMA as their basic access scheme in the downlink because of its high data transmission rate capability.

In mobile cellular networks, resource allocation is necessary in both uplink and downlink transmissions. In this thesis, we only consider resource allocation in the downlink transmission. The uplink transmission can be considered as future studies. Taking into account the high data transmission rate capability of OFDMA in the downlink, we have decided to consider OFDMA as our multiple access scheme in this thesis.

1.5 Allocation Problems in Two-Hop Networks

We consider a single VC with a set \mathcal{R} of WPs including the CP. We assume that a set \mathcal{M} of MTs are randomly distributed inside the VC. For data reception, the m -th MT is connected to a set \mathcal{R}_m of WPs such that:

$$\bigcup_{m \in \mathcal{M}} \mathcal{R}_m \subseteq \mathcal{R}. \quad (1.18)$$

Using OFDMA as multiple access scheme, the available bandwidth W is divided into a set \mathcal{S} of orthogonal sub-carriers. We assume that a set $\mathcal{S}_m = \{\mathcal{S}_m^{(0)}, \mathcal{S}_m^{(1)}, \mathcal{S}_m^{(2)}\}$ of subsets of sub-carriers are used to transmit data to the m -th MT, with $\mathcal{S}_m^{(0)}$, $\mathcal{S}_m^{(1)}$, and $\mathcal{S}_m^{(2)}$ being the subsets of sub-carriers used in the direct link¹, the first-hop, and second-hop link respectively. If data transmission is scheduled for all MTs we have:

$$\bigcup_{m \in \mathcal{M}} \left(\mathcal{S}_m^{(0)} \cup \mathcal{S}_m^{(1)} \cup \mathcal{S}_m^{(2)} \right) \subseteq \mathcal{S}. \quad (1.19)$$

The channel capacity C_m of the m -th MT is a function of \mathcal{R}_m , and \mathcal{S}_m ; and it can be expressed as:

$$C_m = f(\Xi(\mathcal{R}_m, \mathcal{S}_m)). \quad (1.20)$$

In Equation (1.20), $\Xi(z)$, and $f(\Xi(z))$ represent respectively the SNR, and the capacity functions of the links z between the CP and an MT, direct links and two-hop links inclusively.

Given \mathcal{M} , \mathcal{R} , and \mathcal{S} , the question is: what is the optimal method to allocate these resources in a single VC in order to maximize the capacity C of that VC? Mathematically, this allocation problem can be formulated as:

$$\arg \max_{\mathcal{R}_1, \dots, \mathcal{R}_{\mathcal{M}}, \mathcal{S}_1, \dots, \mathcal{S}_{\mathcal{M}}} C = \sum_{m \in \mathcal{M}} C_m, \quad \text{Subject to:} \quad (1.21)$$

1. Calculate the channel capacity of each MT using:

$$C_m = f(\Xi(\mathcal{R}_m, \mathcal{S}_m)), \quad \forall m \in \mathcal{M}; \quad (1.22)$$

2. Allocate a set of subsets of sub-carriers to each MT:

$$\mathcal{S}_m = \{\mathcal{S}_m^{(0)}, \mathcal{S}_m^{(1)}, \mathcal{S}_m^{(2)}\}, \quad \mathcal{S}_m^{(0)}, \mathcal{S}_m^{(1)}, \mathcal{S}_m^{(2)} \in \mathcal{S}_m, \quad \forall m \in \mathcal{M}; \quad (1.23)$$

3. Choose the subsets of sub-carriers from the set of sub-carriers \mathcal{S} :

$$\bigcup_{m \in \mathcal{M}} \left(\mathcal{S}_m^{(0)} \cup \mathcal{S}_m^{(1)} \cup \mathcal{S}_m^{(2)} \right) \subseteq \mathcal{S}, \quad \forall m \in \mathcal{M}; \quad (1.24)$$

4. Select a subset of WPs for data transmission to each MT:

$$\mathcal{R}_m, \quad \mathcal{R}_m \subseteq \mathcal{R}, \quad \forall m \in \mathcal{M}; \quad (1.25)$$

¹The link between the CP and an MT

5. Choose the subset of WPs from the set of WPs \mathcal{R} :

$$\bigcup_{m \in \mathcal{M}} \mathcal{R}_m \subseteq \mathcal{R}, \quad \forall m \in \mathcal{M}. \quad (1.26)$$

Three approaches can be used to try to solve this resource allocation problem. Firstly, the problem could be divided into route allocation and sub-carrier allocation. The route allocation and the sub-carrier allocation problems can be solved separately and combined later as a solution. Secondly, we can assume that the WPs and the CP are connected using wired connection and solve the problem of joint allocation of route and sub-carriers in the second-hop link. Lastly, we can consider the joint allocation of route and sub-carrier in the first-hop and second-hop links.

1.5.1 Separate Route and Sub-carrier Allocation

We divide the resource allocation problem into two separate allocation problems, route allocation and sub-carrier allocation.

1.5.1.1 Route Allocation

We assume that $\forall m \in \mathcal{M}$, \mathcal{S}_m is given. This means that the problem of sub-carrier allocation is solved. Our resource allocation problem resumes to find \mathcal{R}_m , $\forall m \in \mathcal{M}$, meaning to determine which set of WPs an MT is connected to for data reception. Hence, the resource allocation problem in Equation (1.21) becomes: given \mathcal{S}_m , $\forall m \in \mathcal{M}$,

$$\arg \max_{\mathcal{R}_1, \dots, \mathcal{R}_{\mathcal{M}}} C = \sum_{m \in \mathcal{M}} C_m, \quad \text{Subject to:} \quad (1.27)$$

1. Calculate the channel capacity of each MT using:

$$C_m = f(\Xi(\mathcal{R}_m, \mathcal{S}_m)), \quad \forall m \in \mathcal{M}; \quad (1.28)$$

2. Select a subset of WPs for data transmission to each MT:

$$\mathcal{R}_m, \quad \mathcal{R}_m \subseteq \mathcal{R}, \quad \forall m \in \mathcal{M}; \quad (1.29)$$

3. Choose the subset of WPs from the set of WPs \mathcal{R} :

$$\bigcup_{m \in \mathcal{M}} \mathcal{R}_m \subseteq \mathcal{R}, \quad \forall m \in \mathcal{M}. \quad (1.30)$$

This type of resource allocation problem is referred to as *route allocation* or *route selection*. It has been investigated in [37, 38]. This allocation design only solves part of our problem.

1.5.1.2 First-Hop and Second-Hop Sub-Carrier Allocation

We suppose that the route allocation problem is solved and that each MT is connected to a subset of selected WPs. This means that $\forall m \in \mathcal{M}$, \mathcal{R}_m is given. Our allocation problem is to find the subsets of sub-carriers $\mathcal{S}_m^{(0)}$, $\mathcal{S}_m^{(1)}$, and $\mathcal{S}_m^{(2)}$, $\forall m \in \mathcal{M}$, allocated in the direct link, the first-hop link, and second-hop link for each MT. If we consider that the same bandwidth W is used in the links between the CP and the WPs, and in the links between the WPs and the MTs, we should take into account that resource allocation between the CP and the WPs is coupled with that between the WPs and the MTs. This is because the primary objective is not to transmit data to the WPs but to the MTs. If plenty of resources are allocated in the first-hop link without enough resources available to relay the data to the MTs, the resources used in the first-hop link are wasted. Furthermore, for complete data delivery, the number of sub-carriers allocated in the second-hop link for data transmission to an MT must equal that allocated in the first-hop link for that MT:

$$|\mathcal{S}_m^{(1)}| = |\mathcal{S}_m^{(2)}|, \quad \mathcal{S}_m^{(1)}, \mathcal{S}_m^{(2)} \in \mathcal{S}_m, \quad \forall m \in \mathcal{M}, \quad (1.31)$$

with $|\mathcal{A}|$ being the cardinal of a set \mathcal{A} . The cardinal of a set is defined as the number of elements in that set, here $|\mathcal{S}_m^{(1)}|$ represents the number of sub-carriers in the set $\mathcal{S}_m^{(1)}$.

Considering that route allocation is done, the second part of our resource allocation problem can be expressed as: given \mathcal{R}_m , $\forall m \in \mathcal{M}$

$$\arg \max_{\mathcal{S}_1, \dots, \mathcal{S}_{\mathcal{M}}} C = \sum_{m \in \mathcal{M}} C_m, \quad \text{Subject to:} \quad (1.32)$$

1. Calculate the channel capacity of each MT using:

$$C_m = f(\Xi(\mathcal{R}_m, \mathcal{S}_m)), \quad \forall m \in \mathcal{M}; \quad (1.33)$$

2. Allocate a set of subsets of sub-carriers to each MT:

$$\mathcal{S}_m = \{\mathcal{S}_m^{(0)}, \mathcal{S}_m^{(1)}, \mathcal{S}_m^{(2)}\}, \quad \mathcal{S}_m^{(0)}, \mathcal{S}_m^{(1)}, \mathcal{S}_m^{(2)} \in \mathcal{S}_m, \quad \forall m \in \mathcal{M}; \quad (1.34)$$

3. Choose the subsets of sub-carriers from the set of sub-carriers \mathcal{S} :

$$\bigcup_{m \in \mathcal{M}} \left(\mathcal{S}_m^{(0)} \cup \mathcal{S}_m^{(1)} \cup \mathcal{S}_m^{(2)} \right) \subseteq \mathcal{S}, \quad \forall m \in \mathcal{M}; \quad (1.35)$$

4. The number of sub-carriers allocated in the first-hop link is equal to that of sub-carriers allocated in the second-hop link:

$$|\mathcal{S}_m^{(1)}| = |\mathcal{S}_m^{(2)}|, \quad \mathcal{S}_m^{(1)}, \mathcal{S}_m^{(2)} \in \mathcal{S}_m, \quad \forall m \in \mathcal{M}. \quad (1.36)$$

Some proposed resource allocation schemes which made the assumptions that the route selection problem is solved can be found in [33, 39, 40, 41, 42, 43].

1.5.1.3 Drawback of This Approach

The solution of the route allocation problem in Equation (1.27) can be coupled with that of the sub-carrier allocation problem in Equation (1.32) to provide a complete solution to our resource allocation problem in Equation (1.21). The disadvantage of this approach is that it cannot provide joint route and subcarrier diversity. Furthermore, in an OFDMA system, the received signal power at an MT on a sub-carrier can vary considerably depending on which WP's link that sub-carrier belongs to. Hence, the previously chosen WP might not provide the best channel quality for this specific sub-carrier.

1.5.2 Joint Route and Second-Hop Sub-Carrier Allocation

A second approach is to consider that the WPs are connected to the CP using dedicated links such as fibre optic. In this case, the set of subsets of subcarriers used to transmit data to the m -th MT becomes $\mathcal{S}_m = \{\mathcal{S}_m^{(0)}, \mathcal{S}_m^{(2)}\}$. This assumption relaxes the constraint in Equation (1.23) in the sense that no more sub-carrier allocation is necessary in the first-hop link between the CP and the WPs. Our resource allocation problem resumes to a *route selection* problem and sub-carrier allocation in the direct and second-hop links which can be formulated as:

$$\arg \max_{\mathcal{R}_1, \dots, \mathcal{R}_{\mathcal{M}}, \mathcal{S}_1, \dots, \mathcal{S}_{\mathcal{M}}} C = \sum_{m \in \mathcal{M}} C_m, \quad \text{Subject to:} \quad (1.37)$$

1. Calculate the channel capacity of each MT using:

$$C_m = f(\Xi(\mathcal{R}_m, \mathcal{S}_m)), \quad \forall m \in \mathcal{M}; \quad (1.38)$$

2. Allocate a set of subsets of sub-carriers to each MT:

$$\mathcal{S}_m = \{\mathcal{S}_m^{(0)}, \mathcal{S}_m^{(2)}\}, \quad \mathcal{S}_m^{(0)}, \mathcal{S}_m^{(2)} \in \mathcal{S}_m, \quad \forall m \in \mathcal{M}; \quad (1.39)$$

3. Choose the subsets of sub-carriers from the set of sub-carriers \mathcal{S} :

$$\bigcup_{m \in \mathcal{M}} (\mathcal{S}_m^{(0)} \cup \mathcal{S}_m^{(2)}) \subseteq \mathcal{S}, \quad \forall m \in \mathcal{M}; \quad (1.40)$$

4. Select a subset of WPs for data transmission to each MT:

$$\mathcal{R}_m, \quad \mathcal{R}_m \subseteq \mathcal{R}, \quad \forall m \in \mathcal{M}; \quad (1.41)$$

5. Choose the subset of WPs from the set of WPs \mathcal{R} :

$$\bigcup_{m \in \mathcal{M}} \mathcal{R}_m \subseteq \mathcal{R}, \quad \forall m \in \mathcal{M}. \quad (1.42)$$

This resource allocation problem has been investigated in [31].

1.5.2.1 Drawback of This Approach

Though this approach can provide route and frequency diversity, unfortunately the solution of using a dedicated connection between the CP and the WPs is not always viable. It can be costly depending on the type of connection used. Furthermore, if wired connection is used, the network becomes less flexible when it comes to network extension to accommodate new market demand.

1.5.3 Joint Route and Sub-Carrier Allocation

A third approach is to assume that there was no previous route selection. We can consider the joint allocation of routes and sub-carriers in the first-hop and second-hop links. We assume that there is no direct connection with the CP, which means that $\forall m \in \mathcal{M}$, $\mathcal{S}_m = \{\mathcal{S}_m^{(1)}, \mathcal{S}_m^{(2)}\}$. The allocation problem can be formulated as:

$$\arg \max_{\mathcal{R}_1, \dots, \mathcal{R}_{\mathcal{M}}, \mathcal{S}_1, \dots, \mathcal{S}_{\mathcal{M}}} C = \sum_{m \in \mathcal{M}} C_m, \quad \text{Subject to:} \quad (1.43)$$

1. Calculate the channel capacity of each MT using:

$$C_m = f(\Xi(\mathcal{R}_m, \mathcal{S}_m)), \quad \forall m \in \mathcal{M}; \quad (1.44)$$

2. Allocate a set of subsets of sub-carriers to each MT:

$$\mathcal{S}_m = \{\mathcal{S}_m^{(1)}, \mathcal{S}_m^{(2)}\}, \quad \mathcal{S}_m^{(1)}, \mathcal{S}_m^{(2)} \in \mathcal{S}_m, \quad \forall m \in \mathcal{M}; \quad (1.45)$$

3. Choose the subsets of sub-carriers from the set of sub-carriers \mathcal{S} :

$$\bigcup_{m \in \mathcal{M}} \left(\mathcal{S}_m^{(1)} \cup \mathcal{S}_m^{(2)} \right) \subseteq \mathcal{S}, \quad \forall m \in \mathcal{M}; \quad (1.46)$$

4. The number of sub-carriers allocated in the first-hop link is equal to that allocated in the second-hop link:

$$|\mathcal{S}_m^{(1)}| = |\mathcal{S}_m^{(2)}|, \quad \mathcal{S}_m^{(1)}, \mathcal{S}_m^{(2)} \in \mathcal{S}_m, \quad \forall m \in \mathcal{M}; \quad (1.47)$$

5. Select a subset of WPs for data transmission to each MT:

$$\mathcal{R}_m, \quad \mathcal{R}_m \subseteq \mathcal{R}, \quad \forall m \in \mathcal{M}; \quad (1.48)$$

6. Choose the subset of WPs from the set of WPs \mathcal{R} :

$$\bigcup_{m \in \mathcal{M}} \mathcal{R}_m \subseteq \mathcal{R}, \quad \forall m \in \mathcal{M}. \quad (1.49)$$

Depending on the data relaying method used at the WP, resource allocation schemes related to this allocation problem can be categorized in two groups, *time division relaying schemes*, and *frequency division relaying schemes*.

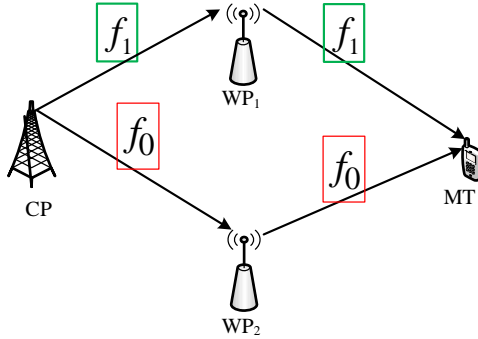


Figure 1.11: Time division relaying

1.5.3.1 Time Division Relaying Schemes

We suppose that the frequency in-use in the first-hop link between the CP and a WP is the same as that reused by that WP to transmit to an MT (see Figure 1.11):

$$\mathcal{S}_{m,r}^{(1)} = \mathcal{S}_{m,r}^{(2)}, \quad \mathcal{S}_{m,r}^{(1)} \subseteq \mathcal{S}_m^{(1)}, \quad \mathcal{S}_{m,r}^{(2)} \subseteq \mathcal{S}_m^{(2)}, \quad \forall m \in \mathcal{M}, \quad \forall r \in \mathcal{R}_m; \quad (1.50)$$

with $\mathcal{S}_{m,r}^{(1)}$, and $\mathcal{S}_{m,r}^{(2)}$ being respectively the subsets of sub-carriers allocated in the first-hop link between the CP and the r -th WP for data transmission to the m -th MT, and in the second-hop link between the r -th WP and the m -th MT. With such assumption, to prevent self-interference, the WPs are not allowed to transmit and receive simultaneously in the same timeframe. The WPs are constrained to transmit and receive in two different timeframes. Figure 1.11 illustrates the case of a single MT and two WPs where the same frequency is used to transmit in the first-hop and second-hop links. These schemes can be referred to as *time division relaying schemes* and an example can be found in [34].

Though time division relaying schemes consider the joint allocation of routes and sub-carriers, the constraint on the sub-carrier in the first-hop link to be the same as that in the second-hop link removes any degree of frequency diversity which might exist between the two hops. Furthermore, the channel conditions of a sub-carrier could fluctuate considerably between the two hops which will result in a poor resultant link between the CP and the MT.

1.5.3.2 Frequency Division Relaying Schemes

In contrast to time division relaying scheme, a different method is to assign two different frequencies for data reception and transmission in the first-hop link and second-hop link respectively (see Figure 1.12):

$$\mathcal{S}_{m,r}^{(1)} \neq \mathcal{S}_{m,r}^{(2)}, \quad \mathcal{S}_{m,r}^{(1)} \subseteq \mathcal{S}_m^{(1)}, \quad \mathcal{S}_{m,r}^{(2)} \subseteq \mathcal{S}_m^{(2)}, \quad \forall m \in \mathcal{M}, \quad \forall r \in \mathcal{R}_m. \quad (1.51)$$

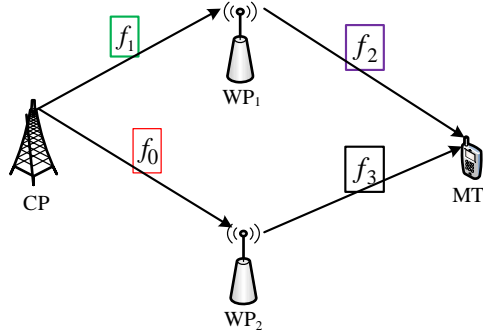


Figure 1.12: Frequency division relaying

Since the frequency allocated to transmit data between the CP and WP differs from that assigned between the WP and the MT, a WP can transmit and receive concurrently in the same timeframe. The schemes applying such technique can be categorized as *frequency division relaying schemes*. Some references of these schemes are [33, 44, 39].

In a two-hop relaying network, both links are required to be not in bad states for the two-hop transmission to be successful. Allowing different subcarriers to be allocated in each hop link offers the advantage to combine subcarriers with high channel gain in the different hop links. Consequently, in a frequency selective fading environment, frequency division relaying schemes can yield a higher degree of frequency diversity than time division relaying schemes.

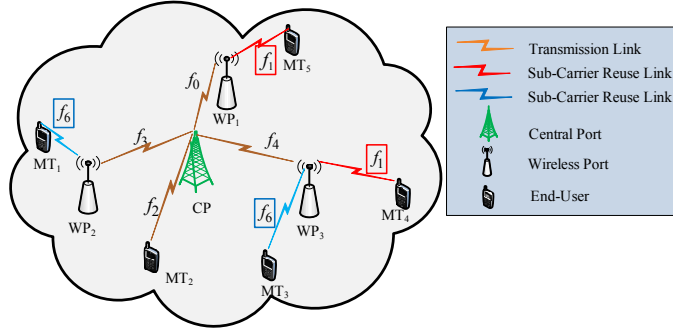


Figure 1.13: Single virtual cell with sub-carrier reuse

1.6 Objective of the Research

In a two-hop network, two-hop links resource allocation is only advantageous to MTs located at the edge of a cell or in the neighbouring of WPs. MTs located in the neighbourhood of the CP do not necessitate any WP connection, and resources should still be allocated to them. Therefore, instead of assuming that there is no direct connection, i.e $\forall m \in \mathcal{M}, \mathcal{S}_m = \{\mathcal{S}_m^{(1)}, \mathcal{S}_m^{(2)}\}$, as we did when introducing the joint route and sub-carrier allocation problem, we also need to consider sub-carrier allocation for direct connections to the CP, i.e $\forall m \in \mathcal{M}, \mathcal{S}_m = \{\mathcal{S}_m^{(0)}, \mathcal{S}_m^{(1)}, \mathcal{S}_m^{(2)}\}$.

The frequency division relaying schemes in [33, 44, 39] do not consider that a sub-carrier can be allocated in two links simultaneously. They assume that the allocated subsets of sub-carriers to the MTs are disjoints:

$$(\mathcal{S}_m^{(1)} \cap \mathcal{S}_m^{(2)}) \cap (\mathcal{S}_p^{(1)} \cap \mathcal{S}_p^{(2)}) = \emptyset, \quad \forall m, p \in \mathcal{M}. \quad (1.52)$$

Consider Figure 1.13, sub-carrier f_6 in use by WP₂ to transmit to MT₁ can be reused with limited added interference by WP₃ to transmit to MT₃. WPs are low transmit power nodes. If intra-cell interference is accounted for in a resource allocation design, a sub-carrier can be reused concurrently in multiple links in a VC.

Including the sub-carriers allocated in the direct links, in a single VC, the sub-carrier reuse design can be mathematically formulated as:

$$|\mathcal{S}_{m,r}^{(2)} \cap \mathcal{S}_{p,w}^{(2)}| \geq 0, \quad \forall m, p \in \mathcal{M}, m \neq p, \quad \forall r \in \mathcal{R}_m, \quad \forall w \in \mathcal{R}_p, r \neq w; \quad (1.53)$$

$$|\mathcal{S}_{m,r}^{(2)} \cap \mathcal{S}_p^{(0)}| \geq 0, \quad \forall m, p \in \mathcal{M}, \quad \forall r \in \mathcal{R}_m; \quad (1.54)$$

$$|\bigcap_{m \in \mathcal{M}} \mathcal{S}_m| \geq 0, \quad \forall m \in \mathcal{M}. \quad (1.55)$$

1.6.1 Single Cell Allocation Problem

Taking into account that resource allocation is necessary for direct link transmission, assuming that a sub-carrier can be assigned concurrently in multiple

links, the joint route and sub-carrier allocation problem in a single VC can be formulated as:

$$\arg \max_{\mathcal{R}_1, \dots, \mathcal{R}_{\mathcal{M}}, \mathcal{S}_1, \dots, \mathcal{S}_{\mathcal{M}}} C = \sum_{m \in \mathcal{M}} C_m, \quad \text{Subject to:} \quad (1.56)$$

1. Calculate the channel capacity of an MT using:

$$C_m = f(\Xi(\mathcal{R}_m, \mathcal{S}_m)), \quad \forall m \in \mathcal{M}; \quad (1.57)$$

$\Xi(z)$, and $f(\Xi(z))$ represent respectively the signal-to-interference-plus-noise power ratio (SINR), and the channel capacity functions of the links z between the CP and MT in a VC. The effect of intra-cell interference in the VC is taken into account when evaluating $\Xi(z)$.

2. Allocate a set of subsets of sub-carriers to each MT:

$$\mathcal{S}_m = \{\mathcal{S}_m^{(0)}, \mathcal{S}_m^{(1)}, \mathcal{S}_m^{(2)}\}, \quad \mathcal{S}_m^{(0)}, \mathcal{S}_m^{(1)}, \mathcal{S}_m^{(2)} \in \mathcal{S}_m, \quad \forall m \in \mathcal{M}; \quad (1.58)$$

3. Choose the subsets of sub-carriers from the set of sub-carriers \mathcal{S} :

$$\bigcup_{m \in \mathcal{M}} \left(\mathcal{S}_m^{(0)} \cup \mathcal{S}_m^{(1)} \cup \mathcal{S}_m^{(2)} \right) \subseteq \mathcal{S}, \quad \forall m \in \mathcal{M}; \quad (1.59)$$

4. The number of sub-carriers allocated in the first-hop link is equal to that allocated in the second-hop link:

$$|\mathcal{S}_m^{(1)}| = |\mathcal{S}_m^{(2)}|, \quad \mathcal{S}_m^{(1)}, \mathcal{S}_m^{(2)} \in \mathcal{S}_m, \quad \forall m \in \mathcal{M}; \quad (1.60)$$

5. Select a subset of WPs for data transmission to each MT:

$$\mathcal{R}_m, \quad \mathcal{R}_m \subseteq \mathcal{R}, \quad \forall m \in \mathcal{M}; \quad (1.61)$$

6. Choose the subset of WPs from the set of WPs \mathcal{R} :

$$\bigcup_{m \in \mathcal{M}} \mathcal{R}_m \subseteq \mathcal{R}, \quad \forall m \in \mathcal{M}; \quad (1.62)$$

7. Frequency division relaying is assumed. Considering the two-hop links belonging to the m -th MT, the sub-carriers used to transmit in the first-hop link to the r -th WP should be different from that used by that WP to transmit to MT_m :

$$\mathcal{S}_{m,r}^{(1)} \neq \mathcal{S}_{m,r}^{(2)}, \quad \mathcal{S}_{m,r}^{(1)} \subseteq \mathcal{S}_m^{(1)}, \quad \mathcal{S}_{m,r}^{(2)} \subseteq \mathcal{S}_m^{(2)}, \quad \forall m \in \mathcal{M}, \quad \forall r \in \mathcal{R}_m; \quad (1.63)$$

8. A sub-carrier can be reused simultaneously in multiple links:

$$\begin{aligned} & |\mathcal{S}_{m,r}^{(2)} \cap \mathcal{S}_{p,w}^{(2)}| \geq 0, \quad \forall m, p \in \mathcal{M}, m \neq p, \quad \forall r \in \mathcal{R}_m, \quad \forall w \in \mathcal{R}_p, r \neq w; \\ & |\mathcal{S}_{m,r}^{(2)} \cap \mathcal{S}_p^{(0)}| \geq 0, \quad \forall m, p \in \mathcal{M}, \quad \forall r \in \mathcal{R}_m; \\ & \left| \bigcap_{m \in \mathcal{M}} \mathcal{S}_m \right| \geq 0, \quad \forall m \in \mathcal{M}. \end{aligned} \quad (1.64)$$

1.6.2 Multi-Cell Allocation Problem

In a multi-cell environment, the channel capacity of mobile wireless networks deteriorates considerably because of co-channel interference. Therefore, when designing a resource allocation scheme, it is a must to consider the effect of inter-cell interference in the system.

Consider a system with a set \mathcal{V} of VCs. In the v -th VC, (VC_v), a set \mathcal{R}_v of WPs including the CP ensure the data transmission between the CN and a set \mathcal{M}_v of MTs. The available bandwidth of the v -th VC is divided into a set \mathcal{S}_v of orthogonal sub-carriers. The WPs and CP are assumed to be able to transmit concurrently in the same timeframe using different sub-carriers in the first-hop and second-hop links. A sub-carrier can be reused simultaneously in multiple links in a VC. A set $\mathcal{S}_{m,v} = \{\mathcal{S}_{m,v}^{(0)}, \mathcal{S}_{m,v}^{(1)}, \mathcal{S}_{m,v}^{(2)}\}$ of subsets of sub-carriers are to be allocated to the m -th MT in the v -VC ($MT_{m,v}$). $\mathcal{S}_{m,v}^{(0)}$, $\mathcal{S}_{m,v}^{(1)}$, and $\mathcal{S}_{m,v}^{(2)}$ represent respectively the subsets of sub-carriers allocated in the direct, the first-hop, and the second-hop links for data transmission to $MT_{m,v}$. Denote the set of WPs in the v -th VC to which $MT_{m,v}$ is connected for data transmission by $\mathcal{R}_{m,v}$. The multi-cell resource allocation problem can be formulated as:

$$\arg \max_{\mathcal{R}_{1,v}, \dots, \mathcal{R}_{\mathcal{M}_v,v}, \mathcal{S}_{1,v}, \dots, \mathcal{S}_{\mathcal{M}_v,v}} C = \sum_{m \in \mathcal{M}} C_{m,v}, \quad \text{Subject to:} \quad (1.65)$$

1. Calculate the channel capacity of an MT using:

$$C_{m,v} = f(\Xi(\mathcal{R}_{m,v}, \mathcal{S}_{m,v})), \quad \forall m \in \mathcal{M}_v; \quad (1.66)$$

$\Xi(z)$, and $f(\Xi(z))$ represent respectively the SINR, and the channel capacity functions of the links z between the CP and MT in a VC. The effect of intra-cell and inter-cell interference inside each VC and between the different VCs is accounted for when evaluating $\Xi(z)$.

2. Allocate a set of subsets of sub-carriers to each MT:

$$\mathcal{S}_{m,v} = \{\mathcal{S}_{m,v}^{(0)}, \mathcal{S}_{m,v}^{(1)}, \mathcal{S}_{m,v}^{(2)}\}, \quad \mathcal{S}_{m,v}^{(0)}, \mathcal{S}_{m,v}^{(1)}, \mathcal{S}_{m,v}^{(2)} \in \mathcal{S}_v, \quad \forall m \in \mathcal{M}_v; \quad (1.67)$$

3. Choose the subsets of sub-carriers from the set of sub-carriers \mathcal{S}_v :

$$\bigcup_{m \in \mathcal{M}_v} \left(\mathcal{S}_{m,v}^{(0)} \cup \mathcal{S}_{m,v}^{(1)} \cup \mathcal{S}_{m,v}^{(2)} \right) \subseteq \mathcal{S}_v, \quad \forall m \in \mathcal{M}_v; \quad (1.68)$$

4. The number of sub-carriers allocated in the first-hop link is equal to that allocated in the second-hop link:

$$|\mathcal{S}_{m,v}^{(1)}| = |\mathcal{S}_{m,v}^{(2)}|, \quad \mathcal{S}_{m,v}^{(1)}, \mathcal{S}_{m,v}^{(2)} \in \mathcal{S}_v, \quad \forall m \in \mathcal{M}_v; \quad (1.69)$$

5. Select a subset of WPs for data transmission to each MT:

$$\mathcal{R}_{m,v}, \quad \mathcal{R}_{m,v} \subseteq \mathcal{R}_v, \quad \forall m \in \mathcal{M}_v; \quad (1.70)$$

6. Choose the subset of WPs from the set of WPs \mathcal{R}_v :

$$\bigcup_{m \in \mathcal{M}_v} \mathcal{R}_{m,v} \subseteq \mathcal{R}_v, \quad \forall m \in \mathcal{M}_v; \quad (1.71)$$

7. Frequency division relaying is assumed. Consider the set of two-hop links of $\text{MT}_{m,v}$, the sub-carriers used to transmit in the first-hop link to the r -th WP should be different from that used by that WP to transmit to $\text{MT}_{m,v}$:

$$\mathcal{S}_{m,r,v}^{(1)} \neq \mathcal{S}_{m,r,v}^{(2)}, \quad \mathcal{S}_{m,r,v}^{(1)} \subseteq \mathcal{S}_{m,v}^{(1)}, \quad \mathcal{S}_{m,r,v}^{(2)} \subseteq \mathcal{S}_{m,v}^{(2)}, \quad \forall m \in \mathcal{M}_v, \quad \forall r \in \mathcal{R}_{m,v}; \quad (1.72)$$

8. A sub-carrier can be reused simultaneously in multiple links:

$$\begin{aligned} |\mathcal{S}_{m,r,v}^{(2)} \cap \mathcal{S}_{p,w,v}^{(2)}| &\geq 0, & \forall m, p \in \mathcal{M}_v, m \neq p, & \forall r \in \mathcal{R}_{m,v}, & \forall w \in \mathcal{R}_{p,v}, r \neq w; \\ |\mathcal{S}_{m,r,v}^{(2)} \cap \mathcal{S}_{p,v}^{(0)}| &\geq 0, & \forall m, p \in \mathcal{M}_v, & \forall r \in \mathcal{R}_{m,v}; \\ |\bigcap_{m \in \mathcal{M}_v} \mathcal{S}_{m,v}| &\geq 0, & \forall m \in \mathcal{M}_v. \end{aligned} \quad (1.73)$$

1.6.3 Objective

The resource allocation problems defined above in Equation (1.56) and Equation (1.65) are non-deterministic polynomial-time hard (NP-hard) resource allocation problems and cannot be solved using existing allocation algorithms. Their optimal solution would require exhaustive search which is not practical in real systems. To the best of the author's knowledge, these resource allocation problems have not yet been solved in the literature. Our objective is to provide some element of solution to these problems.

1.7 Thesis Contribution

As element of solution to the joint route and sub-carrier allocation problem in a two-hop network, we have considered the following approaches:

1. To solve the joint route and sub-carrier allocation problem, in Chapter 2 we design the joint allocation of route and sub-carrier as a *logical route* allocation problem. We derive the numerical expression involved in the logical route allocation problem, and formulate the allocation problem in single cell and multi-cell environment.
2. To reduce the computational complexity of the allocation problems in Equation (1.56) and Equation (1.65), in Chapter 3, we propose a sub-optimal successive allocation scheme (SAS) which considers the successive allocation of the logical route per MT. We study the performance of the successive scheme in a single cell and a multi-cell environment.
3. The successive scheme is not resilient to intra-cell and inter-cell interference. Hence, in Chapter 4, we study some iterative allocation schemes to alleviate the effect of intra-cell interference in a single VC. We propose a sequential iterative allocation scheme (SIS) and study its performance in a multi-cell environment.
4. Though the SIS can lessen the effect of intra-cell and inter-cell interference in a two-hop network, its performance could not approximate that of the optimal solution. Hence, in Chapter 5, to approximate the optimal solution, we model the allocation problem using the idea of the evolution theory. We propose an evolutionary allocation scheme (EAS) and show that it can achieve similar performance with the optimal exhaustive allocation scheme in a single VC. We later extend the study to a multi-cell environment.
5. Chapter 6 presents a summary of the proposed allocation schemes. Future and prospective work are also discussed.

CHAPTER 2

Resource Allocation Problem Formulation

The development of new wireless devices capable of using live streaming applications and other data hungry applications has created a high demand for increasing the data transmission rate in mobile wireless networks. The macro-cell-based network architecture cannot satisfy that augmentation of the data transmission rate without increasing the transmission power, particularly for a user located at the cell-edge.

By reducing the distance between the transmission station and the receiving device, multi-hop networks can augment the data transmission rate of cell-edge users without increasing the transmission power [8, 9, 10, 11, 12, 13, 14, 15, 16]. Taking into account that a migration step will be necessary to move from a single hop architecture to a multi-hop architecture, a two-hop network can be considered as a transition network design for the next generation of mobile cellular networks.

In order to provide high data transmission rate in the downlink, many recent wireless transmission technologies have considered OFDMA as the access scheme [35, 36]. Researchers involved in radio resource allocation have extensively investigated the application of OFDMA because of its multi-user diversity and its resiliency against frequency selective channels [26, 29, 30, 27, 28]. Therefore, OFDMA can be considered as the access scheme of choice for future mobile cellular networks aiming at providing high data transmission rate.

In a two-hop network, the joint allocation of routes and sub-carriers in the first-hop and second-hop link can provide route a frequency diversity [44]. Furthermore, frequency division relaying schemes can provide higher degree of frequency diversity than time division relaying schemes. Most of the frequency division relaying schemes proposed in the literature do not consider the problem of route selection [33, 39, 40]. If they do, they can only be applied in a single user case [44].

Multi-cell interference can degrade the capacity of a network considerably. Therefore, inter-cell interference should be taken into account when designing a resource allocation scheme.

The limitation and the high cost of wireless spectrum in mobile cellular networks create the necessity to develop algorithms aiming at increasing the spectrum efficiency. In a two-hop network, the enhancement of the spectrum efficiency can be achieved by allowing a sub-carrier to be allocated simultane-

ously in multiple links.

In Chapter 1, we defined and detailed the problem of joint route and sub-carrier allocation with frequency reused in single cell and multi-cell environment for two-hop networks. As discussed in Chapter 1, this allocation problem has not yet been solved in the literature. In this chapter, we design the joint route and sub-carrier allocation problem using a new concept called logical route. We derive the numerical expressions related to the allocation problem and formulate the resource allocation problem as a logical route optimization allocation problem, for single cell and multi-cell environments.

2.1 Parallel Relaying Transmission

The allocation of resources in a two-hop cellular network is closely related to the method of data transmission considered. Therefore, in order to formulate our allocation problem, we will first define the data transmission method used.

2.1.1 Physical Route

We consider a single VC with a set \mathcal{R} of R WPs including the CP, a set \mathcal{M} of M MTs, and a bandwidth W . We define a *physical route* as the path a transmitted data from the CP takes on to reach an MT. It can be a direct route if it describes a direct link between the CP and the MT (See Figure 2.1). If the transmitted data is relayed by a WP, the physical route is said to be a two-hop link route. Since we consider downlink transmission, the first-hop link is the link between the CP and a WP, and the second-hop link represents the link between the WP and an MT. In Figure 2.1, we illustrate the physical routes using dashed-dotted lines. Three physical routes enable the communication between the CP and MT_1 , one direct link route and two 2-hop link routes. A physical route is represented by a WP (CP included) and an MT. $LR(MT_1, CP, 6, 6)$ is used for consistency.

2.1.2 Logical Route

We divide the available bandwidth W into a set \mathcal{S} of S orthogonal sub-carriers. We assume that the same bandwidth is used in the direct links and in the first-hop and second-hop links. We define a *logical route* (LR) as a set of a physical route and sub-carriers allocated along each link of the physical route. In the case of a direct route, a logical route is constructed using the CP and one sub-carrier. To prevent self-interference at a WP and consequently enable frequency division relaying, we assign two different sub-carriers in the first-hop and second-hop links if the physical route is a two-hop link route. Figure 2.1 illustrates a logical route constructed along the physical route going through WP_1 , (WP_1, MT_1) , between the CP and MT_1 . In the logical route

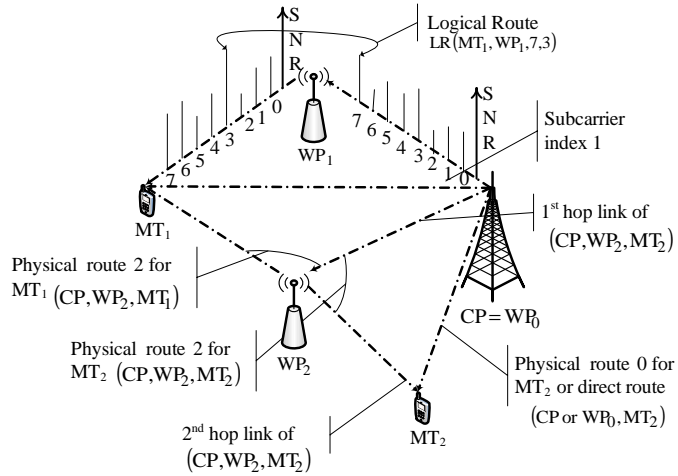


Figure 2.1: Physical and logical route

$LR(MT_1, WP_1, 7, 3)$, the sub-carrier index 7 is assigned in the first-hop link and sub-carrier index 3 in the second-hop link.

2.1.3 Data Transmission Method

We suppose that the transmitting data of the m -th MT (MT_m) at the CP is divided into D_m data streams $d_1^{(m)}, d_2^{(m)}, \dots, d_{D_m}^{(m)}$. In the *parallel relaying transmission* methods, these data streams are transmitted simultaneously from the CP to MT_m using D_m parallel logical routes [44]. Figure 2.2 illustrates a parallel relaying transmission of four data streams $d_1^{(1)}, d_2^{(1)}, d_3^{(1)}$, and $d_4^{(1)}$ to MT_1 . The data streams $d_1^{(1)}, d_2^{(1)}, d_3^{(1)}$, and $d_4^{(1)}$ are transmitted simultaneously from the CP using the respective logical routes $LR(MT_1, WP_1, 1, 5)$, $LR(MT_1, CP, 6, 6)$, $LR(MT_1, WP_2, 3, 7)$, and $LR(MT_1, WP_2, 5, 4)$. Though only one sub-carrier is necessary to construct a logical route in the direct link, this notation $LR(MT_1, CP, 6, 6)$ is used for consistency.

2.1.4 Joint Route and Sub-Carrier Allocation

With the parallel relaying transmission method, the allocation of routes and sub-carriers is carried out simultaneously using the concept of logical route. We denote $l_e(m, r, k_i, k_j)$ the e -th logical route allocated to the m -th MT via the r -th physical route (or WP_r), k_i and k_j being respectively the sub-carriers assigned in the first-hop and second-hop links. We consider a set \mathcal{L}_m of D_m logical routes allocated to the m -th MT:

$$\begin{aligned} \mathcal{L}_m = & \{l_0(m, 0, k_i, k_i), \dots, l_e(m, 0, k_n, k_n), l_{e+1}(m, r, k_j, k_h), \dots, l_{D_m}(m, w, k_t, k_s)\}, \\ & \forall r, w \in \mathcal{R}, \quad r \neq 0, \quad w \neq 0, \quad \forall k_i, k_n, k_j, k_h, k_t, k_s \in \mathcal{S}. \end{aligned} \quad (2.1)$$

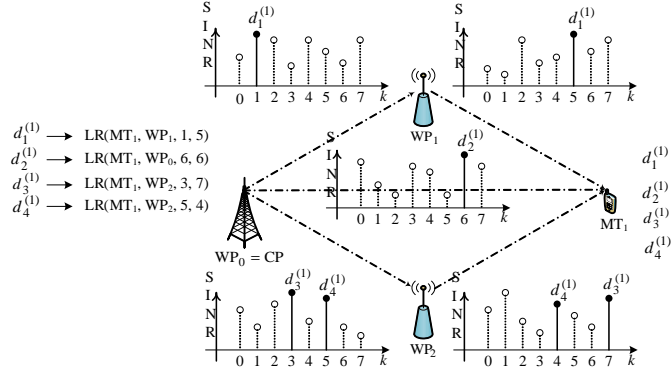


Figure 2.2: Parallel relaying transmission

Recall that in the Chapter 1, we have defined the set of subsets of sub-carriers allocated to the m -th MT by $\mathcal{S}_m = \{\mathcal{S}_m^{(0)}, \mathcal{S}_m^{(1)}, \mathcal{S}_m^{(2)}\}$. In the set \mathcal{L}_m of logical routes, the sub-carriers $\{k_i, \dots, k_n\}$ allocated in the direct link logical routes $\{l_0(m, 0, k_i, k_i), \dots, l_e(m, 0, k_n, k_n)\}$ represent the elements of the subset $\mathcal{S}_m^{(0)}$. The sub-carriers k_j, \dots, k_t assigned in the first-hop links of logical routes $l_{e'}(m, r, k_j, k_h), \dots, l_{L_m}(m, w, k_t, k_s)$ are those of the subset $\mathcal{S}_m^{(1)}$, and k_h, \dots, k_s assigned in the second-hop links are those of the subset $\mathcal{S}_m^{(2)}$. Furthermore, the WPs $0, \dots, r, \dots, w$ of the set \mathcal{L}_m of logical routes represent the elements of the subset \mathcal{R}_m of routes allocated to the m -th MT as defined previously. Therefore, the problem of joint route and sub-carrier allocation can be formulated as a logical route allocation problem.

2.1.5 Data Modulation in Parallel Relaying

The implementation of the parallel relaying transmission requires some data modulation techniques based on OFDMA. The different data modulation techniques applied at the CP, the WPs, and the MTs are detailed in the following sections.

2.1.5.1 CP Data Modulation

At the CP, the transmitting data of each MT is divided into a subset of data streams:

$$\begin{aligned} \mathcal{D}_1 &= \{d_1^{(1)}, d_2^{(1)}, \dots, d_i^{(1)}, \dots, d_{D_1}^{(1)}\}, \\ &\quad \vdots \quad \vdots \\ \mathcal{D}_m &= \{d_1^{(m)}, d_2^{(m)}, \dots, d_i^{(m)}, \dots, d_{D_m}^{(m)}\}, \\ &\quad \vdots \quad \vdots \\ \mathcal{D}_M &= \{d_1^{(M)}, d_2^{(M)}, \dots, d_i^{(M)}, \dots, d_{D_M}^{(M)}\}. \end{aligned}$$

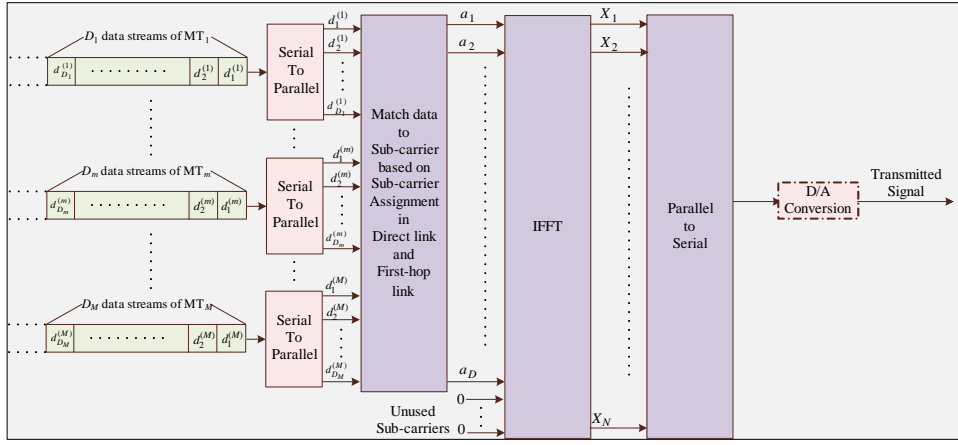


Figure 2.3: Data modulation at the CP

$d_i^{(m)}$ represents the i -th data element of the data streams that belongs to the m -th MT. Each subset of data streams is converted from a serial stream to a parallel stream (see Figure 2.3).

Depending on the logical route allocation to each MT, the parallel data streams are matched to the position of their sub-carrier respective. We assume that a set of D_m logical routes is allocated to the m -th MT, with \mathcal{I}_m being the set of sub-carrier indices allocated in the direct and first-hop links of the logical routes. We designate by $g_i(m)$ the function which returns the set \mathcal{I}_m when given the index m of the m -th MT:

$$\mathcal{I}_m = g_i(m), \quad \forall m \in \mathcal{M}. \quad (2.2)$$

We denote by $\Lambda(\mathcal{I}_m, \mathcal{D}_m)$ the mapping function that, given a set of sub-carrier indices \mathcal{I}_m and a subset of data \mathcal{D}_m , assigns the indices to the given data and match them to their sub-carrier position respective to produce a subset of mapped data \mathcal{A}_m :

$$\mathcal{A}_m = \Lambda(\mathcal{I}_m, \mathcal{D}_m), \quad \forall m \in \mathcal{M}, \quad (2.3)$$

with \mathcal{A}_m being the subset of mapped data for the m -th MT. The mapped data subsets for all MTs are obtained as:

$$\begin{aligned} \mathcal{A}_1 &= \Lambda(g_1(1), \mathcal{D}_1), \\ &\vdots \quad \vdots \end{aligned} \quad (2.4)$$

$$\mathcal{A}_m = \Lambda(g_i(m), \mathcal{D}_m), \quad (2.5)$$

$$\vdots \quad \vdots \quad (2.6)$$

$$\mathcal{A}_M = \Lambda(g_i(M), \mathcal{D}_M).$$

The mapped data set \mathcal{A} before the OFDM modulation is given as:

$$\begin{aligned} \mathcal{A} &= \{\mathcal{A}_1, \dots, \mathcal{A}_m, \dots, \mathcal{A}_M\}, \\ \mathcal{A} &= \{a_1, a_2, \dots, a_D\}, \quad \text{with } D = D_1 + D_2 + \dots + D_M. \end{aligned} \quad (2.7)$$

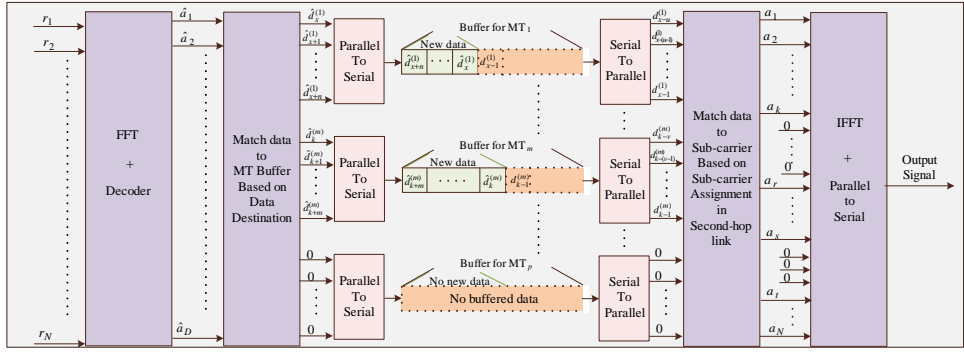


Figure 2.4: Parallel relaying implementation at a WP

The mapped data set is converted to the OFDM symbols X_1, X_2, \dots, X_N , through the means of IFFT. Zeros are inserted to the mapped data set if necessary for IFFT processing. Parallel to serial conversion is carried out. After further processing, the signal is transmitted from the CP to the WPs and MTs.

2.1.5.2 WP Data Demodulation and Modulation

At a WP the received OFDM symbols $\{\hat{r}_1, \hat{r}_2, \dots, \hat{r}_N\}$ are processed using FFT and decoded to recover the estimated mapped data $\hat{\mathcal{A}} = \{\hat{a}_1, \hat{a}_2, \dots, \hat{a}_D\}$. By applying the mapping inverse operation $\Lambda^{-1}(\cdot)$ to the estimated mapped data, the set of data streams of each MT can be recovered as:

$$\begin{aligned} \{\hat{d}_1^{(1)}, \hat{d}_2^{(1)}, \dots, \hat{d}_{D_1}^{(1)}\} &= \Lambda^{-1}(g_i(1), \hat{\mathcal{A}}); \\ &\vdots \quad \vdots \quad \vdots \\ \{\hat{d}_1^{(m)}, \hat{d}_2^{(m)}, \dots, \hat{d}_{D_m}^{(m)}\} &= \Lambda^{-1}(g_i(m), \hat{\mathcal{A}}); \\ &\vdots \quad \vdots \quad \vdots \\ \{\hat{d}_1^{(M)}, \hat{d}_2^{(M)}, \dots, \hat{d}_{D_M}^{(M)}\} &= \Lambda^{-1}(g_i(M), \hat{\mathcal{A}}). \end{aligned} \quad (2.8)$$

During the recovering process any data which was not destined to the WP is discarded. Hence, in Figure 2.4, these data elements are represented by 0. The Figure 2.4 illustrates the data modulation at a WP.

The recovered data of each MT is either buffered or processed for transmission to the MTs. The same data modulation technique used at the CP is applied at the WP to relay the data to the MTs. The only difference is that instead of using the indices of sub-carriers of the direct and first-hop links, a WP uses the indices of sub-carriers assigned in the second hop link for the logical routes going through that WP.

2.1.5.3 MT Data Demodulation

The designated data of an MT can be transmitted from multiple WPs including the CP. Therefore, the data transmission to an MT can be regarded as the

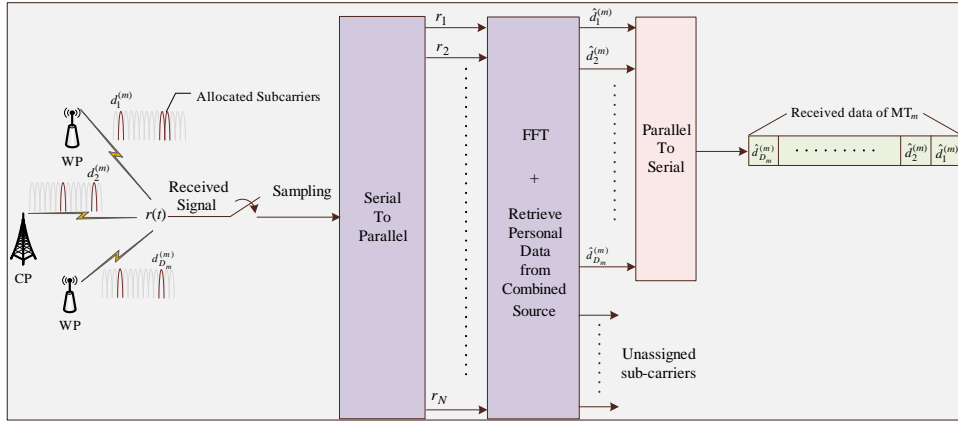


Figure 2.5: Parallel relaying implementation at an MT

uplink of an OFDMA system where multiple MTs are transmitted to a base station using different allocated group of sub-carriers. A brief illustration of data demodulation at an MT is shown in Figure 2.5.

2.2 Single Virtual Cell

The concept of logical route can be used to represent the joint route and sub-carrier allocation in a two-hop network. Using the concept of logical route, parallel relaying transmission can be implemented. We have defined above the different modulation techniques involved in the implementation of parallel relaying transmission. In the following, we formulate the joint route and sub-carrier allocation problem using the concept of logical route in a single VC.

2.2.1 Numerical expressions

Let us consider a single VC with a set \mathcal{R} of R WPs including the CP. The CP is referred to as WP₀ for simplicity. The available bandwidth in the VC is denoted by W . Suppose that a set \mathcal{M} of M MTs are distributed inside the VC. An MT can be connected to one or multiple WPs (CP included) simultaneously for data reception. We say data reception because we assume the downlink transmission. We assume that parallel relaying transmission method is used to transmit data from the CP to an MT.

2.2.1.1 Logical Route SINR

In the absence of interference, the SNR γ of a sub-carrier k at node y when the desired transmitted signal is from node x is given by:

$$\gamma_{x-y}(k) = \frac{P_{x-y}(k)}{N}. \quad (2.9)$$

$P_{x-y}(k)$ is the received signal power at *node y* and N is the noise power spectral. If another device is transmitting using the same sub-carrier, interference from that node is created at *node y*. In the presence of interference, the SINR at *node y* is expressed as:

$$\beta_{x-y}(k) = \frac{P_{x-y}(k)}{N + I_{z-y}(k)}, \quad (2.10)$$

where $I_{z-y}(k)$ represents the interference power from the *interfering device z* to *node y* at the sub-carrier k .

In our study, we consider the received signal power $P_{x-y}(k)$ at *node y* in a sub-carrier k to be modelled as the product of the log-normally distributed shadowing loss δ_{x-y} , the instantaneous channel fading gain $H_{x-y}(k)$, the path-loss $d_{x-y}^{-\alpha}$ between *node x* and *node y*, and the transmit power $P_x(k)$ of *node x* at the sub-carrier k :

$$P_{x-y}(k) = P_x(k) \cdot d_{x-y}^{-\alpha} \cdot 10^{-\delta_{x-y}/10} \cdot |H_{x-y}(k)|^2, \quad (2.11)$$

with d_{x-y} and α being respectively the propagation distance between *node x* and *node y*, and the path-loss exponent. Similarly, as the desired received signal power, the interfering received signal power at *node y*, in the sub-carrier k , when an interfering *node z* is transmitting in that same sub-carrier, is given as:

$$I_{z-y}(k) = P_z(k) \cdot d_{z-y}^{-\alpha} \cdot 10^{-\delta_{z-y}/10} \cdot |H_{z-y}(k)|^2. \quad (2.12)$$

Consider our system of a set \mathcal{R} of R WPs including the CP. We have assumed that a sub-carrier can be reused simultaneously in multiple links. Therefore, there could exist multiple interfering nodes transmitting using the same sub-carrier k inside the VC. In this case, the total interfering signal power at *node y* at the k -th sub-carrier should be expressed as:

$$I_{\text{tot.-}y}(k) = \sum_{\substack{z \in \mathcal{R} \\ z \neq x}} \left(P_z(k) \cdot d_{z-y}^{-\alpha} \cdot 10^{-\delta_{z-y}/10} \cdot |H_{z-y}(k)|^2 \right) \quad (2.13)$$

In a single cell environment, based on Equations (2.10), (2.11), and (2.13), the SINR at a *node y*¹, when the desired transmit signal is from a *node x*² at the k -th sub-carrier, can be expressed as:

$$\begin{aligned} \beta_{x-y}(k) &= \frac{P_{x-y}(k)}{N + I_{\text{tot.-}y}(k)} \\ &= \frac{\frac{P_x(k)}{N} d_{x-y}^{-\alpha} 10^{-\delta_{x-y}/10} |H_{x-y}(k)|^2}{1 + \sum_{\substack{z \in \mathcal{R} \\ z \neq x}} \left(\frac{P_z(k)}{N} d_{z-y}^{-\alpha} 10^{-\delta_{z-y}/10} |H_{z-y}(k)|^2 \right)}. \end{aligned} \quad (2.14)$$

¹Can be a WP or an MT

²Can be a WP or the CP

We consider the e -th logical route $l_e(m, r, k_i, k_j)$ allocated to the m -th MT via the r -th physical route (or WP_r), with k_i and k_j being respectively the sub-carriers allocated in the first-hop and second-hop links. If WP_r is the CP ($r = 0$), the logical route is a direct link logical route ($k_i = k_j$), and the SINR of the logical route can be calculated using Equation (2.14) since there is only one link. However, in the case of a two-hop link logical route, the link with the smaller SINR determines the success or failure of the transmission. Therefore, the SINR of a two-hop link logical route is the minimum of the SINRs of each hop link. Hence, the SINR $\Gamma(l_e(m, r, k_i, k_j))$ of $l_e(m, r, k_i, k_j)$ is given as:

$$\Gamma(l_e(m, r, k_i, k_j)) = \begin{cases} \beta_{WP_0-MT_m}(k_i), & \text{if } r = 0, \text{ or } k_i = k_j; \\ \min(\beta_{WP_0-WP_r}(k_i), \beta_{WP_r-MT_m}(k_j)), & \text{else.} \end{cases} \quad (2.15)$$

2.2.1.2 System Capacity

In Chapter 1, we defined the channel capacity of a channel as:

$$C = \log(1 + \gamma) \quad (2.16)$$

where γ represents the SNR of the channel. In a multi-carrier system of S sub-carriers, in the presence of interference, a sub-carrier k has a capacity C_k [1]:

$$C_k = \frac{1}{S} \log_2(1 + \beta_k) \quad (2.17)$$

where β_k represents the SINR of the sub-carrier k . Hence, the capacity $C(l_e(m, r, k_i, k_j))$ of the e -th logical route $l_e(m, r, k_i, k_j)$ located to the m -th MT via the r -th WP can be expressed as:

$$C(l_e(m, r, k_i, k_j)) = \frac{1}{S} \log_2 \left\{ 1 + \Gamma(l_e(m, r, k_i, k_j)) \right\}. \quad (2.18)$$

Suppose that in the VC a set \mathcal{D}_m of D_m logical routes is allocated to the m -th MT, the channel capacity of that MT is given as:

$$C(\mathcal{D}_m) = \frac{1}{S} \sum_{e=1}^{D_m} \log_2 \left\{ 1 + \Gamma(l_e(m, r, k_i, k_j)) \right\} \quad (2.19)$$

Denote the set Ψ of all allocated logical routes in the VC as :

$$\Psi = \{\mathcal{D}_1, \mathcal{D}_2, \dots, \mathcal{D}_M\}. \quad (2.20)$$

The total channel capacity of the system is given as:

$$C(\Psi) = \frac{1}{S} \sum_{m=1}^M \sum_{e=1}^{D_m} \log_2 \left\{ 1 + \Gamma(l_e(m, r, k_i, k_j)) \right\}. \quad (2.21)$$

2.2.2 Sub-Carrier Reuse

To increase the number of logical route candidates per WP and consequently maximize the number of two-hop link logical routes that can be allocated in the VC, we assume that a sub-carrier can be assigned simultaneously in multiple links. In the absence of this intra-cell sub-carrier reuse, the maximum number of two-hop link logical routes, which can be assigned in a VC, does not exceed half of the number of sub-carriers in that VC, $\sum_{1 \leq m \leq M} D_m \leq S/2$. By allowing a sub-carrier to be reused concurrently in multiple links, we can increase the number of logical routes which can be allocated to $\sum_{1 \leq m \leq M} D_m \leq S$. To allow a sub-carrier to be reused simultaneously in multiple links, certain constraints have to be applied:

1. A WP cannot use the same sub-carrier to transmit and receive simultaneously in a timeframe.
2. Multiple WPs cannot use the same sub-carrier to transmit concurrently to an MT, and neither can the CP reuse the same sub-carrier to transmit to multiple WPs in the same timeframe.
3. If the above constraints are respected, a sub-carrier allocated in a first-hop link in a logical route can be reassigned simultaneously in a second-hop link in an other logical route and vice versa.
4. With respect to the first two constraints, a sub-carrier assigned to an MT in a second-hop link can be reused concurrently to transmit data to another MT in a second-hop link.
5. The number of allocated logical routes in a VC cannot exceed the number of sub-carriers available in that VC.

2.2.3 Single Cell Logical Route Allocation Problem

Given a set \mathcal{M} of WPs including the CP, a set \mathcal{M} of MTs, and a set \mathcal{S} of subcarriers in the VC, the objective is to find the optimal solution candidate that will maximize the total channel capacity of the VC with the sub-carrier reuse constraints defined previously. Hence, the logical route allocation problem in a single VC is formulated as:

$$\arg \max_{\Psi = \{\mathcal{D}_1, \mathcal{D}_2, \dots, \mathcal{D}_M\}} = \frac{1}{S} \sum_{m=1}^M \sum_{e=1}^{D_m} \log_2 \left\{ 1 + \Gamma(l_e(m, r, k_i, k_j)) \right\}, \quad \text{subject to: } (2.22)$$

1. A WP cannot use the same sub-carrier to transmit and receive simultaneously in a timeframe:

$$\begin{aligned} & \forall l_e(m, r, k_i, k_j) \in \Psi, \quad \forall l_{e'}(m', r', k_{i'}, k_{j'}) \in \Psi, \\ & \begin{cases} k_i = k_j \Leftrightarrow r = 0; \\ k_i \neq k_j \Leftrightarrow r \neq 0; \end{cases} \quad \text{and} \quad \begin{cases} k_i = k_{j'} \Rightarrow r \neq r'; \\ k_{i'} = k_j \Rightarrow r \neq r'. \end{cases} \end{aligned} \quad (2.23)$$

2. Multiple WPs cannot use the same sub-carrier to transmit concurrently to an MT, neither can the CP reuse the same sub-carrier to transmit to multiple WPs in the same timeframe:

$$\begin{aligned} \forall l_e(m, r, k_i, k_j) \in \Psi, \quad \forall l_{e'}(m', r', k_{i'}, k_{j'}) \in \Psi, \\ \begin{cases} k_i = k_{i'} \Rightarrow l_e = l_{e'}; \\ k_j = k_{j'} \Rightarrow m \neq m' \text{ and } r \neq r'. \end{cases} \end{aligned} \quad (2.24)$$

3. A sub-carrier allocated in a first-hop link in a logical route can be re-assigned simultaneously in a second-hop link in an other logical route, and vice versa. Denoting Ω the problem space containing the set of solution candidates in the VC, $\Omega = \{\Psi : \Psi \text{ is a solution candidate}\}$:

$$\begin{aligned} \exists \Psi' \in \Omega \quad \text{so that} : l_e(m, r, k_i, k_j) \in \Psi \text{ and } l_{e'}(m', r', k_{i'}, k_{j'}) \in \Psi', \\ \text{with } k_i = k_{j'} \text{ or } k_{i'} = k_j, \text{ and } r \neq r'. \end{aligned} \quad (2.25)$$

4. A sub-carrier assigned to an MT in a second-hop link can be reused concurrently to transmit data to another MT in a second-hop link:

$$\begin{aligned} \exists \Psi' \in \Omega \quad \text{so that} : l_e(m, r, k_i, k_j) \in \Psi \text{ and } l_{e'}(m', r', k_{i'}, k_{j'}) \in \Psi', \\ \text{with } k_j = k_{j'}, m \neq m', \text{ and } r \neq r'. \end{aligned} \quad (2.26)$$

5. The number of allocated logical routes ψ in a VC cannot exceed the number of sub-carriers available in that VC:

$$\psi = \sum_{m=1}^M D_m \leq S. \quad (2.27)$$

2.3 Multi-Cell Environment

Multiple cells form a mobile cellular network. The reuse of the same frequency in group of these cells produces inter-cell interference which can degrade the channel capacity of the system. Therefore, for practical purposes, it is a must to include the effect of inter-cell interference in the performance analysis of a wireless system. In this section, we derive the mathematical expressions of the logical route allocation problem while taking into account inter-cell interference in the system.

2.3.1 Numerical expressions

Consider the downlink transmission in a system with a set \mathcal{V} of V VCs. In the v -th VC (VC_v), a set \mathcal{R}_v of R_v WPs and a CP establish the data transmission between the core network and a set \mathcal{M}_v of M_v MTs. The available bandwidth of the v -th VC is divided into a set \mathcal{S}_v of S_v sub-carriers. To study the worst case scenario, we consider that all VCs operate on the same bandwidth. The WPs and CP are assumed to be able to transmit concurrently in the same timeframe using different sub-carriers in the first-hop and second-hop links. Data transmission from the CP to an MT is enabled using the parallel relaying transmission method.

2.3.1.1 Logical Route SINR

In Equation (2.13), we derived the total interference at a node in a single VC. Equation (2.13) only takes into account intra-cell interference added by the reuse of sub-carriers inside a VC. In a multi-cell environment, interference occurs from neighbouring communications in other VCs using the same sub-carrier. Suppose that *node* x located in VC_v is transmitting to *node* y also located in the same VC. The total interfering received signal power at the k -th sub-carrier at a *node* y is given by:

$$I_{\text{tot.}-y}(k) = \sum_{u \in \mathcal{V}} \sum_{\substack{z \in \mathcal{R}_u \\ (z,u) \neq (x,v)}} \left(P_{z,u}(k) \cdot d_{z-y}^{-\alpha} \cdot 10^{-\delta_{z-y}/10} \cdot |H_{z-y}(k)|^2 \right), \quad (2.28)$$

where $P_{z,u}(k)$, d_{z-y} , δ_{z-y} , and $H_{z-y}(k)$ denote respectively the transmit power of the interfering *node* z located in the u -th VC, the distance, the log-normally distributed shadowing loss, and the instantaneous channel fading gain between *node* y and *node* z . This total interference in Equation (2.28) include not only intra-cell interference in VC_v but also inter-cell interference from communications in other VCs.

In a multi-cell environment, the SINR at *node* y located in the v -th VC for

a desired transmit signal from *node x* at the k -th sub-carrier is expressed as:

$$\begin{aligned}\beta_{x-y}(k) &= \frac{P_{x-y}(k)}{N + I_{\text{tot.}-y}(k)} \\ &= \frac{\frac{P_{x,v}(k)}{N} d_{x-y}^{-\alpha} 10^{-\delta_{x-y}/10} |H_{x-y}(k)|^2}{1 + \sum_{\substack{u \in \mathcal{V} \\ (z,u) \neq (x,v)}} \sum_{z \in \mathcal{R}_u} \left(\frac{P_{z,u}(k)}{N} \cdot d_{z-y}^{-\alpha} \cdot 10^{-\delta_{z-y}/10} \cdot |H_{z-y}(k)|^2 \right)}.\end{aligned}\quad (2.29)$$

$P_{x,v}(k)$, and $P_{z,u}(k)$ represent respectively the transmit power at the k -th sub-carrier of *node x* located in VC_v and *node z* located in VC_u .

We denote $l_e(v, m, r, k_i, k_j)$ the e -th logical route allocated to the m -th MT ($\text{MT}_{m,v}$) via the r -th WP ($\text{WP}_{r,v}$) in the v -th VC, with k_i and k_j being the sub-carriers assigned in the first-hop and second-hop links respectively. Similarly as in Equation (2.15), the SINR of $l_e(v, m, r, k_i, k_j)$ is given as:

$$\Gamma(l_e(v, m, r, k_i, k_j)) = \begin{cases} \beta_{\text{WP}_{0,v}-\text{MT}_{m,v}}(k_i), & \text{if } r = 0, \text{ or } k_i = k_j; \\ \min(\beta_{\text{WP}_{0,v}-\text{WP}_{r,v}}(k_i), \beta_{\text{WP}_{r,v}-\text{MT}_{m,v}}(k_j)), & \text{else.} \end{cases}\quad (2.30)$$

2.3.1.2 System Channel Capacity

In a multi-cell environment, the channel capacity of the e -th logical route allocated to the $\text{MT}_{m,v}$ via $\text{WP}_{r,v}$ is given by:

$$C(l_e(v, m, r, k_i, k_j)) = \frac{1}{S_v} \log_2 \left\{ 1 + \Gamma(l_e(v, m, r, k_i, k_j)) \right\}.\quad (2.31)$$

Let $\mathcal{D}_{m,v}$ be the set of $D_{m,v}$ logical routes allocated to $\text{MT}_{m,v}$ in the v -th VC, the channel capacity $C_{m,v}$ of $\text{MT}_{m,v}$ can be calculated as:

$$C_{m,v}(\mathcal{D}_{m,v}) = \frac{1}{S_v} \sum_{e=1}^{D_{m,v}} \log_2 \left\{ 1 + \Gamma(l_e(v, m, r, k_i, k_j)) \right\}.\quad (2.32)$$

We designate by Ψ_v the set of ψ_v logical routes allocated to all M_v MTs in that VC:

$$\Psi_v = \{\mathcal{D}_{1,v}, \mathcal{D}_{2,v}, \dots, \mathcal{D}_{M_v,v}\}.\quad (2.33)$$

The total channel capacity $C(\Psi_v)$ of VC_v is the summation of the capacity of all logical routes allocated to all MTs in that VC and it is evaluated as:

$$C(\Psi_v) = \frac{1}{S_v} \sum_{m=1}^{M_v} \sum_{e=1}^{D_{m,v}} \log_2 \left\{ 1 + \Gamma(l_e(v, m, r, k_i, k_j)) \right\}.\quad (2.34)$$

2.3.2 Multi-Cell Logical Route Allocation Problem

The same sub-carrier reuse constraints described previously for a single VC is applied to each VC in the multi-cell environment. Furthermore, we assume that all VCs operate on the same bandwidth. We formulate logical route allocation problem in a multi-cell environment as follow: given a set \mathcal{R}_v of R_v WPs, a set \mathcal{M}_v of M_v MTs, and a set \mathcal{S}_v of S_v sub-carriers in the v -th VC, while taking into account the sub-carrier reuse constraints in the VC we aim at finding the optimal solution candidate Ψ_v^* of logical routes which maximizes the total channel capacity of that VC:

$$\arg \max_{\Psi_v = \{\mathcal{D}_{1,v}, \mathcal{D}_{2,v}, \dots, \mathcal{D}_{M_v,v}\}} = \frac{1}{S_v} \sum_{m=1}^{M_v} \sum_{e=1}^{D_{m,v}} \log_2 \left\{ 1 + \Gamma(l_e(v, m, r, k_i, k_j)) \right\}, \quad \text{Subject to:} \quad (2.35)$$

1. In a VC, a WP cannot use the same sub-carrier to transmit and receive simultaneously in the same timeframe:

$$\begin{aligned} & \forall l_e(v, m, r, k_i, k_j) \in \Psi_v, \quad \forall l_{e'}(v, m', r', k_{i'}, k_{j'}) \in \Psi_v, \\ & \begin{cases} k_i = k_j \Leftrightarrow r = 0; \\ k_i \neq k_j \Leftrightarrow r \neq 0; \end{cases} \quad \text{and} \quad \begin{cases} k_i = k_{j'} \Rightarrow r \neq r'; \\ k_{i'} = k_j \Rightarrow r \neq r'. \end{cases} \end{aligned} \quad (2.36)$$

2. In a VC, multiple WPs cannot transmit concurrently on the same sub-carrier to an MT, neither can the CP reuse the same sub-carrier to transmit to multiple WPs in the same timeframe:

$$\begin{aligned} & \forall l_e(v, m, r, k_i, k_j) \in \Psi_v, \quad \forall l_{e'}(v, m', r', k_{i'}, k_{j'}) \in \Psi_v, \\ & \begin{cases} k_i = k_{i'} \Rightarrow l_e = l_{e'}; \\ k_j = k_{j'} \Rightarrow m \neq m', \text{ and } r \neq r'. \end{cases} \end{aligned} \quad (2.37)$$

3. A sub-carrier allocated in a first-hop link in a logical route can be reassigned simultaneously in a second-hop link in an other logical route, and vice versa inside a VC. Denoting Ω_v the problem space containing the set of solution candidates in the v -th VC, $\Omega_v = \{\Psi_v : \Psi_v \text{ is a solution candidate}\}$,

$$\exists \Psi'_v \in \Omega_v \quad \text{so that: } l_e(v, m, r, k_i, k_j) \in \Psi_v \text{ and } l_{e'}(v, m', r', k_{i'}, k_{j'}) \in \Psi'_v, \quad \text{with } k_i = k_{j'} \text{ or } k_{i'} = k_j, \text{ and } r \neq r'. \quad (2.38)$$

4. A sub-carrier assigned to an MT in a second-hop link can be reused concurrently to transmit data to another MT in a second-hop link inside a VC:

$$\exists \Psi'_v \in \Omega_v \quad \text{so that: } l_e(v, m, r, k_i, k_j) \in \Psi_v \text{ and } l_{e'}(v, m', r', k_{i'}, k_{j'}) \in \Psi'_v, \quad \text{with } k_j = k_{j'}, m \neq m', \text{ and } r \neq r'. \quad (2.39)$$

5. The number of allocated logical routes ψ_v in a VC cannot exceed the number of sub-carriers available in that VC:

$$\forall v \in \mathcal{V}, \quad \psi_v = \sum_{m=1}^{M_v} D_{m,v} \leq S_v. \quad (2.40)$$

2.4 Resource Allocation Problem Complexity

Using the parallel relaying transmission method, we have modelled the joint route and sub-carrier allocation problem into a logical route allocation problem. With the sub-carrier constraints defined above, the logical route allocation problems in a single cell and multi-cell environments formulated in Equation (2.22) and in Equation (2.22) are NP-hard optimization problems and cannot be solved by conventional allocation algorithms found in the literature. Their optimal solutions would require an exhaustive search.

In a VC, as the number of MTs increases, the number of logical route candidates to evaluate increases considerably. The optimal allocation scheme which requires exhaustive search implements the simultaneous allocation of the logical routes. The implementation of simultaneous allocation of the logical routes becomes extremely complex in a multi-user and multi-cell environment. If D logical routes have to be allocated to a single MT, the number of combinations \mathfrak{D} that will be evaluated without applying sub-carrier reuse in the simultaneous allocation scheme is given by this formula:

$$\mathfrak{D} = \sum_{i=0}^D \frac{R^{D-i} \cdot S!}{(S - 2D + i)! (D - i)! i!}. \quad (2.41)$$

S and R represents respectively the number of sub-carriers and WPs in a single cell. With sub-carrier reuse applied in a multi-user environment, the number of combinations that will be evaluated increases exponentially. Figure 2.4 shows the number of combinations to evaluate in the simultaneous allocation scheme to allocate $S/2$ logical routes to a single user.

Taking into account the complexity of the exhaustive allocation scheme, our objective is to propose resource allocation schemes that can approximate the optimal solution while taking practicality into consideration.

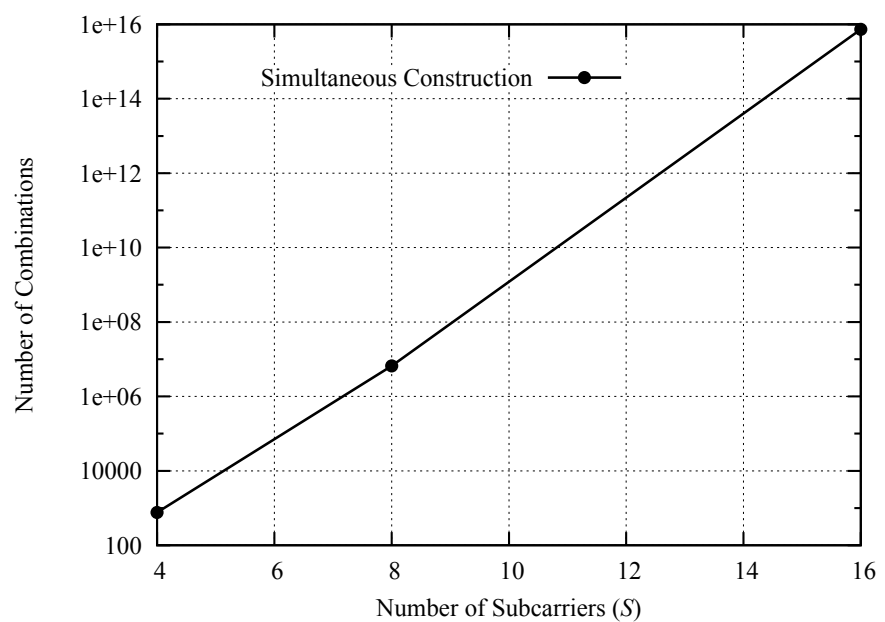


Figure 2.6: Number of combinations to evaluate in the exhaustive search

CHAPTER 3

Successive Allocation Scheme

In Chapter 2, we formulated the joint route and sub-carrier allocation problem in a two-hop network as a logical route allocation problem. The optimal solution of the logical route allocation problem requires an exhaustive search with high computational complexity and might not be applicable in a practical system. To reduce computational complexity, in this chapter, we propose a successive allocation scheme (SAS). We study the performance of the successive scheme in a single cell and in a multi-cell environment.

3.1 Single Cell Network

We consider a single VC, a set \mathcal{M} of M MTs and a set \mathcal{R} of R WPs (CP included). We denote by MT_m the m -th MT and by WP_r the r -th WP, with WP_0 being the CP, in the VC. The bandwidth of the VC is divided into a set \mathcal{S} of S sub-carriers. Parallel relaying transmission is used to transmit data to an MT. We assume that a sub-carrier can be reused simultaneously in multiple links based on the sub-carriers constraints defined in Section 2.2.2 on page 43.

For the m -th MT, we denote the e -th logical route candidate constructed via the r -th WP as $l_e^*(m, r, k_i, k_j)$, k_i and k_j being respectively the sub-carriers assigned in the first-hop and second-hop links. We denote $\mathcal{L}_{m,r}^*$ the set of logical route candidates of the m -th MT via the r -th WP, and by $\mathfrak{L}_{m,r}^* = (l_{ij})$ the matrix associated with $\mathcal{L}_{m,r}^*$,

$$\mathfrak{L}_{m,r}^* = (l_{ij}), \quad 1 \leq i, j \leq S, \quad (3.0a)$$

$$l_{i,j} = \begin{cases} 0 & \text{if } l_e^*(m, r, k_i, k_j) \text{ is available for allocation,} \\ 1 & \text{else.} \end{cases} \quad (3.0b)$$

The elements l_{ij} of the matrix $\mathfrak{L}_{m,r}^*$ take on values 0 or 1 indicating whether or not the logical route using the sub-carrier k_i and k_j in the set of logical route candidates $\mathcal{L}_{m,r}^*$ is available or not for allocation. The row index i and the column index j of the matrix $\mathfrak{L}_{m,r}^*$ represent respectively the sub-carrier index assigned in the first-hop and second-hop links of the logical route candidate $l_e^*(m, r, k_i, k_j)$.

At the initial state, before logical route allocation, taking into account that a single sub-carrier is necessary for logical route belonging to the direct route,

the allocation matrix candidate of the m -th MT via the WP_0 is a square matrix of dimension $S \times S$ with 0 as diagonal elements and 1 as non-diagonal elements:

$$\mathfrak{L}_{m,0}^* = \begin{pmatrix} l_{1,1} & \dots & l_{1,j} & \dots & l_{1,S} \\ \vdots & \ddots & \vdots & \vdots & \vdots \\ l_{i,1} & \dots & l_{i,j} & \dots & l_{i,S} \\ \vdots & \vdots & \vdots & \ddots & \vdots \\ l_{S,1} & \dots & l_{S,j} & \dots & l_{S,S} \end{pmatrix} = \begin{pmatrix} 0 & \dots & 1 & \dots & 1 \\ \vdots & \ddots & \vdots & \vdots & \vdots \\ 1 & \dots & 0 & \dots & 1 \\ \vdots & \vdots & \vdots & \ddots & \vdots \\ 1 & \dots & 1 & \dots & 0 \end{pmatrix}$$

For all WPs different from the CP, two sub-carriers are necessary to construct a logical route. According to the first sub-carrier reuse constraint in Chapter 2, a WP cannot receive and transmit simultaneously in the same sub-carrier. Therefore at the initial state, the allocation matrix candidate $\mathfrak{L}_{m,r}^*$ of the m -th MT via the r -th WP with $r \neq 0$ is constructed as:

$$\mathfrak{L}_{m,r}^* = \begin{pmatrix} l_{1,1} & \dots & l_{1,j} & \dots & l_{1,S} \\ \vdots & \ddots & \vdots & \vdots & \vdots \\ l_{i,1} & \dots & l_{i,j} & \dots & l_{i,S} \\ \vdots & \vdots & \vdots & \ddots & \vdots \\ l_{S,1} & \dots & l_{S,j} & \dots & l_{S,S} \end{pmatrix} = \begin{pmatrix} 1 & \dots & 0 & \dots & 0 \\ \vdots & \ddots & \vdots & \vdots & \vdots \\ 0 & \dots & 1 & \dots & 0 \\ \vdots & \vdots & \vdots & \ddots & \vdots \\ 0 & \dots & 0 & \dots & 1 \end{pmatrix}$$

3.1.1 Sub-Carrier Reuse Constraints Implementation

The first sub-carrier reuse constraint states that a WP cannot transmit and receive simultaneously using the same sub-carrier. In order to implement this constraint, we suppose that $l_e(m, r, k_i, k_j)$ is the e -th logical route allocated to the m -th MT via r -th WP with $r \neq 0$. The sub-carrier indices used in the first-hop and second-hop links being i and j respectively, the first sub-carrier constraint is implemented by modifying the allocation matrix candidate of all MTs for that WP as follow:

If $l_e(m, r, k_i, k_j)$ is allocated :

$$\begin{cases} \forall u \in \mathcal{M}, \quad \forall l_{i,t} \in \mathfrak{L}_{u,r}^*, \quad l_{i,t} = 1, \quad 1 \leq t \leq S; \\ \forall u \in \mathcal{M}, \quad \forall l_{j,t} \in \mathfrak{L}_{u,r}^*, \quad l_{j,t} = 1, \quad 1 \leq t \leq S; \\ \forall u \in \mathcal{M}, \quad \forall l_{t,i} \in \mathfrak{L}_{u,r}^*, \quad l_{t,i} = 1, \quad 1 \leq t \leq S; \\ \forall u \in \mathcal{M}, \quad \forall l_{t,j} \in \mathfrak{L}_{u,r}^*, \quad l_{t,j} = 1, \quad 1 \leq t \leq S. \end{cases} \quad (3.1)$$

The second sub-carrier reuse constraint prevents multiple WPs to transmit concurrently on the same sub-carrier to an MT, or the CP to reuse the same sub-carrier to transmit to multiple WPs in the same timeframe. Let us consider again that $l_e(m, r, k_i, k_j)$ is allocated to the m -th MT via r -th WP with $r \neq 0$. The sub-carrier of index j is allocated in the second-hop link and therefore

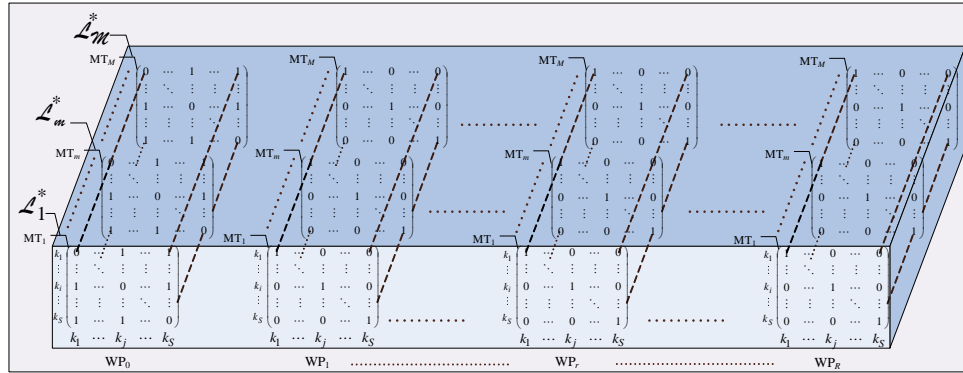


Figure 3.1: Initial allocation matrices

cannot be reused by any WP to transmit to MT_m . This constraint is implemented as follows:

If $l_e(m, r, k_i, k_j)$ is allocated :

$$\forall w \in \mathcal{R}, \quad \forall l_{t,j} \in \mathcal{L}_{m,w}^*, \quad l_{t,j} = 1, \quad 1 \leq t \leq S. \quad (3.2)$$

In the first-hop link, the sub-carrier of index i is allocated. Hence, the CP cannot reuse it to transmit to any other WP, nor to transmit directly to any MT. This constraint is implemented as follows:

If $l_e(m, r, k_i, k_j)$ is allocated :

$$\forall u \in \mathcal{M}, \quad \forall w \in \mathcal{R}, \quad \forall l_{i,t} \in \mathcal{L}_{u,w}^*, \quad l_{i,t} = 1, \quad 1 \leq t \leq S. \quad (3.3)$$

By modifying the allocation matrix candidates for all MTs after each logical route allocation, the third and fourth sub-carrier reuse constraints can be applied. The fifth sub-carrier reuse constraint is a trivial consequence of the second sub-carrier reuse constraint because the number of logical routes which can be allocated is limited by the number of sub-carriers available for first-hop transmission and direct link transmission.

3.1.2 Single Cell Successive Allocation Scheme

Suppose that a set \mathcal{D}_m of D_m logical routes are to be allocated to the m -th MT. We define a solution candidate $\Psi = \{\mathcal{D}_1, \mathcal{D}_2, \dots, \mathcal{D}_m, \dots, \mathcal{D}_M\}$ as the set of allocated logical route to all MTs. In the SAS, these subsets of logical routes $\mathcal{D}_1, \mathcal{D}_2$, and \mathcal{D}_m are allocated successively. First, the first best set \mathcal{D}_1 of logical routes which maximizes the total channel capacity of the VC is allocated to MT_1 . Second, the best set \mathcal{D}_2 which maximizes the total channel capacity with respect to intra-cell interference is allocated to MT_2 . The process continues until a set \mathcal{D}_M of logical routes is allocated to the last MT.

Let us denote by $\mathcal{L}_m^* = \{\mathcal{L}_{m,0}^*, \mathcal{L}_{m,1}^*, \dots, \mathcal{L}_{m,R}^*\}$ the set of all logical route candidates of the m -th MT. In Figure 3.1, we illustrate the initial allocation

matrix candidates $(\mathcal{L}_1^*, \mathcal{L}_2^*, \dots, \mathcal{L}_M^*)$ for all MTs. Figure 3.1 shows the initial allocation matrices for all MTs. We note the temporary set of logical routes allocated to the m -th MT as \mathcal{L}_m . Suppose that logical route allocation has been completed for $m - 1$ MTs, the allocation of a set \mathcal{D}_m of logical routes to the m -th MT is carried out as follows in **Algorithm 1** on page 55.

In this scheme, we suppose that the CP can obtain the channel state information (CSI) of all links in the VC. This allocation algorithm will be implemented at the CP. Therefore, this allocation scheme is a centralized allocation scheme. Once the best logical route allocation has been determined, the CP will inform the WPs and the MTs about the respective routes and sub-carriers allocation.

3.1.3 Successive Allocation Scheme Complexity

In Figure 2.4 on page 49 we plotted the number of combinations that should be evaluated to allocate $S/2$ logical routes to a single MT in a system with R WPs and S sub-carriers when simultaneous construction are used to allocate the logical routes. In the SAS, by applying sub-carrier reuse, the maximum number of allocated logical routes can be increased up to S logical routes. In the SAS, the maximum number of combinations $\mathfrak{O}_{D_K}^{\max}$ to evaluate to allocate D_K logical routes to K MTs can be reduced to:

$$\mathfrak{O}_{D_K}^{\max} = \sum_{i=0}^{D_K-1} \{(S-i) + (S-1)(S-i)R\} \quad (3.4)$$

with

$$D_K = \sum_{m=1}^{K \leq M} D_m \leq S. \quad (3.5)$$

In Figure 3.2, we plot the maximum number of combinations to evaluate with sub-carrier reuse applied in the case of SAS compared with that of the exhaustive allocation scheme. Figure 3.2 was obtained for a system with $R = 7$ WPs, and $K = M = 1$ MT. The number of allocated logical routes was considered to be the same as the number of subcarriers in the case of the SAS ($D_1 = S$), and half that of the number of subcarriers without subcarrier reuse for the exhaustive allocation scheme ($D_1 = S/2$). It can be noted that successively allocating logical routes can drastically reduce the number of combinations to be evaluated.

3.1.4 Simulation Assumptions and System Model

We use the Monte Carlo simulation method to evaluate the channel capacity when applying SAS. For convenience, we consider the VC to be of a hexagonal shape with the WPs equally distanced of a distance d from a CP placed at the center of a single VC. Figure 3.3 presents the cell layout used. In Figure 3.3, d_0 represents the radius of the VC. The MTs are randomly located in the VC. This simulation is carried out for a single VC.

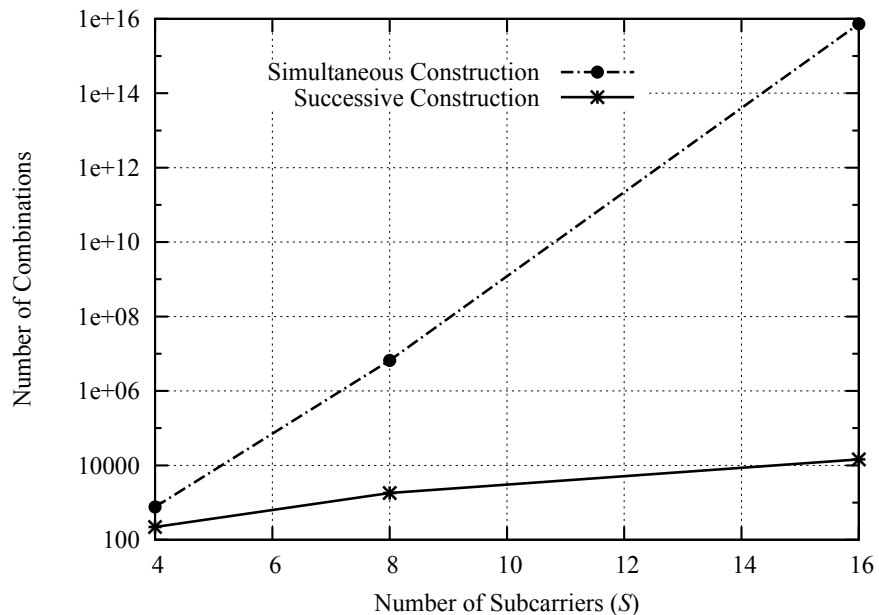


Figure 3.2: Number of combinations for SAS and optimal scheme

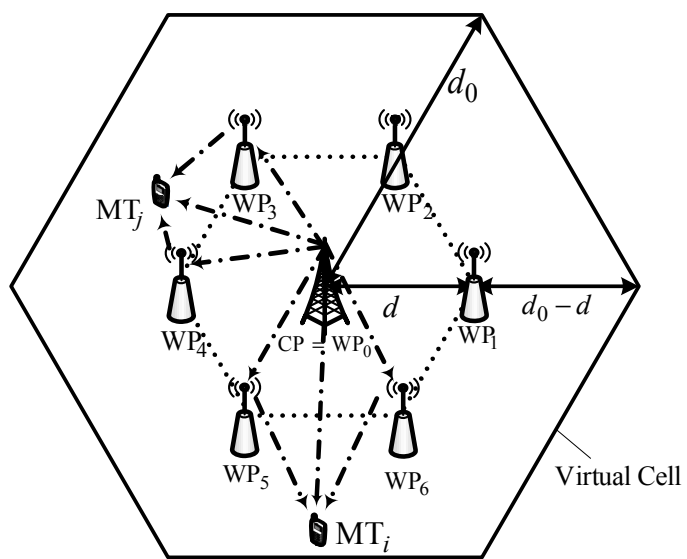


Figure 3.3: Virtual cell layout

Algorithm 1: Single Cell Successive Allocation Scheme

Input: \mathcal{M} , \mathcal{R} , \mathcal{S} , \mathcal{L}_p^* and \mathcal{D}_p , $\forall p < m$.
Output: Allocate D_m logical routes to MT_m

```

begin
    step 1   /* Initialization of logical route candidates */
    Initialize  $\mathcal{L}_m^*$  and  $\mathfrak{L}_{m,w}^*$   $\forall w \in \mathcal{R}$  based on constraints (3.1)– (3.3);
    /* Successive allocation of logical routes */
    step 2   repeat
        foreach  $l_e^*(m, r, k_i, k_j) \in \mathcal{L}_m^*$  do
            foreach  $p \in \mathcal{M}, p \leq m$  do
                foreach  $l_h(p, r', k_{i'}, k_{j'}) \in \mathcal{D}_p$  do
                    | Execute the Procedure InterferenceSinceCell;
                end
                /* Recalculate SINR and capacity */
                Evaluate  $\Gamma(l_e^*(m, r, k_i, k_j))$  using Equation (2.15) on
                page 42;
                Evaluate  $\Gamma(l'_h(p, r', k_{i'}, k_{j'}))$  using Equation (2.15) on
                page 42;
                Recalculate  $C_p(\mathcal{D}_p)$  using Equation (2.19) on page 42;
            end
            Update  $\mathcal{L}_m \leftarrow l_e^*(m, r, k_i, k_j)$ ;
            Evaluate  $C_m(\mathcal{L}_m)$  using Equation (2.19) on page 42;
        end
        /* Choose best logical route candidate */
        Choose  $l_e^*(m, r, k_i, k_j)$  according to Equation (2.22) on page 43;
        Add  $l_e^*(m, r, k_i, k_j)$  to  $\mathcal{D}_m$ ;
        /* Update the set of logical route candidates */
        Modify  $\mathfrak{L}_{m,w}^*$ ,  $\forall w \in \mathcal{R}$ , and update  $\mathcal{L}_m^*$  based on
        Equations (3.1)– (3.3);
    until  $D_m$  logical routes are allocated to  $MT_m$ ;
end

```

Procedure InterferenceSinceCell

Input: $l_e^*(m, r, k_i, k_j)$, and $l_h(p, r', k_{i'}, k_{j'})$

Output: $l_e^*(m, r, k_i, k_j)$, and $l_h(p, r', k_{i'}, k_{j'})$ with interference

begin

/* Evaluate interference from existing communications */

if ($k_i = k_{i'}$ or $k_i = k_{j'}$) and $k_i = k_j$ **then**

| Evaluate $\beta_{WP_0-MT_m}(k_i)$ using Equation (2.14) on page 41;

end

if ($k_i = k_{i'}$ or $k_i = k_{j'}$), and $k_i \neq k_j$ **then**

| Evaluate $\beta_{WP_0-WP_r}(k_i)$ using Equation (2.14) on page 41;

end

if ($k_j = k_{i'}$ or $k_j = k_{j'}$), and $k_i \neq k_j$ **then**

| Evaluate $\beta_{WP_r-MT_m}(k_j)$ using Equation (2.14) on page 41;

end

/* Evaluate interference to existing communications */

if ($k_{i'} = k_i$ or $k_{i'} = k_{j'}$), and $k_{i'} = k_{j'}$ **then**

| Evaluate $\beta_{WP_0-MT_p}(k_{i'})$ using Equation (2.14) on page 41;

end

if ($k_{i'} = k_i$ or $k_{i'} = k_{j'}$), and $k_{i'} \neq k_{j'}$ **then**

| Evaluate $\beta_{WP_0-WP_{r'}}(k_{i'})$ using Equation (2.14) on page 41;

end

if ($k_{j'} = k_i$ or $k_{j'} = k_{j'}$), and $k_{i'} \neq k_{j'}$ **then**

| Evaluate $\beta_{WP_{r'}-MT_p}(k_{j'})$ using Equation (2.14) on page 41;

end

end

We denote by P_t the total transmit power in the VC. P_0 represents the average transmit power of the CP for which the received SNR at d_0 is 0dB, i.e:

$$\frac{P_0 d_0^{-\alpha}}{SN} = 1. \quad (3.6)$$

N and S represent the noise power per subcarrier and the number of subcarriers in the VC. It is assumed that the noise power spectral is the same for all sub-carriers. We define the normalized transmission power as $P_n = P_t/P_0$. The transmission power of a WP depends on the number of allocated logical routes from this WP. A WP which is not transmitting is considered to be in off mode. The total transmit power of the VC is uniformly distributed among the allocated logical routes. We suppose that each link of a two-hop logical route uniformly shares the allocated power for this logical route.

We consider a multipath frequency selective fading channel with $L = 8$ propagation paths. The paths are considered to be independently Rayleigh distributed with uniformly distributed average power delay profile and equidistant delays. The delay between two consecutive paths is considered to be equal to the inverse of the sub-carrier spacing during the FFT process.

We consider a path-loss exponent $\alpha = 4$, a standard deviation of the log-normally distributed shadowing loss $\delta = 8$ dB.

The performance of SAS is compared with that of the conventional SHN. The same assumptions regarding power allocation and MT locations in the two-hop VCN (VCN) is considered for the SHN.

3.1.5 Simulation Performance

Firstly, we consider that $M = 2$ MTs are randomly located in the VC. The bandwidth of the VC is divided into $S = 8$ sub-carriers. $D_m = 4$ logical routes are allocated per MT. Since we allow sub-carrier reuse, the number of logical routes that can be allocated in the VCN can be equal to the number of subcarriers in the VC. In the SHN, we allocated the first best sub-carriers to the first MT, and the remaining ones to the second MT.

In Figure 3.4, we plot the ergodic channel capacity of the two-hop VCN for the distance ratio $d/d_0 = 0.4$, $d/d_0 = 0.6$, and $d/d_0 = 0.8$, respectively. We notice that the channel capacity of the two-hop VCN outperforms that of the SHN for low transmission power. For instance, for the distance ratio $d/d_0 = 0.4$, the channel capacity of the two-hop VCN exceeds that of the SHN by more than 35% for a normalized transmission power $P_n = 0$ dB. This is because multihop networks can provide better channel capacity than SHN for low transmission power by reducing the transmitting distance between the end-MT and the transmitting station.

Considering Figure 3.4, we also observe that as the distance ratio increases the channel capacity of the VCN approaches that of the SHN. This is because the more the WPs are distanced from the CP, the more the VCN tends to act like a SHN as illustrated in Figure 3.5 and Figure 3.6. In Figure 3.5 and 3.6,

we plot the usage of each WP, for different values of the distance ratio, for a single MT randomly located. We notice that as the distance ratio increases, most of the chosen logical routes are from the CP which represents the base station for a SHN.

Figure 3.7 represents the plot of the ergodic channel capacity of the VCN for different values of the normalized transmission power, taking the distance ratio d/d_0 as a parameter. It is observed that, for low transmission power, the optimal distance ratio for the location of the WPs can be found in the interval $0.2 \sim 0.4$.

To study the performance of the system as the number of MTs increases, we evaluate the ergodic channel capacity of the two-hop VCN for $S = 32$ sub-carriers and when the number of allocated logical routes per MT is $D_m = 2$.

In Figure 3.8, we plot the ergodic channel capacity of the VCN compared with that of the SHN for different values of the normalized transmission power P_t/P_0 . We observe that, for low transmission power, even if the system is fully loaded to 16 MTs with 2 logical routes per MT, the channel capacity of the VCN remains better than that of the SHN. In case of low transmission power, the noise power level has a greater influence on the channel capacity of a wireless network than the interference power level. That is why low transmission power region is generally referred as the noise dominant transmission power region. In the noise dominant transmission power region, the VCN can provide a better channel capacity than the SHN by shortening the transmission distance between the transmitting stations and the MTs. If the interference dominant transmission power region is considered, it is expected that SHN will provide better channel capacity than the VCN because SHN does not suffer interference between the MTs. We also remark that when the normalized transmission power is $P_t/P_0 = 0\text{dB}$, increasing the number of MTs from 14 to 16 causes the channel capacity of the VCN to decrease. This can be explained by the augmentation of the level of interference between the MTs as the number of MTs increases.

In any network, as the number of users increases, fairness between users should be evaluated. To study the degree of fairness of the VCN, we consider the same system with $S = 32$ sub-carriers and $D_m = 2$ the number of allocated logical routes per MT. We consider that 14 MTs are randomly located in a VC. In Figure 3.9, we plot the probability density function (pdf) of the channel capacity per MT of the VCN compared with that of the SHN, when the total normalized transmission power is $P_t/P_0 = 0\text{dB}$. The distance ratio between the CP and an MT is considered to be $d/d_0 = 0.3$. Since the mean values of the pdf functions for the VCN and the SHN are different, the standard deviation cannot be used to compare the degree of fairness of both architectures. Therefore, we use the coefficient of variation $\rho = \sigma/\mu$ which is the ratio of the standard deviation σ to the mean value μ to evaluate the degree of fairness.

In Figure 3.10, we plot the coefficient of variation of the VCN compared to that of the SHN, based on the total normalized transmission power. Considering Figures 3.9 and 3.10, we observe that, for low transmission power,

the coefficient of variation ρ of the VCN is less than that of the SHN, meaning that the VCN presents a better degree of fairness than the SHN. This is a consequence of multihop networks. By introducing a WP between the CP and an MT located at the edge of the VC, the channel capacity of the MT at the edge increases. Hence, the standard deviation decreases and also the average channel capacity per MT increases.

3.1.5.1 System Throughput

To study the throughput of the system, we consider a system with quadrature phase shift keying (QPSK) as modulation scheme. We assume continuous transmission in all allocated logical routes. The channel condition is considered to be constant during packet transmission. Forward error correction is not considered. Given the SINR at a node y on a sub-carrier k , $\beta_{x-y}(k)$, we define the throughput of that sub-carrier $\Upsilon_{x-y}(k)$ when the desired transmit signal is from node x as:

$$\Upsilon_{x-y}(k) = 1 - \text{per}(\beta_{x-y}(k), B), \quad (3.7)$$

with $\text{per}(\beta_{x-y}(k), B)$ being the packet error rate when B bits are transmitted using that sub-carrier. The packet error rate is calculated as:

$$\text{per}(\beta_{x-y}(k), B) = 1 - \left(1 - p_b(\beta_{x-y}(k))\right)^B, \quad (3.8)$$

where $p_b(\beta_{x-y}(k))$ represents the bit error rate at sub-carrier k . For QPSK modulation, the bit error rate is given as [1]:

$$p_b(\beta_{x-y}(k)) = \frac{1}{2} \text{erfc} \sqrt{\beta_{x-y}(k)}. \quad (3.9)$$

We define the throughput of the e -th logical route allocated to the m -th MT via the r -th WP $\Upsilon(l_e(m, r, k_i, k_j))$, with k_i and k_j being the respective sub-carriers allocated in the first-hop and second-hop links, as :

$$\Upsilon(l_e(m, r, k_i, k_j)) = \begin{cases} \Upsilon_{\text{WP}_0-\text{MT}_m}(k_i), & \text{if } r = 0, \text{ or } k_i = k_j; \\ \min(\Upsilon_{\text{WP}_0-\text{WP}_r}(k_i), \Upsilon_{\text{WP}_r-\text{MT}_m}(k_j)), & \text{else.} \end{cases} \quad (3.10)$$

The throughput of an MT is the summation of the throughput of all allocated logical routes to that MT. If a set \mathcal{D}_m of D_m logical routes are allocated to the m -th MT, the throughput for that MT is given as:

$$\Upsilon(\mathcal{D}_m) = \sum_{e=1}^{D_m} \Upsilon(l_e(m, r, k_i, k_j)). \quad (3.11)$$

For a VC with M MTs where a set Ψ of logical routes are allocated to the MTs, the total throughput of that VC can be pressed as:

$$\Upsilon(\Psi) = \sum_{m=1}^M \sum_{e=1}^{D_m} \Upsilon(l_e(m, r, k_i, k_j)). \quad (3.12)$$

Considering the same system with 14 MTs and 2 logical routes allocated per MT, in Figure 3.11, we plot the throughput of the VCN compared with that of the SHN. In this simulation 500 packets were transmitted and each packet has a size of $B = 512$ bits. Based on Figure 3.11, we observe that, similarly as for the ergodic channel capacity, the throughput of the two-hop networks is higher than that of the SHN. The reason is the same as already explained above. By reducing the transmit distance between the transmit node and the end-MT, VCNs can provide higher throughput than SHN because of the higher achievable SINR gain.

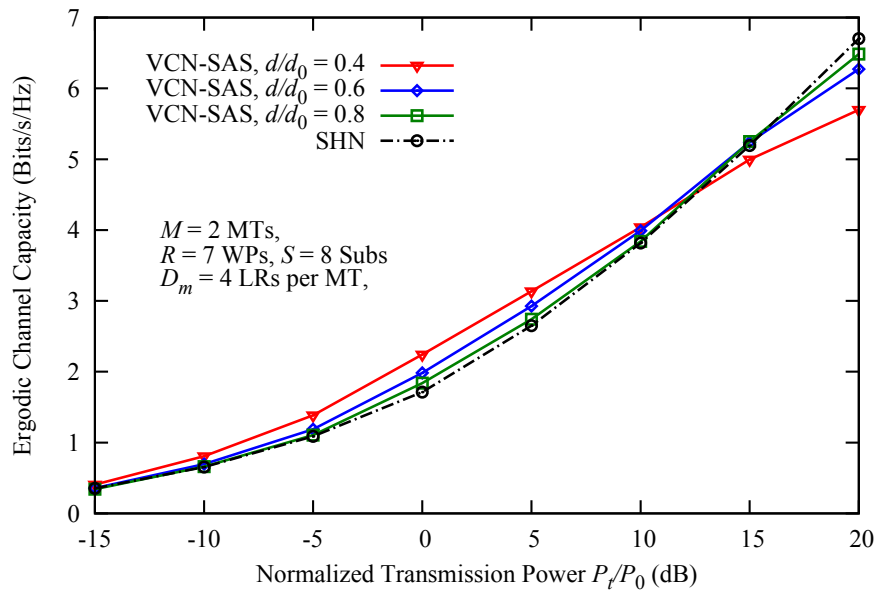
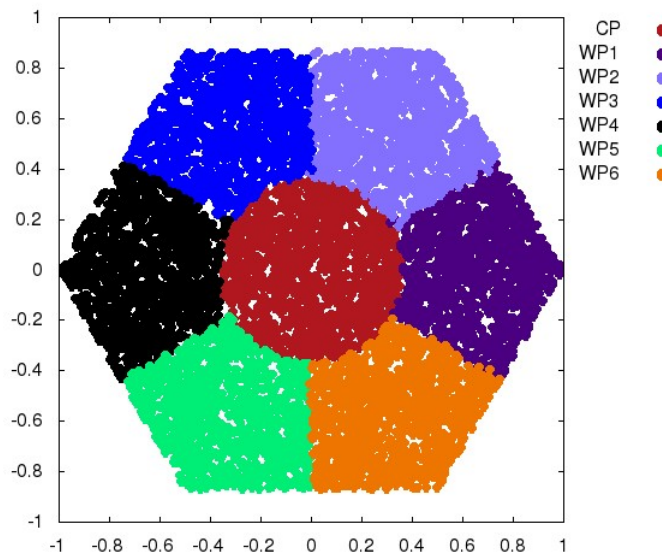


Figure 3.4: Ergodic channel capacity for two MTs

Figure 3.5: Logical route allocation distribution for $d/d_0 = 0.3$

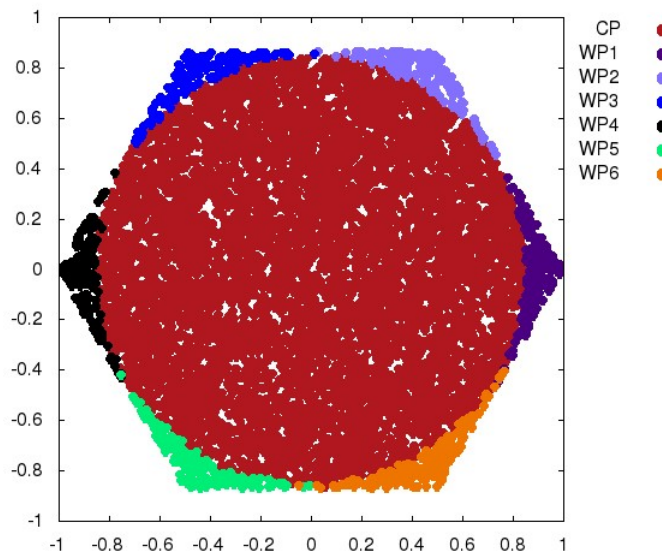
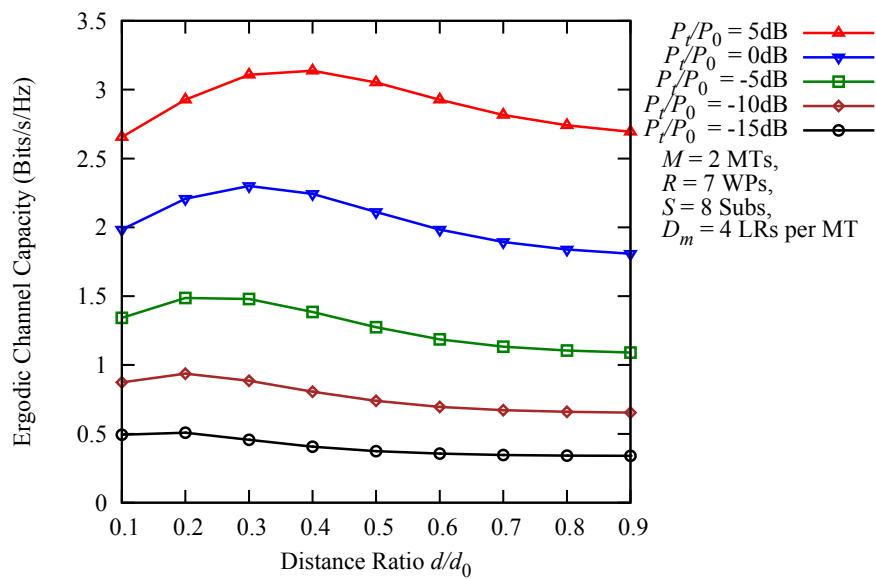
Figure 3.6: Logical route allocation distribution for $d/d_0 = 0.7$ 

Figure 3.7: Ergodic channel capacity based on the distance ratio

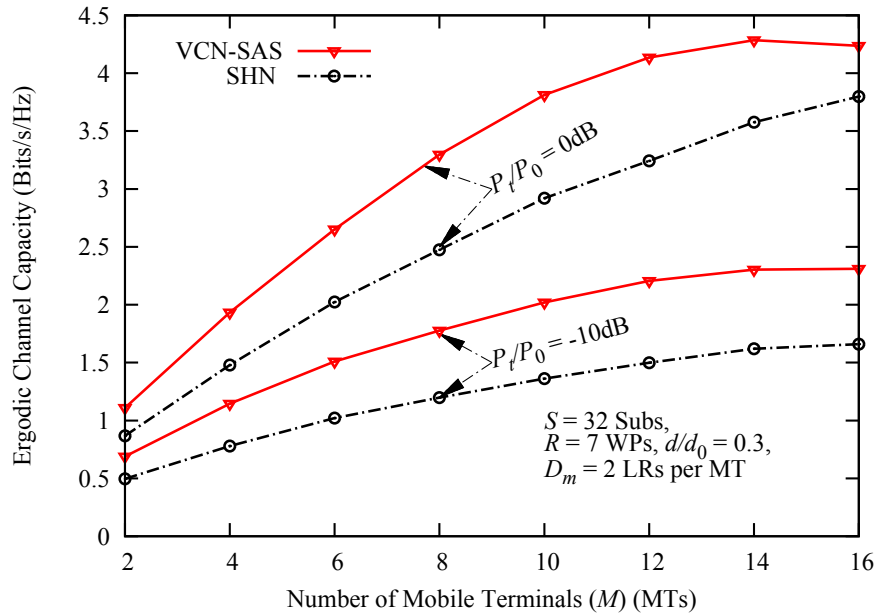


Figure 3.8: Multi-user ergodic channel capacity

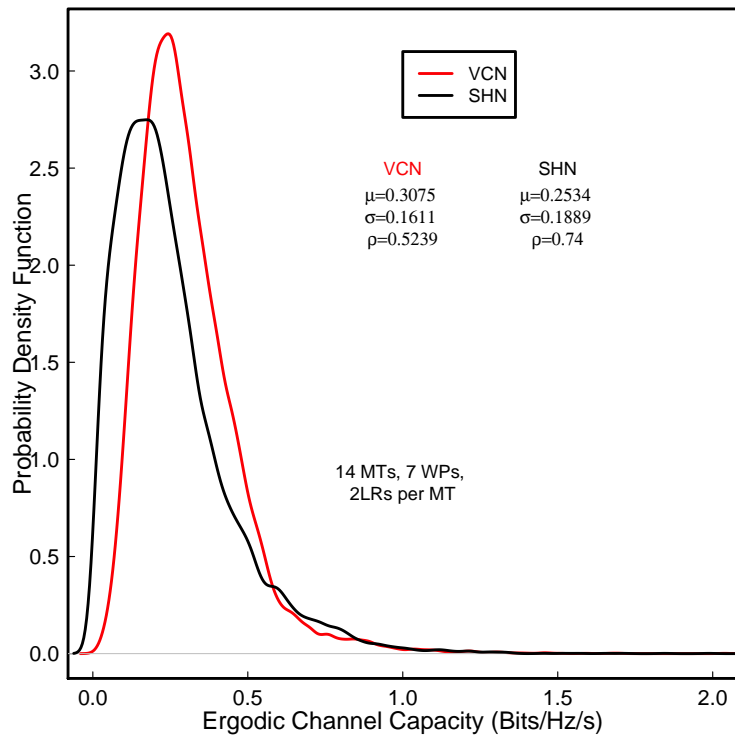


Figure 3.9: PDF of the channel capacity per MT

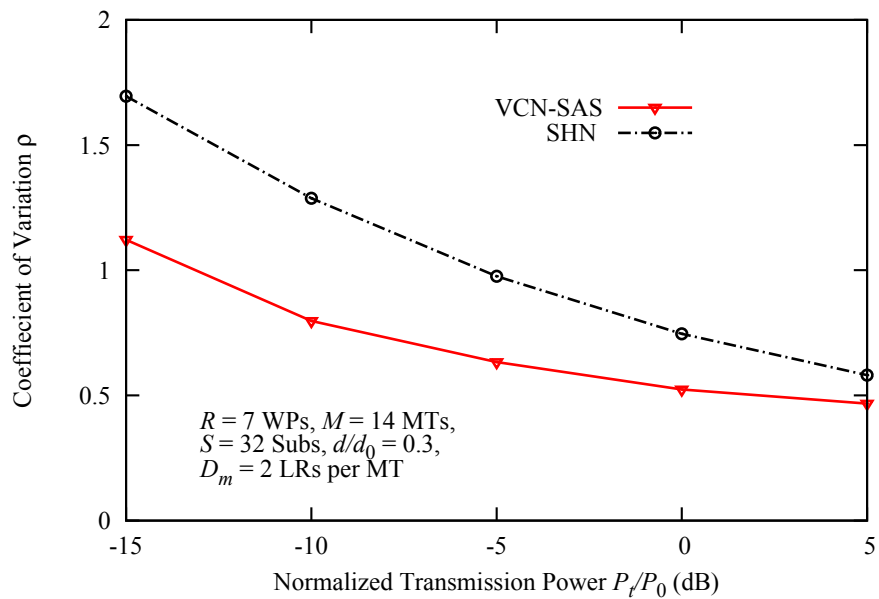


Figure 3.10: Coefficient of variation

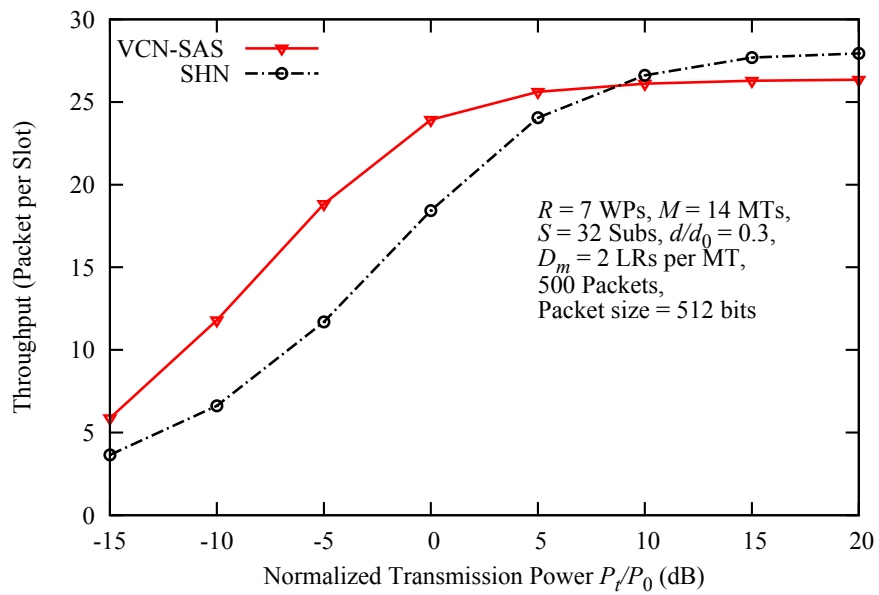


Figure 3.11: Throughput based on normalized transmission power

3.2 Multi-cell Network

In the previous section, we have proposed the SAS considering a single VC. Inter-cell interference was not considered. To introduce the effect of inter-cell interference, in this section, we modify the previously proposed SAS, and study its performance in a multi-cell environment.

We consider a multi-cell system with a set \mathcal{V} of V VCs as defined in section 2.3.1 on page 45. In the v -th VC, the communication between the core network and a set \mathcal{M}_v of M_v MTs is guaranteed by a set of \mathcal{R}_v of R_v WPs including the CP. We denote $\text{MT}_{m,v}$, and $\text{WP}_{r,v}$, the m -th MT and the r -th WP in the v -th VC, $\text{WP}_{v,0}$ being the CP. The same bandwidth is reused in all VCs. We assume that the bandwidth of the v -th VC is divided into a set \mathcal{S}_v of S_v orthogonal sub-carriers. To transmit data from the CP to an MT, in a VC, we apply parallel relaying transmission method.

In the v -th VC, the e -th logical route candidate of $\text{MT}_{m,v}$ via $\text{WP}_{r,v}$ is denoted as $l_e^*(v, m, r, k_i, k_j)$, with k_i and k_j being the sub-carriers assigned in the first-hop and second-hop links respectively. Similarly as in the single cell scenario, we define the set of logical route candidates of $\text{MT}_{m,v}$ via $\text{WP}_{r,v}$ as $\mathcal{L}_{v,m,r}^*$ and the associated allocation matrix as $\mathfrak{L}_{v,m,r}^*$. The associated allocation matrix has the same structure as that defined in Equation (3.0a). We only add the index v in reference to the v -th VC.

$$\mathfrak{L}_{v,m,r}^* = (l_{i,j}), \quad 1 \leq i, j \leq S_v, \quad (3.12a)$$

$$l_{i,j} = \begin{cases} 0 & \text{if } l_e^*(v, m, r, k_i, k_j) \text{ is available for allocation,} \\ 1 & \text{else.} \end{cases} \quad (3.12b)$$

3.2.1 Sub-Carrier Reuse Constraints Implementation

The sub-carrier constraints are implemented the same way as in the single cell scenario. The constraint which states that a WP cannot transmit and receive simultaneously in the same sub-carrier is implemented as follow:

If $l_e(v, m, r, k_i, k_j)$ is allocated :

$$\left\{ \begin{array}{ll} \forall u \in \mathcal{M}_v, \quad \forall l_{i,t} \in \mathfrak{L}_{v,u,r}^*, \quad l_{i,t} = 1, \quad 1 \leq t \leq S_v; \\ \forall u \in \mathcal{M}_v, \quad \forall l_{j,t} \in \mathfrak{L}_{v,u,r}^*, \quad l_{j,t} = 1, \quad 1 \leq t \leq S_v; \\ \forall u \in \mathcal{M}_v, \quad \forall l_{t,i} \in \mathfrak{L}_{v,u,r}^*, \quad l_{t,i} = 1, \quad 1 \leq t \leq S_v; \\ \forall u \in \mathcal{M}_v, \quad \forall l_{t,j} \in \mathfrak{L}_{v,u,r}^*, \quad l_{t,j} = 1, \quad 1 \leq t \leq S_v, \end{array} \right. \quad (3.13)$$

with $l_e(v, m, r, k_i, k_j)$ being an allocated logical route to $\text{MT}_{m,v}$ via $\text{WP}_{r,v}$ in the v -th VC.

We suppose that $l_e(v, m, r, k_i, k_j)$ is allocated to $\text{MT}_{m,v}$ via $\text{WP}_{r,v}$. The second sub-carrier constraint which prevents multiple WPs in the v -th VC to transmit to the same $\text{MT}_{m,v}$ using the same sub-carrier k_j is implemented as

follows:

$$\begin{aligned} & \text{markIf } l_e(v, m, r, k_i, k_j) \text{ is allocated :} \\ & \quad \forall w \in \mathcal{R}_v, \quad \forall l_{t,j} \in \mathcal{L}_{v,m,w}^*, \quad l_{t,j} = 1, \quad 1 \leq t \leq S_v. \end{aligned} \quad (3.14)$$

Obviously the sub-carrier k_i cannot be reused simultaneously by the CP transmit to an other WP or directly to an other MT. Hence, the allocation matrices in the v -th VC are modified as follows:

$$\begin{aligned} & \text{If } l_e(v, m, r, k_i, k_j) \text{ is allocated :} \\ & \quad \forall u \in \mathcal{M}_v, \quad \forall w \in \mathcal{R}_v, \quad \forall l_{i,t} \in \mathcal{L}_{v,u,w}^*, \quad l_{i,t} = 1, \quad 1 \leq t \leq S_v. \end{aligned} \quad (3.15)$$

The other sub-carrier constraints are all applicable inside a VC once the two previous constraints are respected.

3.2.2 Multi-Cell Successive Allocation Scheme

In a multi-cell, we consider that the logical route allocation is carried out in each VC independently. There is no cooperation between the VCs. The aim is to maximize the total channel capacity of each VC independently.

To solve the logical route allocation problem in Equation (2.35) on page 47, the proposed single cell SAS **Algorithm 1** on page 55 has been modified as follows. Suppose that a set $\mathcal{D}_{m,v}$ of $D_{m,v}$ LRs should be allocated to $\text{MT}_{m,v}$ in the v -th VC, we denote a solution candidate of the resource allocation problem in Equation (2.35) by $\Psi_v = \{\mathcal{D}_{1,v}, \mathcal{D}_{2,v}, \dots, \mathcal{D}_{m,v}, \dots, \mathcal{D}_{M_v,v}\}$. The set of all logical route candidates of $\text{MT}_{m,v}$ is indicated by $\mathcal{L}_{v,m}^* = \{\mathcal{L}_{v,m,0}^*, \mathcal{L}_{v,m,1}^*, \dots, \mathcal{L}_{v,m,R}^*\}$. The temporary set of allocated LRs to $\text{MT}_{m,v}$ is noted as $\mathcal{L}_{v,m}$. Suppose that logical route allocation has been completed for $m - 1$ MTs in the v -th VC, the allocation of $D_{m,v}$ LRs to the m -th MT in the v -th VC is executed as follows in **Algorithm 2** on page 68.

3.2.3 Simulation Assumptions and System Model

To take into account the inter-cell interference generated by a second-tier architecture, a cluster of 19 VCs has been considered (see Figure 3.12). The VCs are assumed to be of a hexagonal shape. Each VC has the same radius d_0 . The CPs are located at the center of the VCs. The distance between the CPs of two neighbouring VCs is $D = d_0\sqrt{3}$. To reduce computational complexity and consequently enable faster running time, a wrap around cluster has been implemented. To illustrate, if VC_1 is the VC of interest, VCs 12, 13, 14, 15, and 16 will be flipped from their position to a new position as shown in Figure 3.13. We consider the VC layout in Figure 3.14 where six WPs are located at the edge of an hexagon and a CP located at the center of the VC. In all VCs, the WPs are placed at an equal distance d from the CP.

Similarly as in the single cell scenario, we define the normalized transmission power in a VC as $P_n = P_t/P_0$. P_t represents the total transmission power

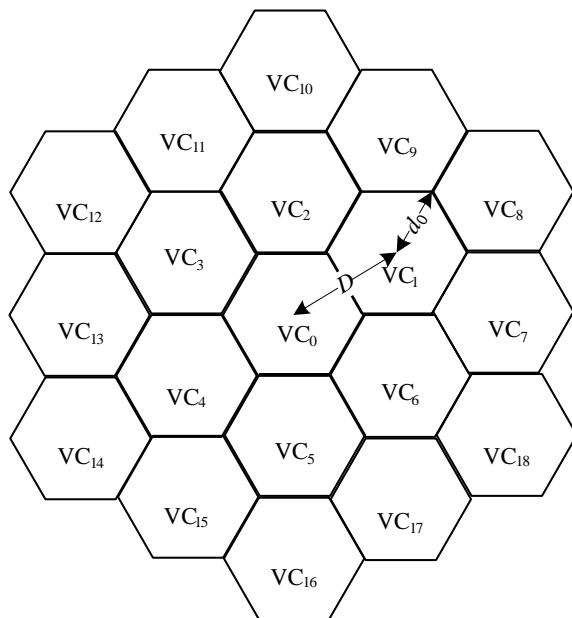


Figure 3.12: Second tier architecture

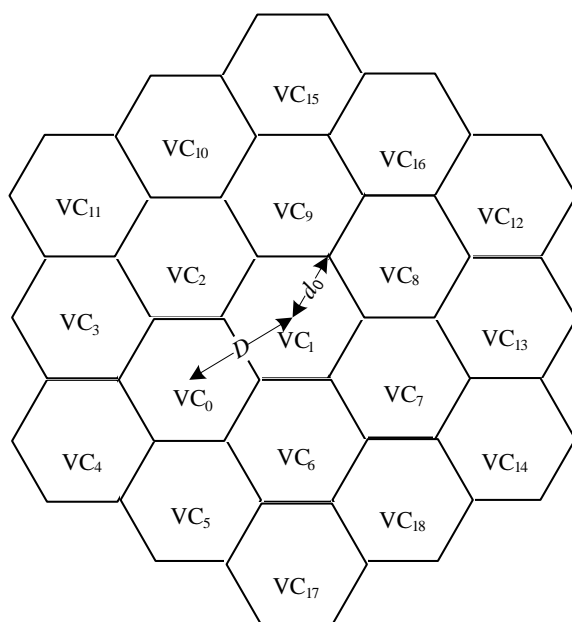


Figure 3.13: Wrap around structure

Algorithm 2: Multi-Cell Successive Allocation Scheme

Input: $\mathcal{V}, \mathcal{M}, \mathcal{R}, \mathcal{S}$, Allocation Completed for $m - 1$ MTs in VC_v .

Output: Allocate $D_{m,v}$ LRs to $\text{MT}_{m,v}$

```

begin
  step 1   /* Initialization of logical route candidates */
  Initialize  $\mathcal{L}_{v,m}^*$  and create  $\mathfrak{L}_{v,m,w}^*$ ,  $\forall w \in \mathcal{R}_v$ , based on
  constraints (2.36)– (2.40) on page 47– 48 and
  Equations (3.13)– (3.15)
  step 2   /* Successive allocation of logical routes */
  repeat
    foreach  $l_e^*(v, m, r, k_i, k_j) \in \mathcal{L}_{v,m}^*$  do
      foreach  $p \in \mathcal{M}_u$ ,  $\forall u \in \mathcal{V}$  do
        foreach  $l_h(u, p, r', k_{i'}, k_{j'}) \in \mathcal{D}_{p,u}$  do
          Execute the
          procedure Procedure InterferenceMultiCell
        end
        /* Recalculate SINR and capacity */
        Evaluate  $\Gamma(l_e^*(v, m, r, k_i, k_j))$  using Equation (2.30) on
        page 46
        Evaluate  $\Gamma(l_h(u, p, r', k_{i'}, k_{j'}))$  using Equation (2.30) on
        page 46
        Recalculate  $C_{p,u}(\mathcal{D}_{p,u})$  using Equation (2.32) on page 46
      end
      Update  $\mathcal{L}_{v,m} \leftarrow l_e^*(v, m, r, k_i, k_j)$ 
      Evaluate  $C_{m,v}(\mathcal{L}_{v,m})$  using Equation (2.32) on page 46
    end
    /* Choose best logical route candidate */
    Choose  $l_e^*(v, m, r, k_i, k_j)$  according to Equation (2.35) on
    page 47
    Add  $l_e^*(v, m, r, k_i, k_j)$  to  $\mathcal{D}_{m,v}$ 
    /* Update of the set of logical route candidates */
    Modify  $\mathfrak{L}_{v,m,w}^*$ ,  $\forall w \in \mathcal{R}_v$ , and update  $\mathcal{L}_{v,m}^*$  based on
    Equations (3.13)– (3.15)
  until  $D_{m,v}$  LRs are allocated to  $\text{MT}_{m,v}$ 
end

```

Procedure InterferenceMultiCell

Input: $l_e^*(v, m, r, k_i, k_j)$, and $l_h(u, p, r', k_{i'}, k_{j'})$
Output: $l_e^*(v, m, r, k_i, k_j)$, and $l_h(u, p, r', k_{i'}, k_{j'})$ with interference
/* Evaluate interference from existing communications */
if ($k_i = k_{i'}$ or $k_i = k_{j'}$) and $k_i = k_j$ **then**
| Evaluate $\beta_{WP_{0,v}-MT_{m,v}}(k_i)$ using Equation (2.29) on page 46;
end
if ($k_i = k_{i'}$ or $k_i = k_{j'}$), and $k_i \neq k_j$ **then**
| Evaluate $\beta_{WP_{0,v}-WP_{r,v}}(k_i)$ using Equation (2.29) on page 46;
end
if ($k_j = k_{i'}$ or $k_j = k_{j'}$), and $k_i \neq k_j$ **then**
| Evaluate $\beta_{WP_{r,v}-MT_{m,v}}(k_j)$ using Equation (2.29) on page 46;
end
/* Evaluate interference to existing communications */
if ($k_{i'} = k_i$ or $k_{i'} = k_j$), and $k_{i'} = k_{j'}$ **then**
| Evaluate $\beta_{WP_{0,u}-MT_{p,u}}(k_{i'})$ using Equation (2.29) on page 46;
end
if ($k_{i'} = k_i$ or $k_{i'} = k_j$), and $k_{i'} \neq k_{j'}$ **then**
| Evaluate $\beta_{WP_{0,u}-WP_{r',u}}(k_{i'})$ using Equation (2.29) on page 46;
end
if ($k_{j'} = k_i$ or $k_{j'} = k_j$), and $k_{i'} \neq k_{j'}$ **then**
| Evaluate $\beta_{WP_{r',u}-MT_{p,u}}(k_{j'})$ using Equation (2.29) on page 46;
end

of a VC and it is equally distributed among the allocated LRs in that VC. We assume that the allocated power to a logical route is the same in all VCs. The assigned power of a two-hop link logical route is shared uniformly between each link of the logical route. In each VC, (suppose the v -th VC here), P_0 is defined as the average transmission power of the CP for which the received signal-to-noise-power ratio at d_0 is 0dB, which means:

$$\frac{P_0 d_0^{-\alpha}}{N S} = 1. \quad (3.16)$$

N and S represent respectively the noise power per subcarrier and the number of subcarriers in the VC.

As already stated, we considered a system with a frequency reuse factor equal to one. This means that the same bandwidth is reused in all VCs simultaneously. The bandwidth of a VC is divided into $S = 32$ orthogonal sub-carriers. For each VC, a path-loss exponent $\alpha = 4$, a standard deviation of the log-normally distributed shadowing loss $\delta = 8$, and $L = 8$ propagation paths independently distributed Rayleigh fading are considered. The propagation paths are considered to have an uniformly distributed average power delay profile. The paths are of equidistant delays. During the FFT process, the inverse of the sub-carriers spacing is considered to be equal to the delay between two consecutive paths.

Monte Carlo simulation method was used to evaluate the performance of SAS in a multi-cell environment. In the simulation, the VCs are chosen randomly. Each time a VC is selected, an MT is generated in that VC. The location of the MTs inside the VCs is random. The simulation was allowed to run until the number of MTs was equivalent in all VCs. The interference from existing communications is added before each allocation. After each allocation, the interference from the allocated sub-carriers to existing communications is taken into account. The VCs were considered to be uniform meaning that they have the same number of MTs, the same total transmission power, and the same number of WPs.

3.2.4 Simulation Performance

Figure 3.15 shows the plots of the ergodic channel capacity per VC of the two-hop VCN and the SHN based on the normalized transmission power P_t/P_0 . The plots are those of the single cell and multi-cell environment. For this simulation case, $M = 14$ MTs are randomly generated in each VC; and $D_m = 2$ LRs are allocated per MT. The VC layout in Figure 3.14 is used in all VCs with $R = 7$ WPs including the CP. The WPs are located at a distance ratio $d/d_0 = 0.3$ from the CP. The dotted lines of Figure 3.15 represent the plots of the ergodic channel capacity of the SHN, and the continuous lines those of the VCN. According to Figure 3.15, in the case of a single cell, the channel capacity of the VCN is greater than that of the SHN only for low transmission power. However, if inter-cell interference is accounted for, the capacity of the VCN remains greater than that of the SHN even for high transmission power.

If a single cell is considered, in the interference dominant transmission power region, the SHN can outperform the VCN because the SHN does not suffer interference between the MTs while the VCN does. However, in the case of multiple cells in the interference dominant transmission power region, inter-cell interference will affect the performance of both network architectures.

In a multi-cell environment, the edge-MTs are mainly those which are affected by inter-cell interference. In the case of the VCN, the edge-MTs suffer from intra-cell and inter-cell interference. In the simulation, an edge-MT is defined as an MT of which the distance ratio d/d_0 from the CP is superior or equal to 0.7 ($d/d_0 \geq 0.7$). Figure 3.16 displays the plots of the probability distribution of the ergodic channel capacity of the edge-MTs of VC_0 for a normalized transmission power $P_t/P_0 = 20\text{dB}$ for the VCN and the SHN, considering both the multi-cell and single cell configurations. The other parameters remained unchanged. As shown in Figure 3.16, in the single cell configuration, the probability distribution of the channel capacity of the edge-MTs in the SHN is better than that of the edge-MTs in the VCN. However, in the multi-cell environment, the probability distribution of channel capacity of the edge-MTs in the SHN becomes worse than that of the edge-MTs in the VCN. This is because the presence of the WPs in the VCN helps to mitigate the effect of intra-cell and inter-cell interference on the edge-MTs, and the VCN can achieve route diversity by using the WPs. This is different for the SHN which has no WP to assist the edge-MTs and to achieve route diversity.

Though the VCN suffers from intra-cell and inter-cell interference, according to the results plotted in Figure 3.16, the VCN can achieve higher ergodic channel capacity than the SHN even for high transmission power. This performance of the VCN compared to that of the SHN is a consequence of the route diversity gain provided by the usage of the WPs in the VCN.

The analysis of the behaviour of both networks in a multi-cell environment for different numbers of MTs is carried out in Figure 3.17. The ergodic channel capacity per VC of the VCN and the SHN, when the normalized transmission power is $P_t/P_0 = -10\text{dB}$ and $P_t/P_0 = 20\text{dB}$ for different loads, is plotted in Figure 3.17. Two logical routes are allocated per MT. Since the number of sub-carriers in a VC is $S = 32$ sub-carriers, the maximum number of MTs which can be served is $M = 16$ MTs. The other parameters remain unchanged.

Figure 3.17 shows that the channel capacity of the VCN remains greater than that of the SHN even when the network is fully loaded to $M = 16$ MTs. The reason is the same as previously explained. In the VCN, because of the usage of WPs, route diversity can be achieved. Furthermore, the WPs in the VCN help to palliate the effect of intra-cell and inter-cell interference on the edge-MTs.

Figure 3.17 also shows that the ergodic channel capacity of the VCN degrades when the number of MTs increases from $M = 14$ MTs to $M = 16$ MTs. This degradation can be understood by the fact that increasing the number of MTs from 14 to 16 also increases the number of sub-carriers which has to be

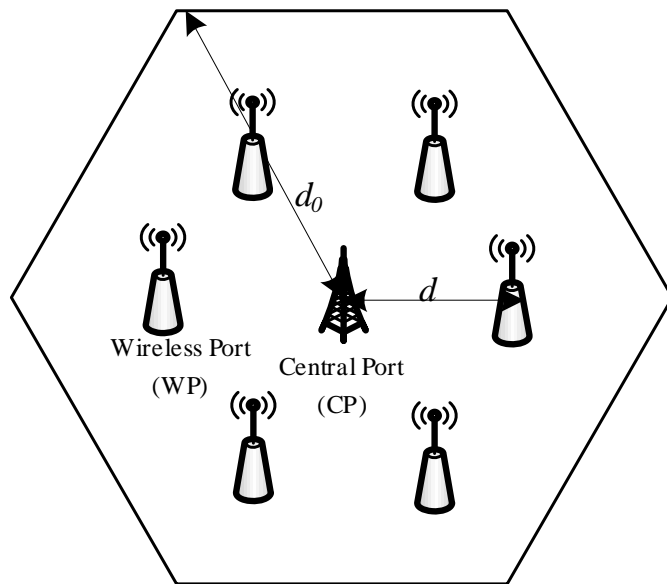


Figure 3.14: First VC layout with six WPs

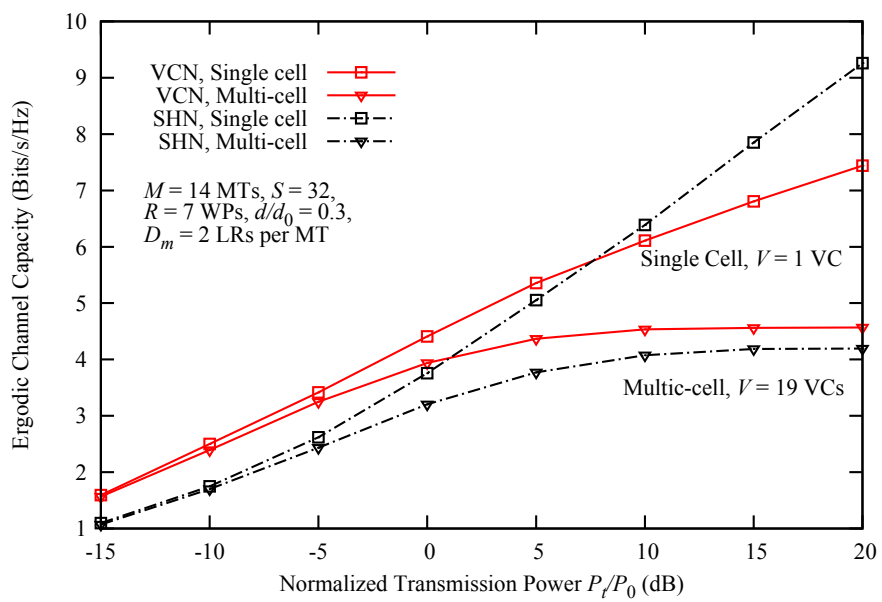


Figure 3.15: Single cell and multi-cell Ergodic channel capacity

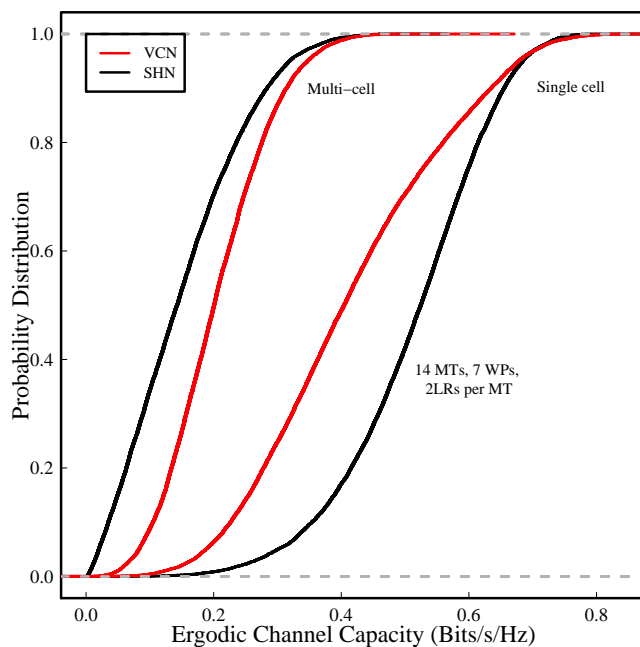
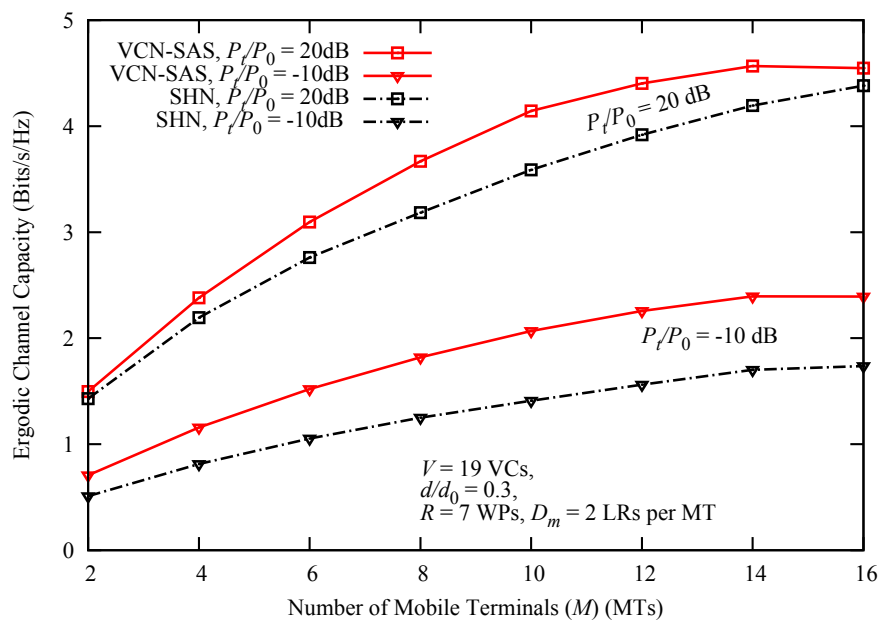
Figure 3.16: Probability distribution of MTs located at $d/d_0 \geq 0.7$ 

Figure 3.17: Multi-user ergodic channel capacity

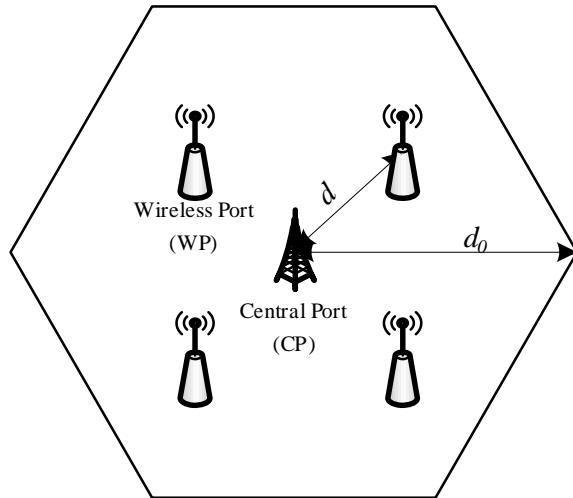


Figure 3.18: Second VC layout with 5 WPs

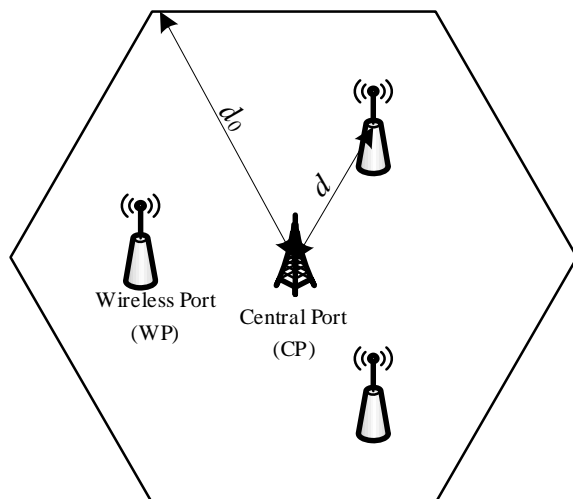


Figure 3.19: Third VC layout with 4 WPs

reused in the VCs. Hence, the interference inside the VC itself also increases. This augmentation of intra-cell interference in the VCs causes the degradation of the ergodic channel capacity of the VCs.

To study the effect of the number of WPs in a VC in the system we consider the following VC layouts (see Figure 3.14, Figure 3.18, and Figure 3.19). Figure 3.14, Figure 3.18, and Figure 3.19 represent the cases of 6, 4, and 3 WPs located at the edge of a hexagon, a square, and an equilateral triangle respectively. In each configuration, the WPs are placed at an equal distance d from the CP.

Figure 3.20 exhibits the plots of the ergodic channel capacity per VC of the

VCN using the three VC layouts in Figure 3.14, Figure 3.18, and Figure 3.19. In a cluster, the same VC layout was used in all VCs. The values of the other parameters are listed in Figure 3.20.

According to Figure 3.20, increasing the number of WPs in the VCs can enhance the ergodic channel capacity. The enhancement of the channel capacity gained in the VCN is due to the reduction of the transmission distance between the transmitting node and the MTs. This reduction is a consequence of the presence of the WPs. By increasing the number of WPs from $R = 4$ WPs to $R = 7$ WPs, the number of MTs for which the transmission distance can be reduced augments. Therefore, further improvement of the channel capacity can be achieved by increasing the number of WPs.

In order to study the relationship between the location of the WPs in a VC and the channel capacity of the VCN, the three different VC layouts described in Figure 3.14, Figure 3.18, and Figure 3.19. are used. As in the simulation above, the same VC layout is applied in all VCs in a cluster.

Figure 3.7 shows the plots of the ergodic channel capacity per VC of the VCN for each configuration based on the distance ratio between the CP and the WPs in a VC. According to Figure 3.7, an optimal distance ratio can be found in the interval $0.2 \sim 0.4$. This optimal location does not depend on the number of WPs in the VCs and neither does it vary considerably with the normalized transmission power.

In order to evaluate the fairness of both systems in the presence of inter-cell interference, the Jain's fairness index is used as the metric of fairness. The Jain's fairness index indicates how fairly resources are shared among the users. Its values lie in the interval $[0, 1]$. The higher the fairness value is, the more fairly the available resources are shared among the MTs. The Jain's fairness index is evaluated using the following Equation [45]:

$$J(x_1, x_2, \dots, x_M) = \frac{1}{M} \sum_{1 \leq m \leq M} \left(\sum_{1 \leq m \leq M} x_m \right)^2 \quad (3.17)$$

In Equation (3.17), x_m represents the ergodic channel capacity of the m -th MT and M the number of MTs in a VC.

Figure 3.22 shows the plots of the Jain's fairness index per VC of the VCN and the SHN based on the normalized transmission power P_t/P_0 . The plots of Figure 3.22 show that the VCN can achieve a better degree of fairness than the SHN. With the introduction of the WPs in the VCN, the channel capacity of the edge-MTs can be improved. Therefore, a better distribution of the total channel capacity can be achieved in the VCN than in the SHN.

If η is the required transmission rate, the outage probability is the probability that the rate exceeds the channel capacity of the MT and it is given by [1]:

$$\begin{aligned} P_{\text{out}}(\eta) &= P(C < \eta) \\ &= F_C(\eta^-). \end{aligned} \quad (3.18)$$

$F_C(c)$ is the cumulative distribution function (CDF) of the channel capacity C , and $F_C(\eta^-)$ is the limit-from-left of $F_C(c)$ at the point $c = \eta$.

Figure 3.23 shows that the VCN can achieve better outage capacity than the SHN in multi-cell environments. These results can be understood by the fact that the VCN has higher channel capacity and better degree of fairness than the SHN in multi-cell environments as noted in Figure 3.23 and Figure 3.23. The WPs in the VCN help to fairly distribute the total channel capacity between the MTs. The performance of the VCN compared to the SHN is a consequence of the route diversity gain that can be achieved by the VCN.

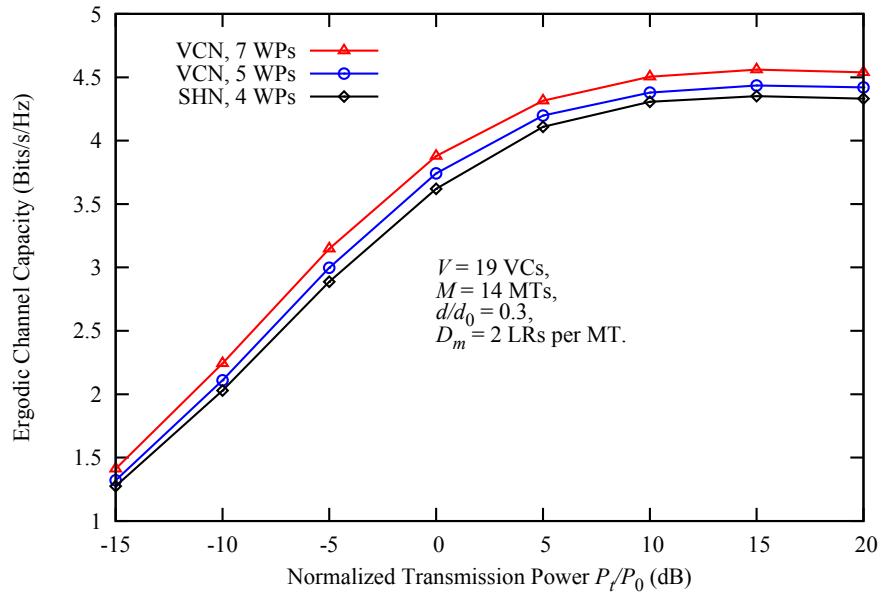
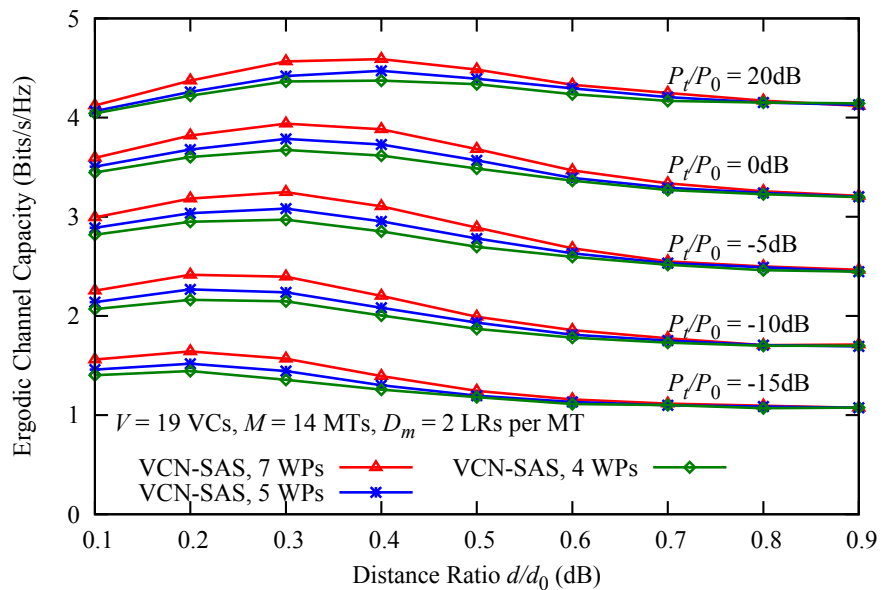
Figure 3.20: Ergodic channel capacity for $R = 4$, $R = 5$, and $R = 7$ WPs

Figure 3.21: Ergodic channel capacity based on the distance ratio

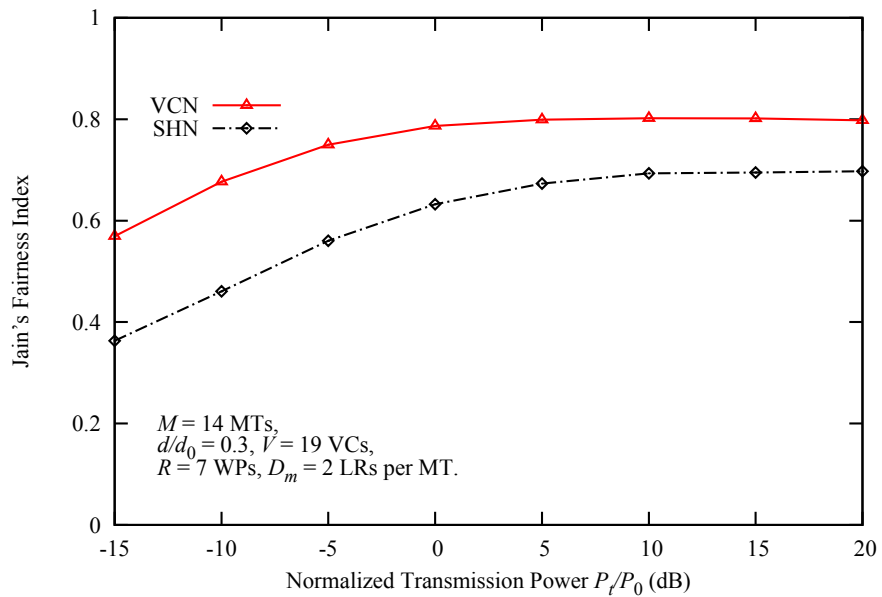


Figure 3.22: Jain's fairness index of the VCN and the SHN

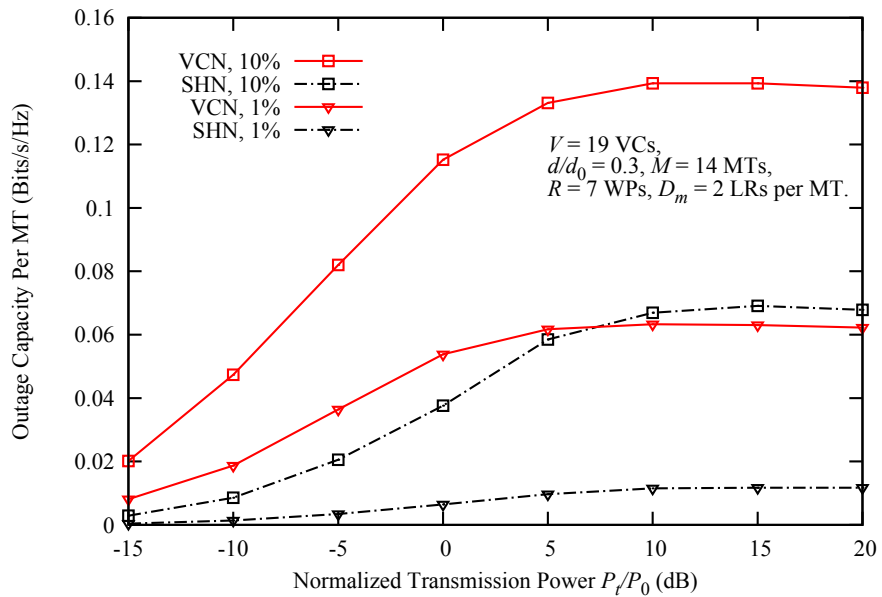


Figure 3.23: Outage channel capacity per MT

3.3 SAS Performance Comparison With Optimal Scheme

To study the performance of SAS compared with the optimal solution, we assume a system of 2 MTs and 8 sub-carriers. Because of the high computational complexity of the optimal solution, we consider a VC with only 3 WPs (the CP included) as illustrated in the Figure 3.24.

In Figure 3.25, we plot the ergodic channel capacity of the VCN when SAS the exhaustive scheme are applied. We remark that the exhaustive scheme slightly outperforms the SAS in the noise dominant transmission power region. The performance gap between the two schemes deepens considerably in the interference dominant transmission power region. The performance of SAS degrades in the interference dominant transmission power region. This degradation is a consequence of the successive allocation of the logical routes implemented by SAS. Successive allocation is not resilient against inter logical route interference.

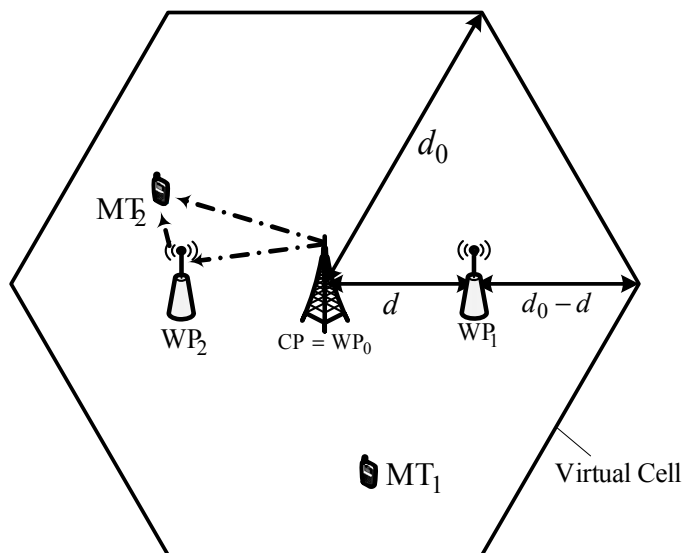


Figure 3.24: Two WPs VC layout

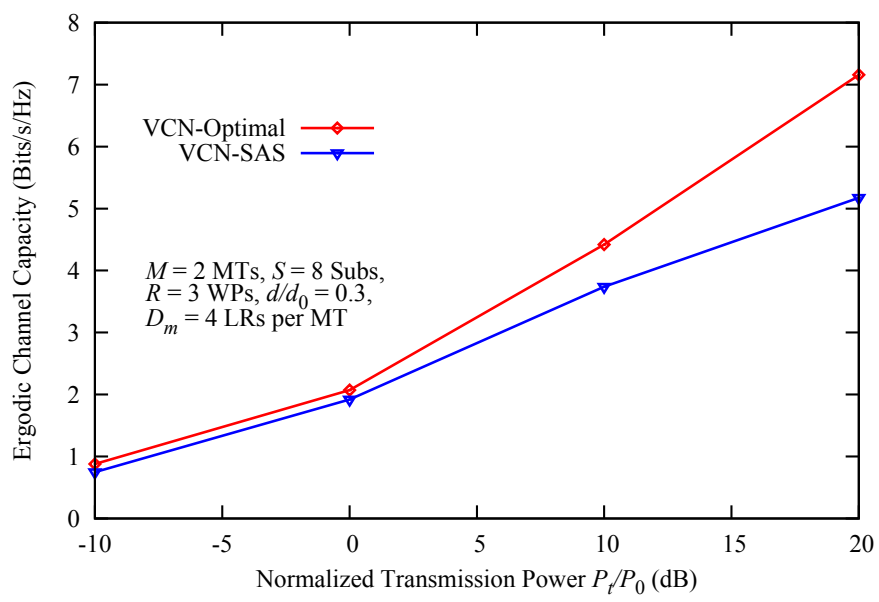


Figure 3.25: Comparison with the optimal solution

3.4 Summary

In this chapter, we have proposed a successive allocation scheme to solve the problem of joint route and sub-carrier allocation in a two-hop network. We have shown that the proposed scheme can reduce considerably the computational complexity of the resource allocation problem compared to the optimal scheme. We study the performance of the SAS in a single cell environment. The SAS applied in a two-hop VCN can increase the channel capacity of the two-hop VCN compared to the SHN.

The SAS has been modified so that it could be applied in a multi-cell environment. We have remarked that in an inter-cell interference scenario, applying the SAS in a two-hop network can provide better outage and ergodic channel capacity than in a single hop network, even in the interference dominant transmission power region.

Though using the SAS the performance of the two-hop VCN outperforms that of the SHN in a multi-cell interference scenario, we remark that the performance of the SAS degrades with interference. Compared with the optimal solution, it could be observed that the optimal solution outperforms greatly the SAS, specifically in the interference dominant transmission power region.

CHAPTER 4

Iterative Allocation Scheme

In Chapter 3, we proposed a successive allocation scheme (SAS) to reduce the computational complexity of the joint route and sub-carrier allocation problem in a two-hop network. The performance of the SAS degrades with interference.

To alleviate the effect of interference between the logical routes and consequently increase the channel capacity of the network in the interference dominant transmission power region, in this chapter, we propose some iterative allocation schemes. First, we study the performance of these iterative schemes in a single VC scenario. The computer simulations show that the iterative schemes can improve the channel capacity of the VCN in the interference dominant transmission power region. Among the proposed iterative allocation schemes, we select a sequential iterative allocation scheme (SIS) and modify it so that it can be applied in a multi-cell environment. We show that the proposed SIS can improve the performance of the network in the interference dominant transmission power region in a multi-cell environment.

4.1 Single Cell Network

In this section, we propose four iterative allocation schemes aiming at improving the performance of the VCN in an intra-cell interference environment. We also study and compare the performance of these iterative schemes and select the most efficient and practical one as the best solution.

We consider the same single VC system described on page 50 with a set \mathcal{R} of R WPs including the CP and a set \mathcal{M} of M MTs randomly distributed in the VC. The system bandwidth is divided into a set \mathcal{S} of S orthogonal sub-carriers. Parallel relaying transmission method is used to transmit data to an MT. We denote by \mathcal{D}_m the set of logical routes which have to be allocated to the m -th MT.

4.1.1 Drawback of Successive Allocation

The SAS proposed in Chapter 3 considers the MTs of a VC to be arranged in a certain order for resource allocation. Though selecting the MTs in a successive order for logical route allocation lessens the complexity of the problem, the channel capacity of the former MTs degrades when interference from the

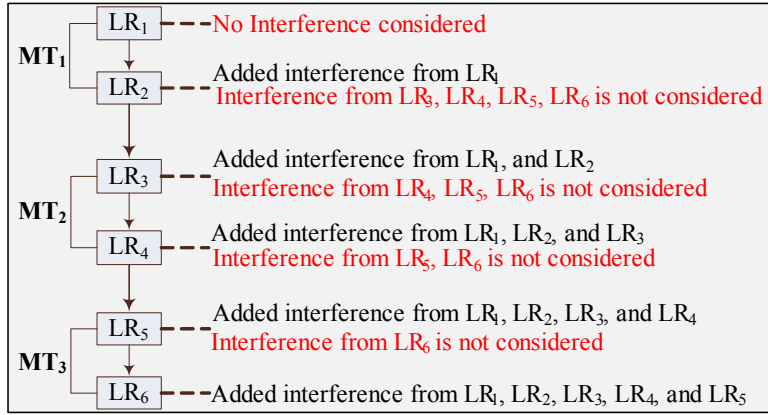


Figure 4.1: Interference scenario in successive allocation

latter MTs is added. This capacity loss can be explained by the fact that while allocating resources to MT_m , interference from MT_h is not taken into account, $h > m$ (see Figure 4.1). Therefore, if any sub-carrier allocated to MT_m is reused in any logical route assigned to MT_h , the channel capacity of MT_m will deteriorate because of interference from MT_h .

We consider the case of 3 MTs and 2 logical routes to be allocated per MT as illustrated in Figure 4.1. When allocating the first logical route to the first MT, no interference from other possible logical route candidates was considered. The only allocation which takes into account interference from all the other communications is the allocation of LR_6 to MT_3 . Hence, if any sub-carrier assigned in LR_1 belonging to MT_1 is reused by any of the other allocated logical routes, the channel capacity of MT_1 might be decreased because of interference from the latter logical route allocation. Furthermore, it should be noted that the same interference problem occurs between logical routes allocated to an MT as the allocation of logical routes to an MT is also conducted in a successive order.

Reallocating logical routes to the m -th MT after allocating logical routes to the h -th MT can provide some improvement of the channel capacity of the VCN. To reduce computational complexity, the reallocation of logical routes to the MTs is considered after logical route allocation for all MTs has been performed. After having completed logical route allocation to all MTs using SAS, we consider two methods to select the MT for which we will perform reallocation, a sequential selection method and a random selection method.

4.1.2 Sequential Iterative Allocation Scheme (SIS)

Assume that the set of M MTs were chosen in the following order for logical route allocation in the SAS:

$$(MT_m)_{m=1}^M = (MT_1, MT_2, \dots, MT_{M-1}, MT_M).$$

The first procedure consists in selecting the MTs in the same order they were chosen for logical route allocation by the SAS. This means that we start reallocating logical routes to the MTs beginning with MT_1 . We refer to this method of iterative allocation as the *sequential iterative allocation scheme* (SIS). At each iteration, in the SIS, the next MT in the sequence is selected for local route allocation. Suppose that reallocation of logical routes has been completed for MT_m at the i -th iteration, at the $(i+1)$ -th iteration, we execute reallocation for MT_{m+1} while the other MTs withhold their allocated logical routes.

Suppose that we perform a number I of iterations. Each iteration of the SIS will provide a solution candidate for the logical route allocation problem described in Equation (2.22) on page 43. We can represent the set of solution candidates generated by the SIS as:

$$\Omega^{(I)} = \{\Psi^{(1)}, \Psi^{(2)}, \dots, \Psi^{(i)}, \dots, \Psi^{(I)}\},$$

where $\Psi^{(i)}$ represents the solution candidate generated by the i -th iteration. At the end of the execution of all iterations, the solution candidate $\Psi^{(*)}$ which maximizes the total channel capacity of the VC according to Equation (2.22) on page 43 is chosen as the best solution. The different steps of the SIS is illustrated in **Algorithm 3** on page 85.

4.1.3 Random Iterative Allocation Scheme

Contrary to SIS where the MTs are selected in a sequential order for logical route reallocation, the random iterative allocation scheme (RIS) randomly chooses an MT for logical route reallocation. For fairness when reallocating logical routes to the MTs, we use a random uniform function $\xi_{\text{unif}}(\mathcal{M})$ which given a set \mathcal{M} of MTs uniformly selects one of the MTs (MT_y) for logical route reallocation:

$$MT_y = \xi_{\text{unif}}(\mathcal{M})$$

The only difference between SIS and RIS is on how the next MT is selected for logical route reallocation. Besides that, anything which has been said regarding SIS remains valid for the RIS. The different steps of the RIS are illustrated in **Algorithm 4** on page 86.

4.1.4 Complexity of SIS and RIS

The added complexity of SIS and RIS resides mainly in the execution of step 2 of **Algorithm 1** on page 55 of the SAS. Thus, to study the complexity of SIS and RIS, we focus on analysing the complexity of step 2 of SAS. In step 2, the allocation of D_m logical routes to MT_m requires the evaluation of a maximum

Algorithm 3: Sequential Iterative Allocation Scheme (SIS)

Input: $\mathcal{M}, \mathcal{R}, \mathcal{S}, I, (MT_m)_{m=1}^M$.
Output: Sequential reallocation of logical routes

```

begin
    /* Successive logical route allocation for all MTs */
    Allocate logical routes to all MTs using Algorithm 1 on page 55;
    /* Iterative reallocation of logical routes to MTs */
    for  $i = 1 : I$  do
        Choose the next MT ( $MT_m$ ) in the sequence  $(MT_m)_{m=1}^M$ ;
        Deallocate the set  $\mathcal{D}_m$  of logical routes of  $MT_m$ ;
        Modify  $\mathcal{L}_{m,w}^*$ ,  $\forall w \in \mathcal{R}$ , and update  $\mathcal{L}_m^*$  based on
        Equations (3.1)– (3.3) on page 51;
        /* Reallocate logical route to  $MT_m$  */
        repeat
            foreach  $l_e^*(m, r, k_i, k_j) \in \mathcal{L}_m^*$  do
                foreach  $p \in \mathcal{M}$  do
                    foreach  $l_h(p, r', k_{i'}, k_{j'}) \in \mathcal{D}_p$  do
                        Execute the Procedure InterferenceSinceCell on
                        page 56;
                    end
                    /* Recalculate SINR and capacity */
                    Evaluate  $\Gamma(l_e^*(m, r, k_i, k_j))$  using Equation (2.15) on
                    page 42;
                    Evaluate  $\Gamma(l_h(p, r', k_{i'}, k_{j'}))$  using Equation (2.15) on
                    page 42;
                    Recalculate  $C_p(\mathcal{D}_p)$  using Equation (2.19) on
                    page 42;
                end
                Update  $\mathcal{L}_m \leftarrow l_e^*(m, r, k_i, k_j)$ ;
                Evaluate  $C_m(\mathcal{L}_m)$  using Equation (2.19) on page 42;
            end
            /* Choose best logical route candidate */
            Choose  $l_e^*(m, r, k_i, k_j)$  according to Equation (2.22) on
            page 43;
            Add  $l_e^*(m, r, k_i, k_j)$  to  $\mathcal{D}_m$ ;
            /* Update the set of logical route candidates */
            Modify  $\mathcal{L}_{m,w}^*$ ,  $\forall w \in \mathcal{R}$ , and update  $\mathcal{L}_m^*$  based on
            Equations (3.1)– (3.3) on page 51;
        until  $D_m$  logical routes are allocated to  $MT_m$ ;
        Add the set  $\mathcal{D}_m$  to the solution candidate  $\Psi^{(i)}$ ;
    end
    Choose  $\Psi^{(*)}$  based on Equation (2.22) on page 43;
end

```

Algorithm 4: Random Iterative Allocation Scheme (RIS)

Input: $\mathcal{M}, \mathcal{R}, \mathcal{S}, I, \xi_{\text{unif}}()$.

Output: Random reallocation of logical routes

begin

/* Successive logical route allocation for all MTs */
 Allocate logical routes to all MTs using **Algorithm 1** on page 55;;
 /* Iterative reallocation of logical routes to MTs */
for $i = 1 : I$ **do**

Select $MT_m = \xi_{\text{unif}}(\mathcal{M})$;
 Deallocate the set \mathcal{D}_m of logical routes of MT_m ;
 Modify $\mathcal{L}_{m,w}^*$, $\forall w \in \mathcal{R}$, and update \mathcal{L}_m^* based on
 Equations (3.1)–(3.3) on page 51;
 /* Reallocate logical route to MT_m */

repeat

foreach $l_e^*(m, r, k_i, k_j) \in \mathcal{L}_m^*$ **do**

foreach $p \in \mathcal{M}$ **do**

foreach $l_h(p, r', k_{i'}, k_{j'}) \in \mathcal{D}_p$ **do**

Execute the **Procedure** InterferenceSinceCell on
 page 56;

end

/* Recalculate SINR and capacity */
 Evaluate $\Gamma(l_e^*(m, r, k_i, k_j))$ using Equation (2.15) on
 page 42;
 Evaluate $\Gamma(l'_h(p, r', k_{i'}, k_{j'}))$ using Equation (2.15) on
 page 42;
 Recalculate $C_p(\mathcal{D}_p)$ using Equation (2.19) on
 page 42;

end

Update $\mathcal{L}_m \leftarrow l_e^*(m, r, k_i, k_j)$;
 Evaluate $C_m(\mathcal{L}_m)$ using Equation (2.19) on page 42;

end

/* Choose best logical route candidate */
 Choose $l_e^*(m, r, k_i, k_j)$ according to Equation (2.22) on
 page 43;
 Add $l_e^*(m, r, k_i, k_j)$ to \mathcal{D}_m ;

/* Update the set of logical route candidates */
 Modify $\mathcal{L}_{m,w}^*$, $\forall w \in \mathcal{R}$, and update \mathcal{L}_m^* based on
 Equations (3.1)–(3.3) on page 51;

until D_m logical routes are allocated to MT_m ;

Add the set \mathcal{D}_m to the solution candidate $\Psi^{(i)}$;

end

Choose $\Psi^{(*)}$ based on Equation (2.22) on page 43;

end

number ζ of logical route candidates. This number ζ can be evaluated using:

$$\zeta(x) = \sum_{i=0}^{D_m-1} \left\{ (S - x - i) + (S - x - i)(S - 1 - i)R \right\},$$

with $0 \leq x = \sum_{\substack{p=1 \\ p \neq m}}^M D_p \leq S$. (4.1)

D_p and x denote respectively the number of logical routes allocated to MT_p and the number of all logical routes allocated to all MTs in the related VC.

Figure 4.2 plots the maximum number ζ of logical route candidates to evaluate in step 2 of SAS in order to allocate $D = 2$ logical routes to the m -th MT. The following parameters were considered: $M = 16$ MTs, $S = 32$ subcarriers, and $R = 7$ WPs including the CP. As it can be observed in Figure 4.2, as the number of MTs for which logical route allocation has been completed increases, the number ζ of logical route candidates to evaluate diminishes exponentially. In this example, while allocating two logical routes to the first MT involves the evaluation of approximately $\zeta = 11,500$ logical route candidates, just about $\zeta = 500$ candidates require evaluation to assign two logical routes to the sixteenth MT. Recall that in the SIS and RIS, logical route allocation is carried out for only one MT per iteration while the other MTs retain their allocated logical routes. Hence, in this current example, each iteration of SIS or RIS would demand the evaluation of roughly $\zeta = 500$ logical route candidates. Reallocating one MT per iteration gives rise to a linear complexity of SIS and RIS on the number I of iterations and the number ζ_{\min} , $\mathcal{O}(I\zeta_{\min})$, with ζ_{\min} being the smallest ζ of Equation (4.1). Therefore, the complexity added by reallocating logical routes using SIS or RIS can be regarded as practical for a limited number of iterations. In this example, the execution of $I = 170$ iterations of SIS (evaluation of approximately 94.000 logical route candidates) results in approximately the same degree of complexity as carrying out logical route allocation to 16 MTs using SAS (evaluation of approximately 97.000 logical route candidates).

4.1.5 Permutational Iterative Allocation Scheme (PIS)

In the SAS, the MTs are selected in a successive order for resource allocation. Since frequency reuse is applied, the order in which the MTs are selected influences the results of the algorithm. In a system with M MTs, there exist $1 \cdot 2 \cdots M$ ways to arrange the MTs. Each of these arrangements is defined as a permutation of the MTs. In a system where M is large, the application of the SAS to each of these permutations is not practical. Therefore, we have decided to apply SAS to some permutations of the MTs generated randomly. The solution candidate of the resource allocation problem in Equation (2.22) on page 43 provided by the i -th permutation $\sigma_i(\mathcal{M})$ is denoted as $\Psi^{(i)}$. For a number of P permutations we denote the set of solution candidates of the

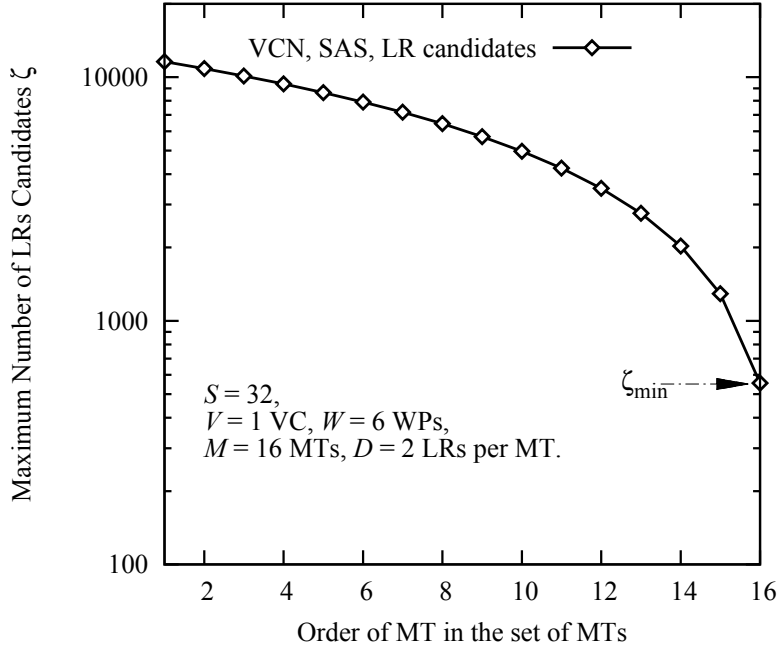


Figure 4.2: Number of logical route candidates to be evaluated based on the order an MT is selected for logical route allocation

permutational iterative allocation scheme (PIS) as:

$$\Omega^{(P)} = \{\Psi^{(1)}, \Psi^{(2)}, \dots, \Psi^{(i)}, \dots, \Psi^{(P)}\}. \quad (4.2)$$

PIS keeps track of the permutation $\Psi^{(*)}$ which provides the highest channel capacity. The Knuth shuffle method is used to generate a random permutation with equal probability. The implementation of PIS is illustrated in **Algorithm 5** on page 89.

4.1.6 Permutational Allocation Scheme Complexity

Taking into account that PIS is the iteration of SAS, its complexity is linear on the number M of MTs and the number P of random permutations generated, $\mathcal{O}(PM\zeta)$. PIS has a higher degree of complexity than SIS and RIS because one iteration of the permutational scheme requires the reallocation for all MTs while SIS and RIS would reallocate only one MT.

4.1.7 Permutational Combined Iterative Scheme (PCIS)

Applying PIS can help find some permutations of the MTs for which the level of interference between the MTs is low. However, PIS does not solve the interference issue resulting from successive allocation of logical routes to the MTs. RIS and SIS were proposed to fix this problem of interference resulting

Algorithm 5: Permutational Iterative Allocation Scheme (PIS)

Input: $\mathcal{M}, \mathcal{R}, \mathcal{S}, P$ Number of permutations.
Output: Random reallocation of logical routes
begin

```
/* Successive logical route allocation for all MTs */  
Allocate logical routes to all MTs using Algorithm 1 on page 55;  
/* Permutational scheme */  
for  $i = 1 : P$  do  
    | Generate the  $i$ -th random permutation  $\sigma_i(\mathcal{M})$ ;  
    | Allocate logical routes to all MTs using Algorithm 1 on page 55  
    | based on their order in  $\sigma_i(\mathcal{M})$ ;  
end  
Choose  $\Psi^{(*)}$  based on Equation (2.22) on page 43;  
end
```

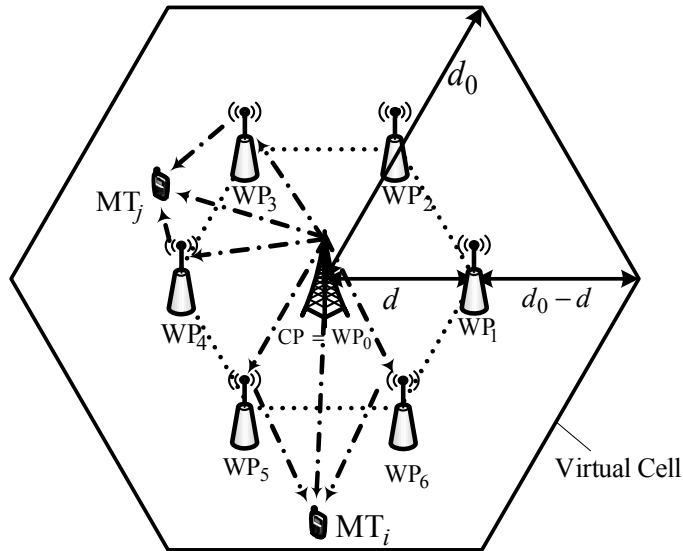


Figure 4.3: Virtual cell layout

from the successive allocation. Hence, the permutational combined iterative scheme (PCIS) combines PIS and SIS aiming at taking advantage of the capability of SIS to tackle the problem of successive allocation. In the PCIS, a random permutation of the MTs is generated, resource allocation is carried out for all MTs using SAS, and reallocation is performed starting from the first MT using SIS. For the i -th permutation $\sigma_i(\mathcal{M})$, I iterations of SIS will generate an optimal solution candidate $\Psi_i^{(*)}$. If P is the number of permutations evaluated, the set of optimal solution candidates generated by PCIS can be noted as:

$$\Omega^{(P)} = \{\Psi_1^{(*)}, \Psi_2^{(*)}, \dots, \Psi_i^{(*)}, \dots, \Psi_P^{(*)}\}. \quad (4.3)$$

The different steps of PICS are illustrated in **Algorithm 6** on page 91.

4.1.8 Permutational Combined Iterative Scheme Complexity

PCIS being a combination of PIS and SIS has a complexity of the order $\mathcal{O}(PM\zeta + PI\zeta_{\min})$. PCIS has a higher degree of complexity than PIS, SIS, and RIS.

4.1.9 Simulation Assumptions and System Model

In order to evaluate the performance of the proposed iterative schemes, we consider a single VC with 7 WPs including a CP located at the center of the VC. The VC is of a hexagonal shape. The WPs are placed at an equal distance d from the CP (see Figure 4.3). With d_0 being the radius of the VC, we define d/d_0 as the distance ratio between the CP and a WP.

Similarly as in the previous chapter, we denote by P_t/P_0 as the normalized transmission power. P_t represents the total transmission power in the VC

Algorithm 6: Permutational Combined Iterative Scheme (PCIS)

Input: $\mathcal{M}, \mathcal{R}, \mathcal{S}, P, I$.

Output: Random reallocation of logical routes

begin

/* Successive logical route allocation for all MTs */

Allocate logical routes to all MTs using **Algorithm 1** on page 55;

/* Permutational scheme */

for $i = 1 : P$ **do**

Generate the i -th random permutation $\sigma_i(\mathcal{M})$;

Allocate logical routes using **Algorithm 3** on page 85 ;

Choose $\Psi_i^{(*)}$ based on Equation (2.22) on page 43;

end

Choose $\Psi^{(*)}$ among the set $\{\Psi_1^{(*)}, \dots, \Psi_i^{(*)}, \dots, \Psi_P^{(*)}\}$ based on
Equation (2.22) on page 43;

end

and P_0 the average transmit power of the CP for which the SNR at d_0 is 0dB (see Equation (InterferenceSinceCell) on page 57). The total transmit power is equally shared among the allocated logical routes. The allocated power of a two-hop link logical route is equally distributed among each link of the logical route. A WP which is not transmitting is considered to be in off mode.

The bandwidth is divided into $S = 32$ sub-carriers. $M = 14$ MTs are generated randomly in the VC, and $D_m = 2$ logical routes are allocated per MT. We consider a path-loss exponent $\alpha = 4$, a standard deviation of the log-normally distributed shadowing loss $\sigma = 8$ dB, and $L = 8$ propagation paths independently distributed Rayleigh fading.

4.1.10 Simulation Performance

Figure 4.4 shows the plot of the ergodic channel capacity of the VCN compared with that of the SHN when the iterative schemes RIS and SIS are applied. This simulation considers the case of $I = 100$ iterations for both RIS and SIS. Figure 4.4 shows that, using SIS and RIS, reallocating the logical routes can increase the ergodic channel capacity of the VCN in the interference dominant transmission power region. By reallocating logical routes to the MTs, SIS and RIS are able to take into account the effect of interference between the logical routes and choose the logical routes which will cause the least interference in the network. Since the SHN does not suffer interference between the logical routes, its channel capacity does not change.

Figure 4.5 compares the performance of the SIS and the RIS. Figure 4.5 shows the plot of the ergodic channel capacity of the VCN based on the number of iterations for a normalized transmission power $P_t/P_0 = 20$ dB. According to Figure 4.5, the number of iterations required by SIS to converge is far smaller than that required by RIS. The first MT is the farthest MT for which interference from the logical routes of other MTs was not considered when doing resource allocation, and the second MT is the second farthest. By starting to reallocate logical routes from the first MT, the SIS can in the first iterations reallocate logical routes to all the farthest MTs for which interference was not considered when doing resource allocation. However, in the RIS, randomly choosing an MT for reallocation does not guarantee that reallocation to the farthest MTs will be done in the first iterations. Hence, SIS converges faster than RIS.

Figure 4.6 shows the plots of the ergodic channel capacity of the VCN and the SHN when the PIS and the PCIS are applied. For the VCN, $P = 10$ random permutations (PIS) and $P = 10$ random permutations with $I = 30$ iterations (PCIS) for the VCN are simulated. For the SHN, the results of $P = 20$ random permutations (PIS) are plotted in the figure. According to Figure 4.6, applying the PIS can increase the channel capacity of the VCN. As already explained, there exist some permutations of the MTs for which the level of interference between the MTs is less than for others. These specific permutations will provide higher channel capacity than the ones which have high

levels of interference. By retaining the permutation with the highest channel capacity, PIS can outperform SAS.

Figure 4.6 also shows that further enhancement can be achieved if $I = 30$ iterations of the SIS are applied to each random permutation (PCIS). This is because though the PIS can improve the channel capacity of the VCN by providing some permutations of the MTs with the lowest interference between the logical routes, it does not solve the interference problem resulting from successive allocation discussed in Section 4.1.1. Therefore, combining SIS with PIS can help to further increase the ergodic channel capacity of the VCN.

Based on Figure 4.6, we observe that even after applying PIS to the SHN, the channel capacity of the SHN does not change. This is because in the SHN there is sub-carrier reuse and therefore no intra-cell interference to mitigate.

According to the results in Figure 4.6, we also notice that the PIS and the PCIS can slightly enhance the channel capacity of the VCN in the noise dominant transmission power region compared to the SAS. PIS and PCIS are both iterative procedures derived from SAS. Being iterative schemes, they can evaluate a bigger set of solution candidates resulting in their enhanced performance compared to SAS.

Applying PCIS in a running system presents some practical challenges because PCIS requires deallocation of all MTs. This means that transmissions to all MTs would need to be stopped if the PCIS has to be applied. Despite its practical challenge, the PCIS can be considered as a valuable candidate to evaluate the performance of the other proposed iterative schemes like SIS. This is because it incorporates both the PIS, which can provide some permutations of the MTs with low interference between the logical routes, and SIS, which can solve the interference issue discussed in section 4.1.1.

Though some of the numbers of logical route candidates to evaluate ζ in the PCIS are greater than those in the SIS, to simplify performance comparison between SIS and PCIS, we assume that the values of ζ in the SIS and in the PCIS are approximately equal. Then, if $M = 14$ MTs, $I = 500$ iterations in the case of the SIS can be compared with $P = 10$ random permutations and $I' = 36$ iterations in the PCIS, $P(M + I') = I = 500$. The simulation results of the above configuration is plotted in Figure 4.7. According to Figure 4.7, the SIS can approximate the performance of the PCIS. Hence, being a less complex allocation scheme than PIS and PCIS, the SIS can be considered as a suitable candidate to alleviate the effect of interference in the VCN.

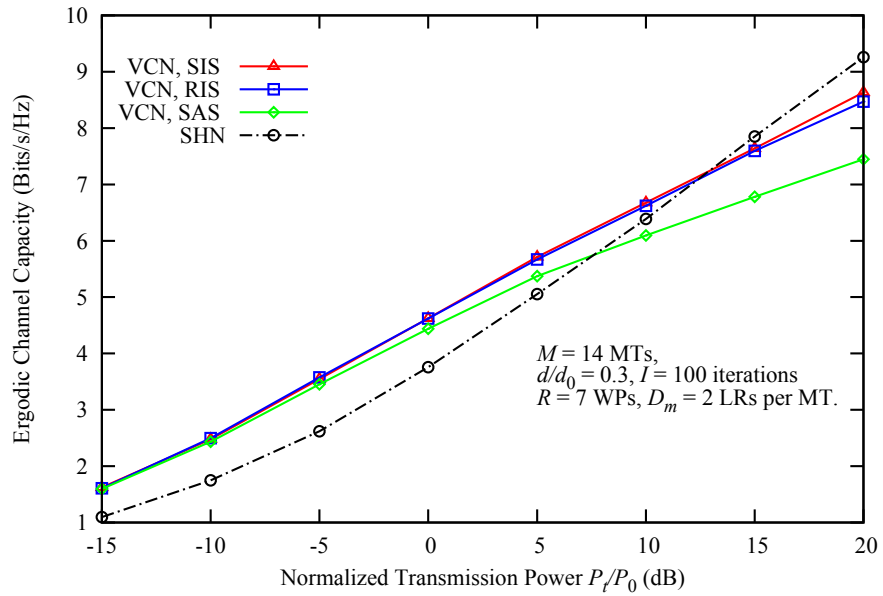


Figure 4.4: Ergodic channel capacity, SIS and RIS

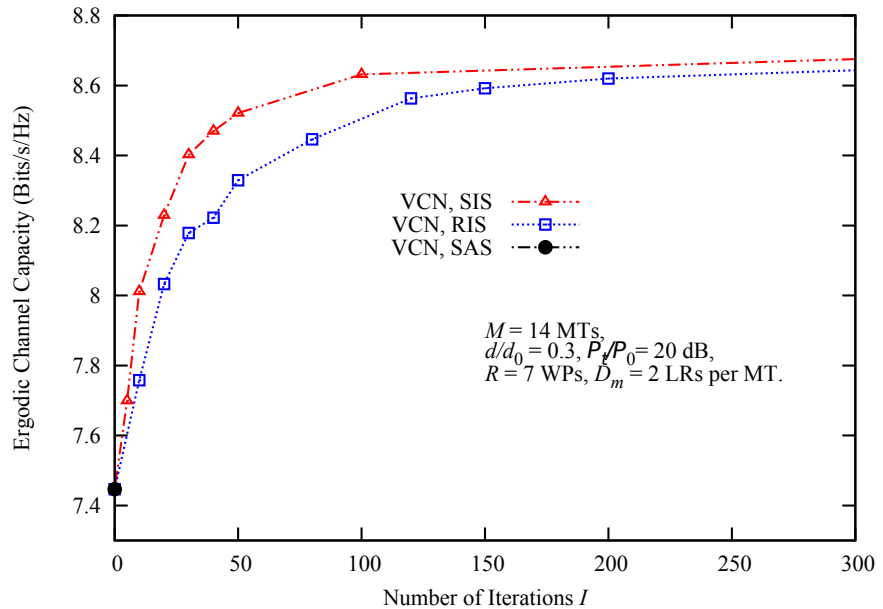


Figure 4.5: Ergodic channel capacity, SIS and RIS performance

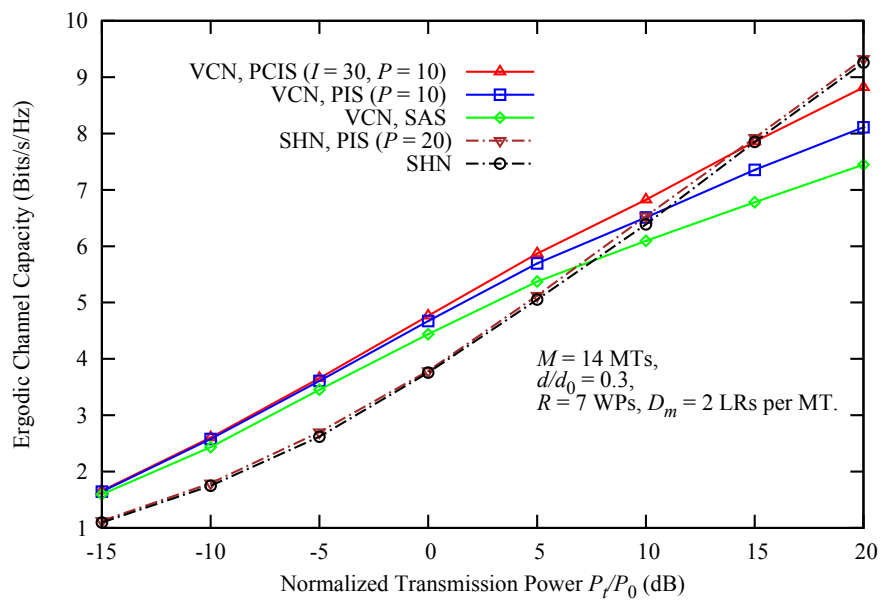


Figure 4.6: Ergodic channel capacity, PIS and PCIS

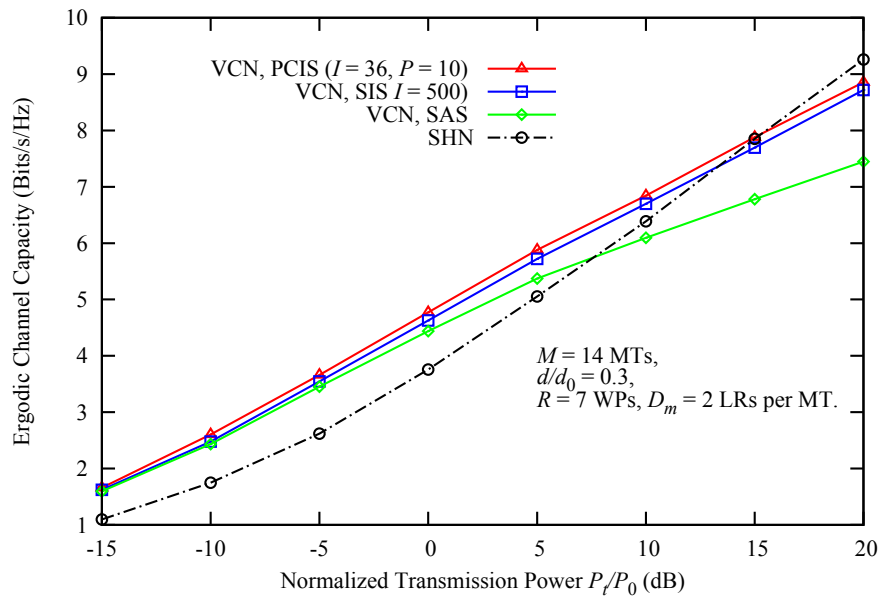


Figure 4.7: Ergodic channel capacity, SIS and PCIS comparison

4.2 Multi-cell Network

In the previous section, we proposed some iterative allocation schemes to improve the performance of the VCN in a single cell environment. Among the proposed iterative schemes, we retained the SIS because of its practical implementation and its performance. In this section, we modify the SIS to study its performance in a multi-cell interference system.

We consider a system with a set \mathcal{V} of V VCs. In the v -th VC, a set of \mathcal{R}_v of R_v WPs including the CP ensure the communication between a set \mathcal{M}_v of M_v MTs and the core network. The bandwidth of the v -th VC is divided into a set \mathcal{S}_v of S_v orthogonal sub-carriers. We assume the implementation of the parallel relaying transmission method to transmit data from the core network to the MTs.

We denote by $l_e^*(v, m, r, k_i, k_j)$ the e -th logical route candidate of the m -th MT ($MT_{m,v}$) going through the r -th WP ($WP_{r,v}$) in the v -th VC (VC_v). The sub-carriers assigned in the first-hop and second-hop links are represented respectively by k_i and k_j . We represent the set of logical route candidates of the $MT_{m,v}$ via $WP_{r,v}$ by $\mathcal{L}_{v,m,r}^*$ and the associated allocation matrix by $\mathfrak{L}_{v,m,r}^*$. We denote by $\mathcal{L}_{v,m}^*$ the set of logical route candidates of $MT_{m,v}$. The implementation of sub-carrier constraints are the same as already defined in Equation (3.13)–(3.15) on page 65.

4.2.1 Multi-Cell Sequential Iterative Allocation Scheme

We consider that a set $\mathcal{D}_{m,v}$ of logical routes is to be allocated to the m -th MT in the v -th VC. Suppose that I_v iterations of the SIS are applied in the v -th VC, we represent the solution candidate of the resource allocation problem in Equation (2.35) on page 47 produced by the i -th iteration by $\Psi_v^{(i)}$; and the optimal solution among these solution candidates as $\Psi_v^{(*)}$. The different steps of the SIS in the v -th VC is given in **Algorithm 7**.

4.2.2 Simulation Assumptions and System Model

A system with a cluster of $V = 19$ VCs positioned as in a second-tier architecture is considered (see Figure 3.12 on page 67). The wrap-around structure displayed in Figure 3.13 on page 67 is implemented as to reduce computational complexity and consequently enable faster running time. In the cluster, the VCs are assumed to be identical in the number of WPs, the VC layout used, the number of MTs, and the allocated bandwidth. The centres of two neighbouring VCs are distanced by $D = d_0\sqrt{3}$, with d_0 being the radius of a VC.

The VCs are considered to be of a hexagonal shape with a CP located at their center. A number of WPs equally distanced from the CP are distributed in each VC. To investigate the effect of the number of WPs on the performance of the VCN, the three VC layouts in Figure 3.14 on page 72, Figure 3.18, and

Algorithm 7: Multi-Cell Sequential Iterative Allocation Scheme (SIS)

Input: $\mathcal{V}, \mathcal{M}_v, \mathcal{R}_v, \mathcal{S}_v, I_v, (MT_m)_{m=1}^{M_v}$.
Output: Sequential reallocation of logical routes

```

begin
    /* Successive logical route allocation for all MTs */
    Allocate logical routes to all MTs using Algorithm 2 on page 68;
    /* Iterative reallocation of logical routes to MTs */
    for  $i = 1 : I$  do
        Choose the next MT ( $MT_{m,v}$ ) in the sequence  $(MT_m)_{m=1}^{M_v}$ ;
        Deallocate the set  $\mathcal{D}_{m,v}$  of logical routes of  $MT_{m,v}$ ;
        Modify  $\mathcal{L}_{v,m,w}^*$ ,  $\forall w \in \mathcal{R}_v$ , and update  $\mathcal{L}_{v,m}^*$  based on
        Equations (3.13)–(3.15) on page 65;
        /* Reallocate logical route to  $MT_{m,v}$  */
        repeat
            foreach  $l_e^*(v, m, r, k_i, k_j) \in \mathcal{L}_{v,m}^*$  do
                foreach  $p \in \mathcal{M}_u$ ,  $\forall u \in \mathcal{V}$  do
                    foreach  $l_h(u, p, r', k_{i'}, k_{j'}) \in \mathcal{D}_{p,u}$  do
                        Execute the Procedure InterferenceMultiCell on
                        page 69;
                    end
                    /* Recalculate SINR and capacity */
                    Evaluate  $\Gamma(l_e^*(v, m, r, k_i, k_j))$  using Equation (2.30)
                    on page 46;
                    Evaluate  $\Gamma(l_h(u, p, r', k_{i'}, k_{j'}))$  using Equation (2.30)
                    on page 46;
                    Recalculate  $C_{p,u}(\mathcal{D}_{p,u})$  using Equation (2.32) on
                    page 46;
                end
                Update  $\mathcal{L}_{v,m} \leftarrow l_e^*(v, m, r, k_i, k_j)$ ;
                Evaluate  $C_{m,v}(\mathcal{L}_{v,m})$  using Equation (2.32) on page 46;
            end
            /* Choose best logical route candidate */
            Choose  $l_e^*(v, m, r, k_i, k_j)$  according to Equation (2.35) on
            page 47;
            Add  $l_e^*(v, m, r, k_i, k_j)$  to  $\mathcal{D}_{m,v}$ ;
            /* Update the set of logical route candidates */
            Modify  $\mathcal{L}_{v,m,w}^*$ ,  $\forall w \in \mathcal{R}_v$ , and update  $\mathcal{L}_{v,m}^*$  based on
            Equations (3.13)–(3.15) on page 65;
            until  $D_{m,v}$  logical routes are allocated to  $MT_{m,v}$ ;
            Add the set  $\mathcal{D}_{m,v}$  to the solution candidate  $\Psi_v^{(i)}$ ;
        end
        Choose  $\Psi_v^{(*)}$  based on Equation (2.35) on page 47;
    end

```

Figure 3.19 on page 74 were considered. The distance between the CP and a WP is noted as d .

A multipath frequency selective fading with $L = 8$ propagation paths is assumed in all VCs. The propagation paths are considered to be independently distributed Rayleigh fading with uniformly distributed average power delay profile and equidistant delays. The delay between two consecutive paths is considered to be equal to the inverse of the sub-carrier spacing during the FFT process. The log-normally distributed shadowing loss, and the path-loss exponent are respectively chosen to be $\sigma = 8$ dB, and $\alpha = 4$, in all VCs.

$M = 14$ MTs are randomly located in each VC. The MTs are considered to be stationary during the simulation run. The allocated bandwidth in a VC is divided into $S = 32$ sub-carriers. In each VC, $D_m = 2$ logical routes are allocated per MT. The normalized transmit power $P_n = P_t/P_0$ of a VC is equally distributed among the allocated logical routes in that VC. A two-hop link logical route uniformly shares the allocated power between each link. P_t denotes the total available transmit power in a VC and P_0 the average transmit power of the CP for which the received SNR at d_0 is equal to 0dB (see Equation (InterferenceMultiCell) on page 70). The total transmit power in all VCs are considered to be equal.

The VCs are selected randomly for resource allocation. In the selected VC, logical route allocation is carried out for one MT. This process is reiterated until the completion of resource allocation to all MTs in all VCs. The SIS is applied after allocation has been completed in all VCs.

4.2.3 Simulation Performance

The dashed and the straight lines in Figure 4.8 represent the respective plots of the ergodic channel capacity, based on the normalized transmission power, of VCN and SHN when SAS and SIS are applied in a single cell environment. In Figure 4.8, the third VC layout with $R = 7$ WPs (see Figure 3.14 on page 72) is considered. A number of $I = 50$ iterations of SIS are applied. From Figure 4.8, it can be concluded that, compared to SAS, SIS can improve the ergodic channel capacity of the VCN in a single cell environment. The ergodic channel capacity of the SHN does not vary when applying SIS in a single cell environment. This is because in the case of a single cell there exists no interference between the logical routes in the SHN. Therefore, in a single cell environment, SIS is efficient only in the VCN to alleviate the effect of intra-cell interference caused by the reuse of sub-carriers. This mitigation of intra-cell interference in the VCN yields the enhancement of the ergodic channel capacity of the VCN.

The plots in Figure 4.9 are those of the ergodic channel capacity of the VCN and the SHN when SAS and SIS are applied in a multi-cell environment. Based on the results in Figure 4.9, SIS can improve the ergodic channel capacity of both networks, VCN and SHN, in a multi-cell environment. In the SHN, this improvement of the channel capacity is mainly observed in the interfer-

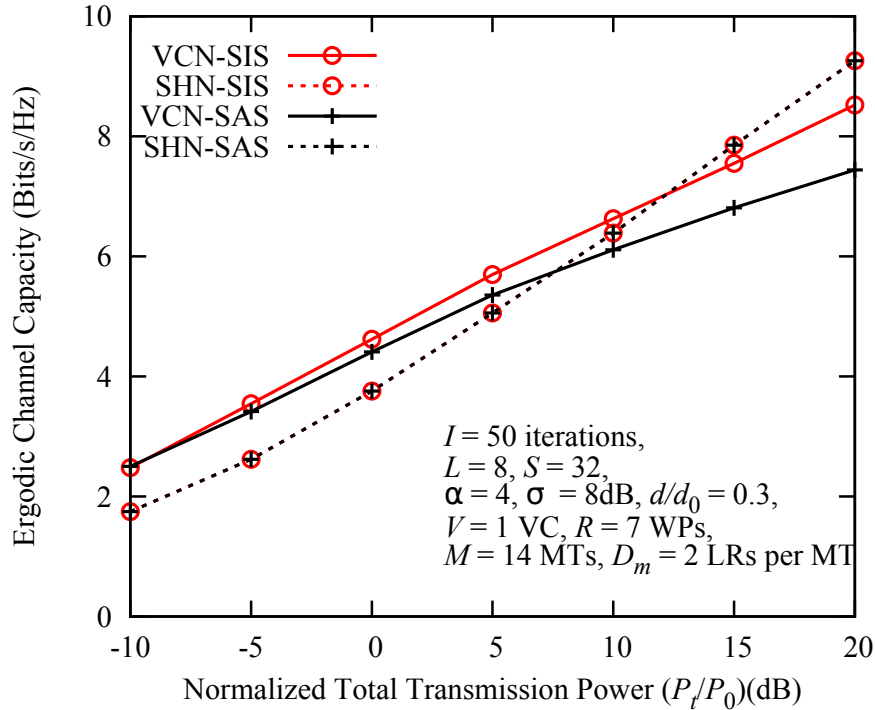


Figure 4.8: SIS and SAS single cell ergodic channel capacity

ence dominant transmission power region. This enhancement of the ergodic channel capacity of these networks is due to the reallocation of logical routes implemented by SIS. By iteratively reallocating logical routes to MTs, SIS is able to find the sets of logical route candidates which create the least intra-cell and inter-cell interference in the VCN and the least inter-cell interference in the SHN.

It should be highlighted that the performance achieved by SIS in the case of the VCN is higher than that gained in the SHN. The analysis of a single cell sheds light on the difference observed between the performances gained in those two networks. As already discussed using Figure 4.8, in a single cell environment the ergodic channel capacity of the SHN does not improve when applying SIS as there is no intra-cell interference in SHN. The additional gain observed in the VCN in a multi-cell environment relates directly to the improvement of the ergodic channel capacity of the VCN resulting from the mitigation of intra-cell interference in the VCN.

The ergodic channel capacity of the VCN, in a multi-cell environment, based on the number of iterations, when the normalized transmission power P_n equals respectively to 5dB, 10dB, and 20dB, are plotted in Fig. 4.10. Figure 4.10 also shows the simulation results when the number of MTs is $M = 10$ MTs for a normalized transmission power of $P_n = 20$ dB. It is remarked that for $M = 14$ MTs, SIS converges after an approximate number of 60 iterations,

regardless of the normalized transmission power. In the case of $M = 10$ MTs, fewer number of iterations are required for SIS to converge. With the specific simulation parameters described in Fig. 4.10, the results suggest that, for the same number of allocated LRs, the number of iterations required for convergence depends on the number of MTs. Furthermore, it can be observed that, for all the cases presented in Fig. 4.10, SIS can improve considerably the ergodic channel capacity of the VCN even if only M iterations are applied. In the case of $M = 14$ MTs and $P_n = 20\text{dB}$, the channel capacity has been increased by 7.65% for $I = 14$ iterations. This significant increase of channel capacity is obtained for $I = 10$ iterations in the case of $M = 10$ MTs (7.17%). Considering the discussion held on the complexity of SIS in subsection 4.1.4 and the results observed in Fig. 4.10, it can be concluded that the achievable gain is worth the complexity added by SIS.

To study the degree of fairness of SIS and SAS in a multi-cell environment, we consider the Jain's fairness index as the performance metric. Figure 4.11 plots the Jain's fairness index, based on the normalized transmission power, of the VCN and the SHN when SAS and SIS are applied in a multi-cell environment. The results in Figure 4.11 show that by applying SIS, a higher degree of fairness can be achieved for both networks in the interference dominant transmission power region. This amelioration of the degree of fairness is a direct consequence of the reallocation of the logical routes. By reallocating logical routes, SIS can enhance the channel capacity of those MTs which suffer the most from interference and subsequently achieve a more equitable distribution of the total channel capacity among the MTs.

In contrast to ergodic channel capacity, the outage channel capacity is more often used to evaluate the practical performance of a system. The $x\%$ outage channel capacity per MT is defined as the highest channel capacity per MT which keeps the outage probability under $x\%$. The outage probability is the probability that the required transmission rate R of an MT exceeds the channel capacity C of that MT. It is given by [1]:

$$P_{\text{out}}(R) = P[C < R] = F_{\text{cum}}(R^-). \quad (4.4)$$

In Eq. (4.4), $F_{\text{cum}}(c)$ denotes the cumulative distribution function of the channel capacity c and $F_{\text{cum}}(R^-)$ the limit-from-left of $F_{\text{cum}}(c)$ at the point $c = R$. Figure 4.12 plots the 1% and 10% outage capacity per MT, based on the normalized transmission power, of the VCN when SIS and SAS are applied in a multi-cell environment. According to Figure 4.12, reallocating logical routes to MTs using SIS can increase the outage channel capacity per MT of the VCN. The reason for this enhancement is the same as already explained in previous discussions. The increase of the ergodic channel capacity and the degree of fairness corroborates the improvement noticed in the outage channel capacity per MT.

Heretofore, the results presented have considered a cluster of $V = 19$ VCs where the VCs are constructed using the third VC layout with $R = 7$ WPs. The

remainder of the discussion will elaborate on the performance of SIS based on the number of WPs used per VC. To facilitate the analysis, the same VC layout is used in all VCs in a cluster.

Figure 4.13 plots the 10% outage channel capacity per MT based on the normalized transmission power when the respective VC layouts are considered, 4 WPs per VC (see Figure 3.19), 5 WPs per VC (see Figure 3.18), and 7 WPs per VC (see Figure 3.14) on page 72. Based on Figure 4.13, increasing the number of WPs per VC can augment the outage channel capacity per MT. This is explained by the fact that adding more WPs to a VC contributes to enhance the degree of route diversity in that VC. This increase of route diversity in the VCs yields additional outage capacity gain per MT in VCs with bigger number of WPs. This added capacity does not include the added signalling overhead generated by the addition of new WPs. It is understood that the achievable capacity might decrease after adding the effect of signalling overhead.

The Jain's fairness index of the VCN based on the normalized transmission power is plotted in Figure 4.14, when different VC layouts are used per cluster. Figure 4.14 shows that the degree of fairness of the VCN can be enhanced by increasing the number of WPs per VC. The reason of this improvement is similar to that of the outage channel capacity discussed above. With the increase of route diversity in VCs with higher number of WPs, a better distribution of the total channel capacity can be obtained.

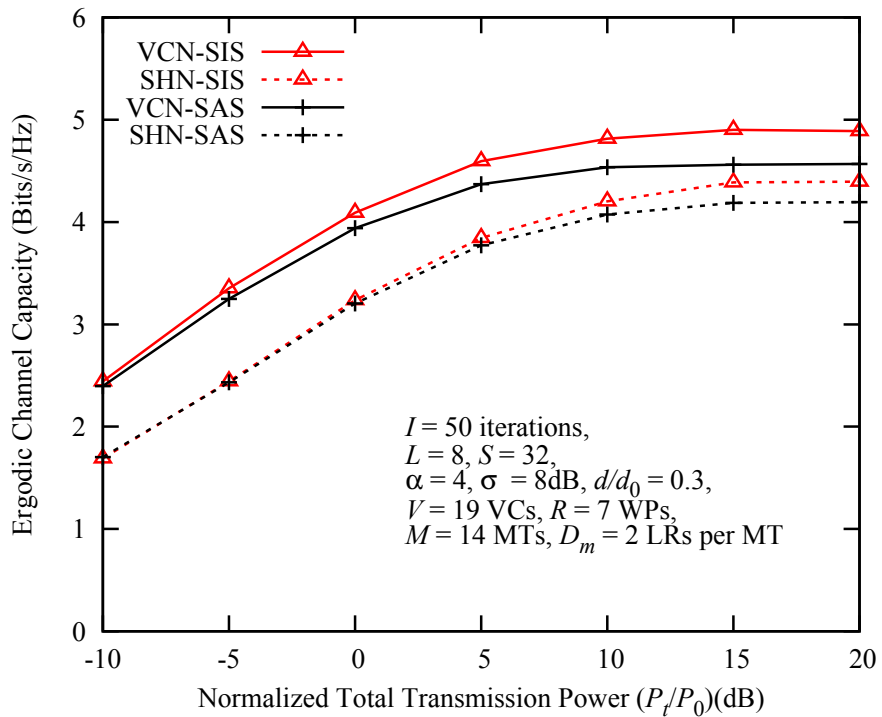


Figure 4.9: SIS and SAS multi-cell ergodic channel capacity

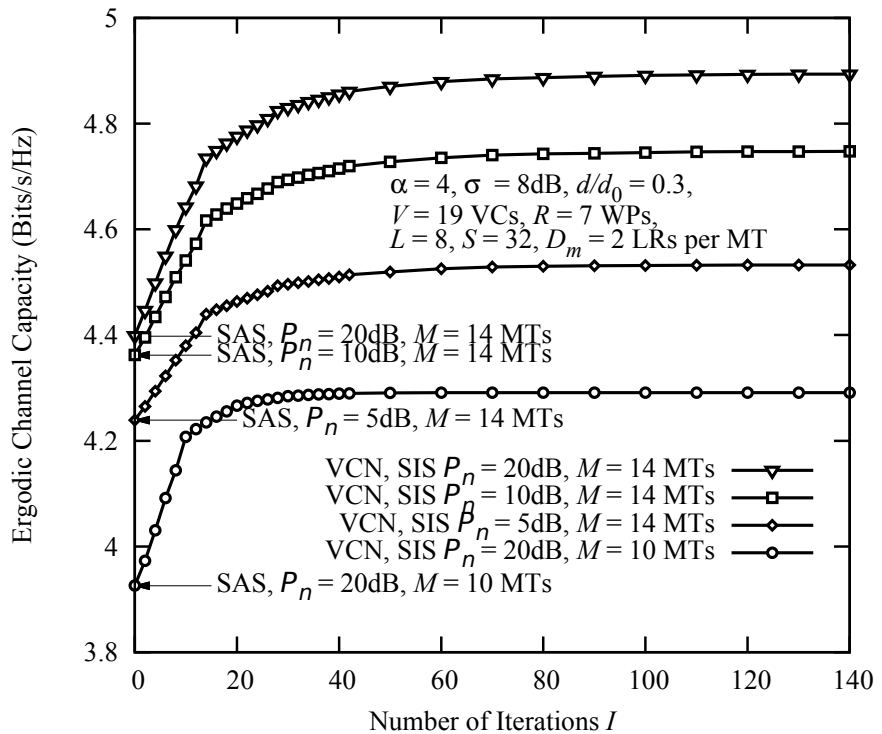


Figure 4.10: Convergence of SIS

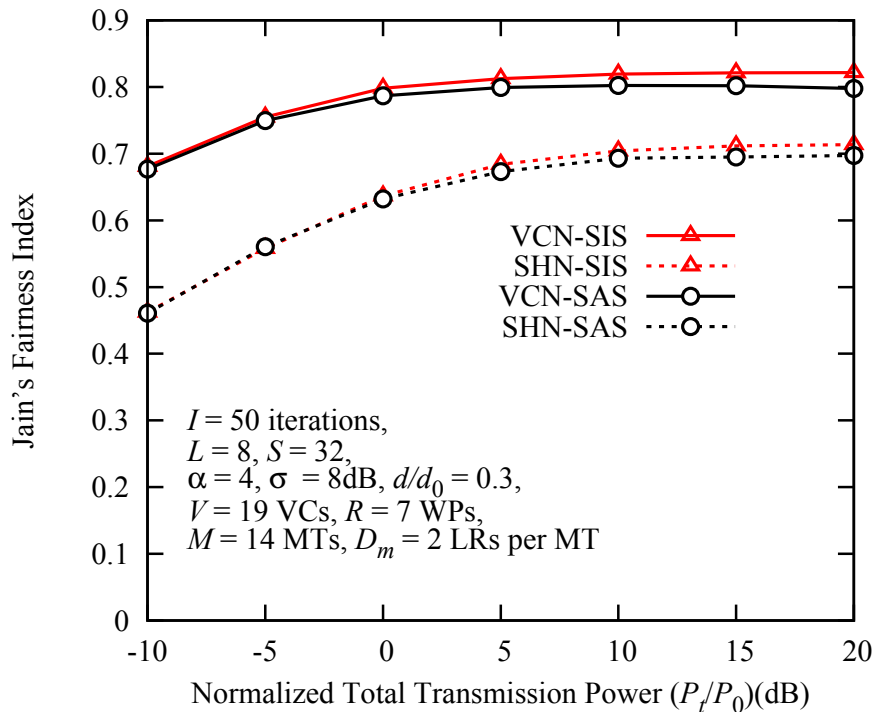


Figure 4.11: Degree of fairness of SIS and SAS

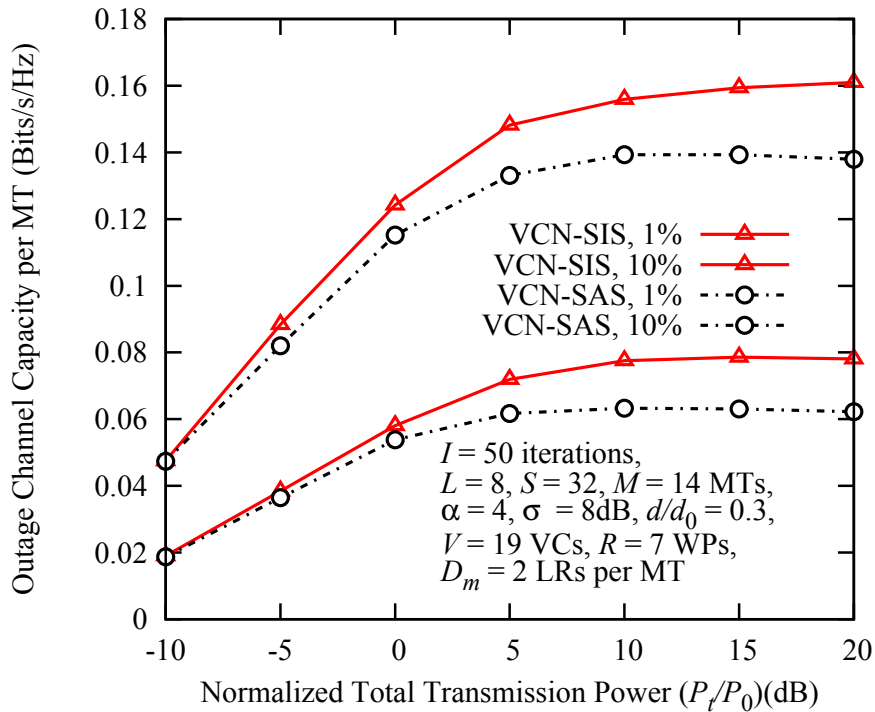


Figure 4.12: VCN, 1% and 10% outage channel capacity per MT

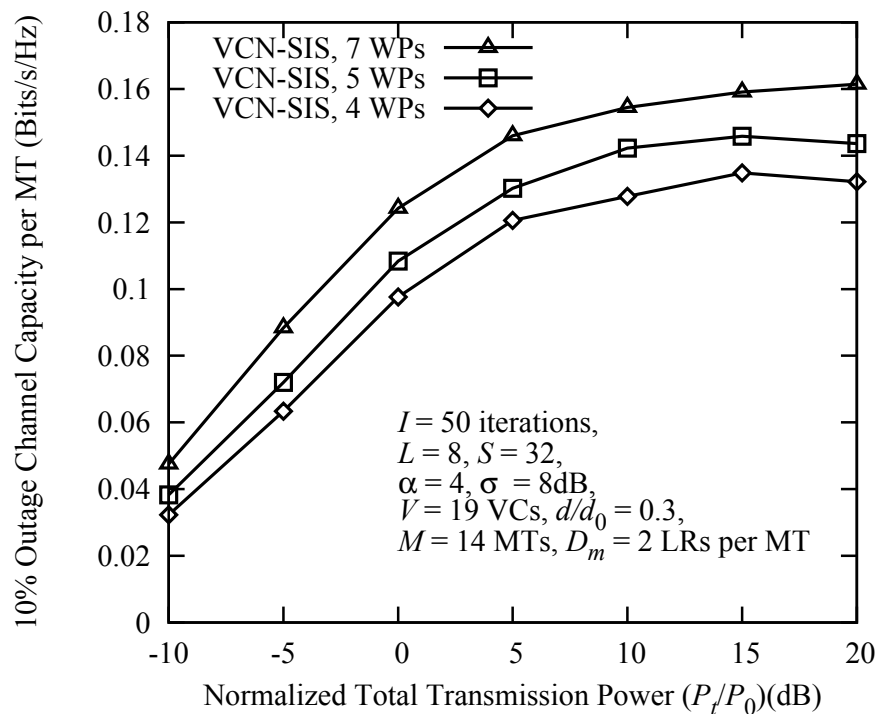


Figure 4.13: VCN, 10% outage capacity for 4, 5, and 7 WPs per VC

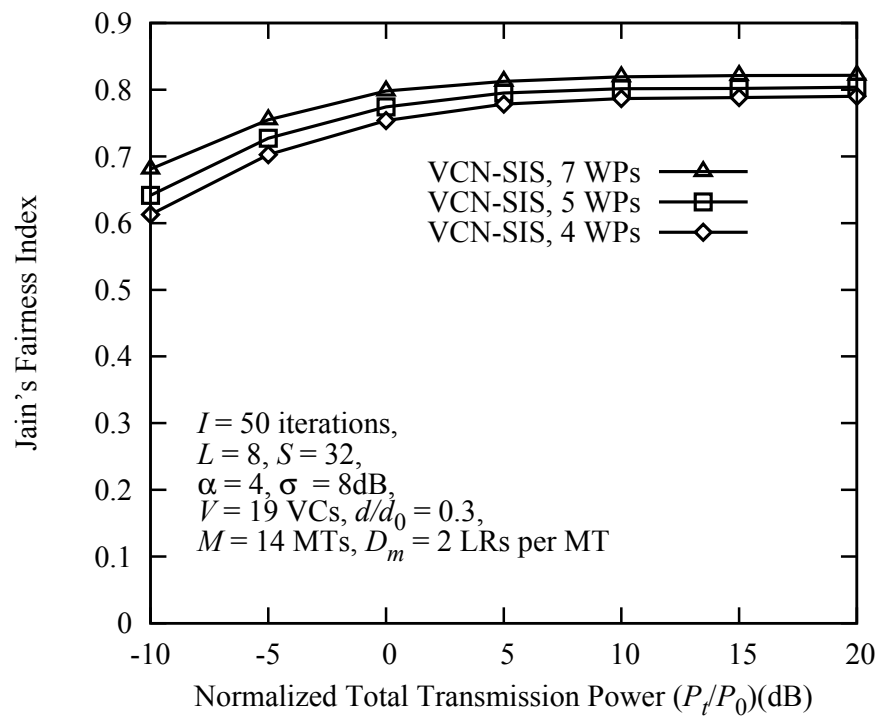


Figure 4.14: VCN, degree of fairness for 4, 5, and 7 WPs per VC

4.3 SIS Performance Comparison With Optimal Scheme

To compare the performance of the SIS with the optimal exhaustive scheme, we consider a single VC with $R = 3$ WPs including the CP as shown in Figure 3.24 on page 80. $M = 2$ MTs are randomly located in the VC and $D_m = 2$ logical routes are allocated per MT. The system bandwidth is divided into $S = 8$ sub-carriers. In Figure 4.15 we plot the ergodic channel capacity for the VCN when SIS, SAS and the exhaustive schemes are applied in a single VC. We observe that though the SIS can help improve the channel capacity of the VCN in the noise dominant transmission power region, it still remains a sub-optimal solution when compared with the optimal exhaustive scheme. This can be understood by the fact that SIS is still a successive scheme being derived from the SAS.

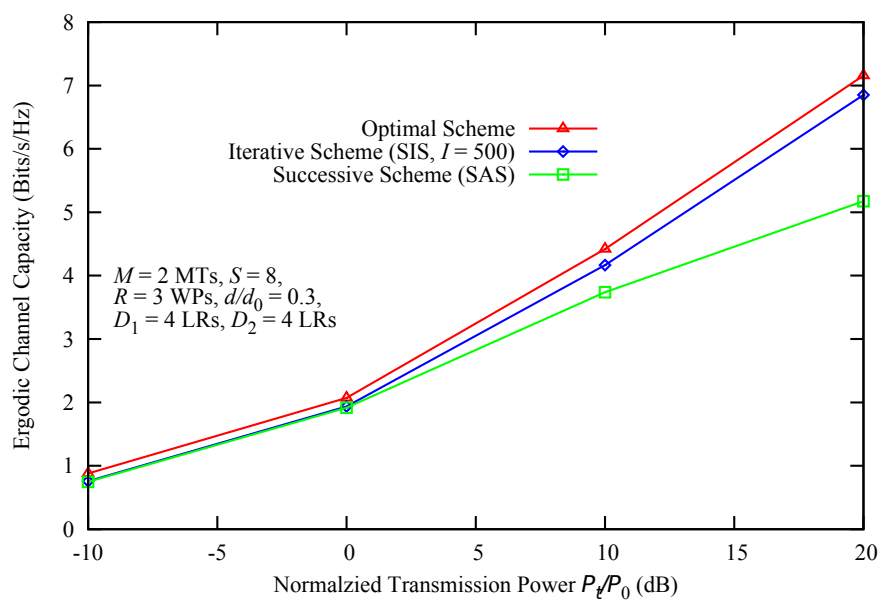


Figure 4.15: Performance of exhaustive, iterative, and successive schemes

4.4 Summary

In Chapter 3, a successive allocation scheme was proposed to solve the problem of joint route and sub-carrier allocation in a two-hop network. Though, applying SAS, the channel capacity of the two-hop networks was greater than that of the SHN for low transmission power, in the interference dominant transmission power region, the performance of the SAS degrades considerably because of intra-cell and inter-cell interference.

In order to improve the channel capacity of the VCN in the interference dominant transmission power region, in this chapter, we have investigated some iterative allocation algorithms. For a single VC, we have proposed a sequential, random, and permutational iterative allocation schemes. The permutational scheme has been later combined with the sequential iterative scheme. We have shown that all the proposed iterative schemes can improve the performance of the VCN in the interference dominant transmission power region for a single VC.

The performance of the sequential iterative scheme SIS has been compared with that of the combined iterative scheme PCIS. It was shown that the performance of the SIS approximates that of the PCIS in a single VC scenario. Taking into account the low computational complexity of the SIS and its performance, SIS was retained as the best practical scheme candidate to improve the channel capacity of the VCN in the interference dominant transmission power region.

In order to study the performance of the SIS in an inter-cell interference scenario, the single cell SIS has been modified to accommodate the study of inter-cell interference. Compared to the SAS, we have shown that SIS can improve the channel capacity of the VCN in the presence of intra-cell and inter-cell interference.

For a single cell, we have compared the performance of the SIS with that of the optimal exhaustive allocation scheme, and that of the SAS. We have remarked that, though compared to SAS, SIS can alleviate the effect of interference in the VCN, SIS still remains a sub-optimal allocation scheme when compared to the optimal allocation scheme. The aim of the next chapter is to propose an allocation scheme which can approximate the performance of the optimal solution.

CHAPTER 5

Evolutionary Allocation Scheme

In our quest for an optimal resource allocation algorithm for a two-hop cellular network, in Chapter 3, we proposed a successive allocation scheme (SAS). The performance of the SAS degrades with interference. To alleviate the effect of interference, in Chapter 4, we studied multiple iterative allocation schemes. Among the different iterative schemes, we selected a sequential iterative allocation scheme (SIS) to improve the capacity of the system in the presence of interference. Though the proposed SIS can lessen the effect of interference in the VCN, it remains a sub-optimal allocation scheme and does not guarantee the same performance as the optimal allocation scheme.

The optimal solution of the allocation problem requires simultaneous allocation of the logical routes. Therefore, in this chapter, to simultaneously allocate the logical routes and consequently approximate the performance of the optimal allocation scheme, we propose an evolutionary allocation scheme based on the evolution theory.

5.1 Evolutionary Algorithm

Evolutionary algorithms are programming methods based on the evolution theory. They have been applied in many research fields such as scheduling [46], combinatorial optimization [47], etc. Their main advantage compared to other optimization methods is their black box where few assumptions regarding the objective functions are necessary. Furthermore, they perform consistently well in many optimization problems like those previously cited. Evolutionary algorithms are inspired by biology mechanisms such as mutation, crossover, natural selection, and survival of the fittest, to refine a solution candidate iteratively. To solve the resource allocation problem in Equation (2.22) on page 43, we model the allocation problem as an evolutionary optimization problem.

5.2 Single Cell Network

We consider a single VC with a set \mathcal{R} of R WPs including the CP. We assume that parallel relaying transmission is used to communicate with a set \mathcal{M} of M MTs located in the VC. The system bandwidth is divided into a set \mathcal{S} of S

orthogonal sub-carriers. We assume that a set \mathcal{D}_m of D_m logical routes is to be allocated to the m -th MT. For further details regarding the system description please refer to section 2.2.1 on page 40.

5.2.1 Evolutionary Allocation Scheme

We denote the t -th solution candidate of the resource allocation problem in Equation (2.22) on page 43 as $\Psi^{(t)} = \{\mathcal{D}_1^{(t)}, \mathcal{D}_2^{(t)}, \dots, \mathcal{D}_m^{(t)}, \dots, \mathcal{D}_M^{(t)}\}$. $\mathcal{D}_m^{(t)}$ represents the set of logical routes allocated to the m -th MT. The set $Pop = \{\Psi^{(1)}, \Psi^{(2)}, \dots, \Psi^{(t)}, \dots, \Psi^{(P)}\}$ of P solution candidates is called a population. This population of candidates is refined using refining procedures. To solve the resource allocation problem in Equation (2.22) on page 43, we implement the nine following methods: *Creation*, *Evaluation*, *Fitness assignment*, *Archiving*, *Selection*, *Mutation*, *Crossover*, *Validation*, and *Reproduction*. They are linked as illustrated in Figure 5.1. We define a *Generation* as the cycle of the application of these four main processes to a population: *Evaluation*, *Fitness Assignment*, *Selection*, and *Reproduction*.

We define the allocation matrix $\mathfrak{T}^{(t)} = (a_{ij}^{(t)})$ of ψ rows and 4 columns associated to the solution candidate $\Psi^{(t)}$ as:

$$\mathfrak{T}^{(t)} = \begin{bmatrix} 1 & a_{12}^{(t)} & a_{13}^{(t)} & a_{14}^{(t)} \\ \vdots & \vdots & \vdots & \vdots \\ 1 & a_{D_1 2}^{(t)} & a_{D_1 3}^{(t)} & a_{D_1 4}^{(t)} \\ 2 & a_{(D_1+1) 2}^{(t)} & a_{(D_1+1) 3}^{(t)} & a_{(D_1+1) 4}^{(t)} \\ \vdots & \vdots & \vdots & \vdots \\ 2 & \vdots & \vdots & \vdots \\ \vdots & \vdots & \vdots & \vdots \\ M & \vdots & \vdots & \vdots \\ \vdots & \vdots & \vdots & \vdots \\ M & a_{\psi 2}^{(t)} & a_{\psi 3}^{(t)} & a_{\psi 4}^{(t)} \end{bmatrix}$$

$$\text{with } 0 \leq a_{i2}^{(t)} \leq R - 1, \quad 1 \leq a_{i3}^{(t)} \leq S, \quad 1 \leq a_{i4}^{(t)} \leq S, \quad \forall i \in \mathbb{N}, 1 \leq i \leq \psi. \quad (5.1)$$

\mathbb{N} represents the set of Natural numbers. The first column of $\mathfrak{T}^{(t)} = (a_{ij}^{(t)})$ contains the indices of the MTs, the second column those of the WPs, the third column those of the sub-carriers assigned in the first hop link or direct link if the WP is the CP, and the fourth column those of the sub-carriers assigned in the second-hop link or direct link if the WP is the CP.

Each row of the allocation matrix $\mathfrak{T}^{(t)}$ represents an allocated logical route. Let us consider the i -row of $\mathfrak{T}^{(t)}$, $\text{Row}_i(\mathfrak{T}^{(t)}) = [a_{i1}^{(t)}, a_{i2}^{(t)}, a_{i3}^{(t)}, a_{i4}^{(t)}]$. This row represents the e -th logical route $l_e(a_{i1}^{(t)}, a_{i2}^{(t)}, a_{i3}^{(t)}, a_{i4}^{(t)})$ allocated to the $a_{i1}^{(t)}$ -th MT via the $a_{i2}^{(t)}$ -th WP, with $a_{i3}^{(t)}$ and $a_{i4}^{(t)}$ being the sub-carriers assigned in

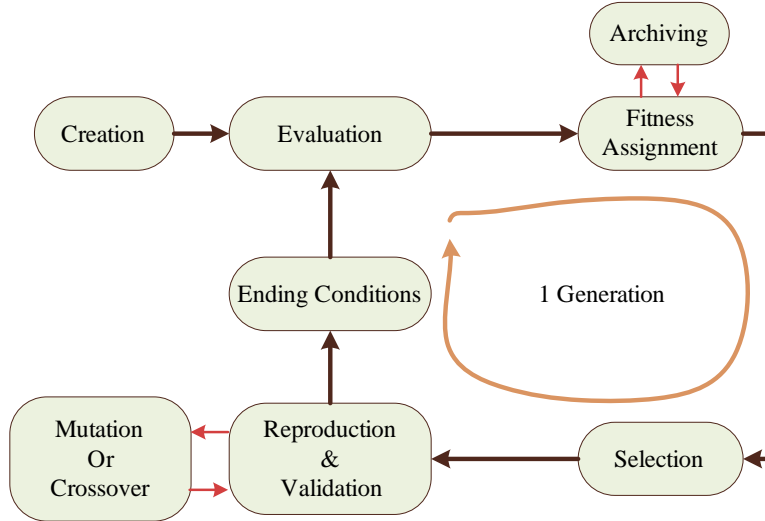


Figure 5.1: Evolutionary Scheme Layout

the first-hop and second-hop links respectively (if $a_{i2}^{(t)} = 0$, $a_{i3}^{(t)} = a_{i4}^{(t)}$). In the matrix $\mathfrak{T}^{(t)}$, the rows Row₁($\mathfrak{T}^{(t)}$) to Row _{D_1} ($\mathfrak{T}^{(t)}$) represent the set $\mathcal{D}_1^{(t)}$ of D_1 logical routes allocated to MT₁, Row _{D_1+1} ($\mathfrak{T}^{(t)}$) to Row _{D_1+D_2} ($\mathfrak{T}^{(t)}$) the set $\mathcal{D}_2^{(t)}$ of D_2 logical routes allocated to MT₂, and so on. Hence, the number of rows ψ of the allocation matrix $\mathfrak{T}^{(t)}$ is equal to the number of logical routes allocated in the VC:

$$\psi = \sum_{m \in \mathcal{M}} D_m \quad (5.2)$$

5.2.1.1 Candidate Validation Method

In the resource allocation problem in Equation (2.22) on page 43, sub-carrier reuse can be applied inside a single VC based on certain reuse constraints. To ensure that each candidate in the population complies to the sub-carrier reuse constraints, we implement a *Validation* method. For the solution candidate $\Psi^{(t)}$ to be a valid candidate, its allocation matrix $\mathfrak{T}^{(t)}$ should satisfy the following rules:

1. The first constraint states that a WP cannot receive and transmit simultaneously in the same sub-carrier. Using the allocation matrix $\mathfrak{T}^{(t)}$, this constraint is translated as:

$$\forall i \in \mathbf{N}, 1 \leq i \leq \psi, \quad \text{if } a_{i2}^{(t)} \neq 0 \Rightarrow a_{i3}^{(t)} \neq a_{i4}^{(t)}; \quad (5.3)$$

$$\forall i, i' \in \mathbf{N}, 1 \leq i, i' \leq \psi, \quad \text{if } a_{i2}^{(t)} = a_{i'2}^{(t)} \Rightarrow a_{i3}^{(t)} \neq a_{i'4}^{(t)} \text{ and } a_{i'3}^{(t)} \neq a_{i4}^{(t)}. \quad (5.4)$$

2. Based on the second constraint, multiple WPs cannot use the same sub-carrier to transmit to an MT. It is implemented as follows:

$$\forall i, i' \in \mathbf{N}, 1 \leq i, i' \leq \psi, \quad \text{if } a_{i1}^{(t)} = a_{i'1}^{(t)} \Rightarrow a_{i4}^{(t)} \neq a_{i'4}^{(t)}. \quad (5.5)$$

Furthermore, according to this same constraint, the CP cannot reuse the same sub-carrier to transmit simultaneously in multiple links. This constraint is implemented as:

$$\forall i, i' \in \mathbf{N}, 1 \leq i, i' \leq \psi, \quad a_{i3}^{(t)} \neq a_{i'3}^{(t)}. \quad (5.6)$$

An obvious constraint which is similar to the previous one is that a WP cannot use the same sub-carrier simultaneously to transmit in multiple second-hop links.

$$\forall i, i' \in \mathbf{N}, 1 \leq i, i' \leq \psi, \quad \text{if } a_{i2}^{(t)} = a_{i'2}^{(t)} \Rightarrow a_{i4}^{(t)} \neq a_{i'4}^{(t)}. \quad (5.7)$$

The *Validation* method is implemented as follows in **Procedure Validate**.

5.2.1.2 Population Creation Method

To implement the evolutionary scheme, we need an initial population of solution candidates for the allocation problem in Equation (2.22) on page 43. These candidates are created only once. The creation stage could be considered as the genesis of the algorithm.

At the creation stage, we create the initial population *Pop* with a fixed number *P* of solution candidates. Each logical route of a candidate is created using a random uniform function $\xi_{\text{unif}}()$. Given a set of elements, the random uniform function returns one of the elements chosen randomly. Using the *Validation* method, each candidate is validated before entering the population.

The WP and the sub-carriers of a logical route are chosen randomly. Taking into account that it is highly probable that the best logical routes for an MT could belong to a group of neighbouring WPs or a single WP, at the creation process, we decide that all logical routes of an MT belong to the same WP which is chosen randomly. Different logical routes of different MTs can belong to different WPs.

Though we select the sub-carriers of a logical route randomly, in order to increase the creation process of the initial population we decide to ensure that each logical route is in accordance with the sub-carrier reuse constraint in Equation (5.6) while being created. If this constraint is not taken into account while creating a logical route, generating the initial population could require a tremendous amount of computational time in the case that $\psi \approx S$. This is because the probability p_r that a candidate is invalid during the creation process increases as the number of logical routes approaches the number of available sub-carriers.

Procedure Validate

Input: $\Psi^{(t)}$, and $\mathfrak{T}^{(t)}$

Output: *valide, non-valide*

begin

 /* Validate candidate based on sub-carrier reuse
 constraints */

 Validate $\mathfrak{T}^{(t)}$ using Equations (5.3)–(5.7);

if $\mathfrak{T}^{(t)}$ passes the test **then**

 | Return *valide*;

end

else

 | Return *non-valide*;

end

end

Procedure Evaluate

Input: P, Pop **Output:** Pop : Population Evaluated**begin** **for** $t = 1 : P$ **do**

/* Take the next candidate in the population */

 $\Psi^{(t)} \leftarrow Pop;$

/* Evaluate interference between logical routes */

foreach $l_e^*(m, r, k_i, k_j) \in \Psi^{(t)}$ and $l_h(p, r', k_{i'}, k_{j'}) \in \Psi^{(t)}$ **do**

Evaluate interference using

 the **Procedure InterferenceSinceCell** on page 56; **end** Evaluate $C(\Psi^{(t)})$ using Equation (2.21) on page 42; **end****end**

Recall that the CP can only use a sub-carrier once. Consider that n logical routes, $n < \psi$, have already been created in the solution candidate $\Psi^{(t)}$. For the candidate $\Psi^{(t)}$ to be a valid candidate according to the reuse constraint in Equation (5.6), the sub-carrier in the $(n+1)$ -th logical route can only be chosen from $S - n$ sub-carriers. Since we use a random uniform function to select the sub-carriers, considering only the constraint in Equation (5.6), the probability for the $(n+1)$ -th logical route to be invalid is:

$$\begin{aligned} p_r &= 1 - \frac{S - n}{S} \\ &= \frac{n}{S}. \end{aligned} \tag{5.8}$$

If $\psi = S$, as n approaches S , the probability for the candidate to be invalid approaches 1. Hence, to reduce computational complexity during the *Creation* method, it is required to apply the sub-carrier reuse constraint in Equation (5.6). We describe the different steps of the *Creation* method in **Procedure Create** on page 114.

5.2.1.3 Population Evaluation Method

In the *Evaluation* procedure, the channel capacity of each solution candidate of the population is evaluated using the objective function Equation (2.21) on page 42. We account interference between the logical routes in a candidate using Equation (2.14) on page 41. The *Evaluation* method is described in the **Procedure Evaluate** on page 113.

5.2.1.4 Archiving Method

In our evolutionary allocation scheme, we define an *Archiving* method. The archiving method has two objectives. First, the *Archiving* method aims at

Procedure Create

Input: $P, \mathcal{R}, \mathcal{M}, \xi_{\text{unif}}(), t = 0$ **Output:** Population Pop **begin** **while** $t < P$ **do** **foreach** $m \in \mathcal{M}$ **do** /* Choose a WP for this MT and update allocation
 matrix $\mathfrak{T}^{(t)}$ */ $r \leftarrow \xi_{\text{unif}}(\mathcal{R})$; Modify $\mathfrak{T}^{(t)}$ accordingly; **for** $d = 1 : D_m$ **do** /* $\mathcal{S}^{(1)}$ set of sub-carriers not yet in-used in
 the first-hop or direct link */ $k_i \leftarrow \xi_{\text{unif}}(\mathcal{S}^{(1)})$ according to Equation (5.6); $k_j \leftarrow \xi_{\text{unif}}(\mathcal{S})$; Modify $\mathfrak{T}^{(t)}$ accordingly; Add $l_d(m, r, k_i, k_j)$ to $\Psi^{(t)}$; **end** **end** Validate $\Psi^{(t)}$ using **Procedure Validate** ; **if** $\Psi^{(t)}$ is valide **then** Add $\Psi^{(t)}$ to the population Pop ; Increment t ; **end** **end****end**

Procedure Archive

Input: φ, Pop_{fit} **Output:** $Arch$ **begin** /* Choose the φ best candidates with no duplication */ $Arch = \{C(\Psi^{(1)}) > C(\Psi^{(2)}) > \dots > C(\Psi^{(\varphi)})\};$ **end**

speeding up the convergence of the scheme by saving in memory a fixed number φ of the best solution candidates of a generation. These best candidates are selected based on their total channel capacity.

The second purpose of the *Archiving* method is to prevent each generation to run out of solution candidates. As we will notice later, in the *Reproduction* method, each candidate is validated before entering the population of the next generation. Since the *Reproduction* involves random changes in a candidate, not all candidates will be a valid candidate after being altered by these changes. At each generation the set of candidates in the archive $Arch$ is added to the current population.

We implement a non-duplicate *Archiving* method based on channel capacity preventing multiple copies of a candidate to be stored. Candidates with same total channel capacity can be highly correlated and lead to a sub-optimal solution. To prevent premature convergence and allow the algorithm to avoid sub-optimal solutions, we decide to keep only candidates which have different total channel capacity. The candidates are chosen in a decreasing order of their total channel capacity. The different steps of the *Archiving* method are implemented as follows in **Procedure Archive**.

5.2.1.5 Fitness Assignment and Archiving

Fitness assignment is the process where a certain value is attributed to a candidate based on its capacity of survival. A candidate with a high fitness value has a higher probability to be selected for mating to produce offspring for the next generation.

In the *Fitness Assignment* method that we have implemented, all candidates are ranked in a decreasing order based on their channel capacity. Those with the highest channel capacity receive the highest ranks. Before assigning a fitness value to the current population, the set of candidates in the archive $Arch$ are added to the population. The different steps are detailed in Part FitAssignArchive.

5.2.1.6 Selection Method

The selection procedure aims at selecting U candidates which will reproduce to create offspring for the next generation. One can implement an *Elite Selection* method where the candidates with the highest fitness values are chosen

Procedure FitAssignArchive

Input: $\varphi, Pop, Arch$ **Output:** New archive $Arch$, Fitted population Pop_{fit} **begin**

```

/* Add archive to the population */
Pop = Pop + Arch;
/* Sort population Pop in decreasing order of the total
   channel capacity */
 $C(\Psi^{(1)}) \geq C(\Psi^{(2)}) \geq \dots \geq C(\Psi^{(t)}) \geq \dots C(\Psi^{(P)})$ ;
/* Rank population Pop ( $A \Rightarrow rank(x)$  means  $A$  receives
   rank  $x$ ) */
 $\Psi^{(1)} \Rightarrow rank(1), \Psi^{(2)} \Rightarrow rank(2), \dots, \Psi^{(P)} \Rightarrow rank(P)$ ;
/* Assign fitness value based on rank to each candidate
   */
 $\Psi^{(1)} \Rightarrow FitValue(1), \Psi^{(2)} \Rightarrow FitValue(2), \dots, \Psi^{(P)} \Rightarrow$ 
 $FitValue(P)$ ;
 $Pop_{fit} = \{\Psi_{fit}^{(1)}, \Psi_{fit}^{(2)}, \dots, \Psi_{fit}^{(P)}\}$ ;
Archive the  $\varphi$  best candidates using Procedure Archive;

```

end

to enter the mating poll *Mate* to create offspring for the next generation. The problem with that selection method is that it can lead to a premature convergence of the algorithm. Furthermore, since we have already implemented a *Elite Fitness Assignment* method where we have attributed the highest rank to the candidate with the highest channel capacity, applying an *Elite Selection* method could prevent the algorithm to avoid sub-optimal solutions.

Instead of implementing an *Elite Selection* method, we have created a *Tournament Selection* method. In the tournament selection method, a candidate is chosen randomly from the fitted population Pop_{fit} . The chosen candidate participates in a number of competitions with other candidates also selected randomly. A competition involves only two candidates, the winner of the previous competition and the newly selected candidate. The winner of the last competition will enter the mating pool *Mate*. We allow a candidate to be selected more than once for competitions. We denote the number competitions or tournament size as T . In **Procedure TournamentSelect** we describe the different steps of the *Tournament Selection* method.

5.2.1.7 Reproduction Method

The reproduction procedure is one of the key functions in evolutionary algorithms. It aims at creating a new population of candidates from an old population. In the old population, only the candidates which were selected during the selection process will mate to produce offspring for the next generation. We have implemented two mating procedures: mutation and crossover. These procedures are explained later in **Procedure Mutate** and **Procedure Crossover**.

With equal probability, a candidate is modified using either mutation or crossover. After a candidate has been modified using one of the mating processes, the offspring which results from that process is validated using the **Procedure Validate**. Only the offspring that are valid would join the population of the next generation. The different steps of the *Reproduction* method are given in **Procedure Reproduce**.

5.2.1.8 Mutation Method

Mutation is the process by which changes occur in a candidate to create a new candidate. Most of the times these changes take place in a random manner. In our mutation method, we have implemented eight random changes. To increase the probability for an offspring to be valid during the validation process, we apply certain control during each change. We ensure that the modified logical routes are partially valid based on the definition of a logical route. This means that two different sub-carriers should be assigned to a logical route belonging to a WP which is not the CP. And if the WP is the CP, the sub-carriers have to be the same.

Procedure TournamentSelect

Input: Pop_{fit} , U , and T **Output:** $Mate$ **begin**

```

for  $u = 1 : U$  do
    /* Choose a winner candidate randomly from  $Pop_{fit}$  */
     $\Psi_{fit}^{(a)} \leftarrow \xi_{unif}(Pop_{fit})$ ;
    /* Start competition */
    for  $t = 1 : T$  do
        /* Choose a candidate randomly */
         $\Psi_{fit}^{(b)} \leftarrow \xi_{unif}(Pop_{fit})$ ;
        /* Choose winner based on maximum fitness value */
         $\Psi_{fit}^{(a)} \leftarrow \max_{fitnessvalue}(\Psi_{fit}^{(a)}, \Psi_{fit}^{(b)})$ ;
    end
    /* Add the winner to the mating poll */
    Add  $\Psi_{fit}^{(a)}$  to  $Mate$ ;
end

```

Procedure Reproduce

Input: *Mate, U***Output:** New *Pop***begin** **for** $u = 1 : U$ **do** /* Take the next candidate $\Psi^{(u)}$ in the mating poll
 Mate */ $\Psi^{(u)} \leftarrow \text{Mate};$

/* Choose process to apply */

switch $x \leftarrow \xi_{\text{unif}}(\{0, 1\})$ **do** **case** $x = 0$ /* Use mutation to create offspring $\Psi_{\text{ofs}}^{(u)}$ */ $\Psi_{\text{ofs}}^{(u)} \leftarrow \text{mutate}(\Psi^{(u)})$ using **Procedure Mutate**; **end** **case** $x = 1$ /* Choose another candidate and apply crossover
 */ $\Psi^{(v)} \leftarrow \xi_{\text{unif}}(\text{Mate});$ $(\Psi_{\text{ofs}}^{(u)}, \Psi_{\text{ofs}}^{(v)}) \leftarrow \text{crossover}(\Psi^{(u)}, \Psi^{(v)})$
 using **Procedure Crossover**; **end** **endsw** Validate $\Psi_{\text{ofs}}^{(u)}$ and $\Psi_{\text{ofs}}^{(v)}$ using **Procedure Validate**; **if** $\Psi_{\text{ofs}}^{(u)}$ or $\Psi_{\text{ofs}}^{(v)}$ are valid **then**

/* Add to the new population */

 Add $\Psi_{\text{ofs}}^{(u)}$ or $\Psi_{\text{ofs}}^{(v)}$ to *Pop*; **end** **end****end**

Definition of Neighbouring WP: Let us denote by d_{rw} the distance between WP_r and WP_w . WP_r is said to be the Neighbouring WP of WP_w written as $r \in \mathfrak{N}(w)$, if WP_r is the closest WP to WP_w :

$$\forall r, w \in \mathcal{R}, \quad r \in \mathfrak{N}(w) \Rightarrow \forall z \in \mathcal{R}, \quad d_{rw} \leq d_{zw}. \quad (5.9)$$

Definition of Neighbouring Logical Route: Consider the allocation matrix $\mathfrak{T}^{(t)}$ associated to the solution candidate $\Psi^{(t)}$. The logical routes $l_{i-1}(\dots)$ and $l_{i+1}(\dots)$ located in rows $\text{Row}_{i-1}(\mathfrak{T}^{(t)})$ and $\text{Row}_{i+1}(\mathfrak{T}^{(t)})$ are defined as the Neighbouring Logical Routes of the logical route $l_i(\dots)$ located in row $\text{Row}_i(\mathfrak{T}^{(t)})$; and we write:

$$l_{i-1}(\dots) \in \mathfrak{N}(l_i(\dots)) \quad \text{and} \quad l_{i+1}(\dots) \in \mathfrak{N}(l_i(\dots)).$$

If $i = 1$, $l_i(\dots)$ has only one neighbour $l_{i+1}(\dots)$ in row $\text{Row}_{i+1}(\mathfrak{T}^{(t)})$. If $i = \psi$, $l_i(\dots)$ has only one neighbour $l_{i-1}(\dots)$ in row $\text{Row}_{i-1}(\mathfrak{T}^{(t)})$.

In the *Mutation* procedure, we randomly select two logical routes $l_u(a_{i1}^{(t)}, a_{i2}^{(t)}, a_{i3}^{(t)}, a_{i4}^{(t)})$ and $l_v(a_{j1}^{(t)}, a_{j2}^{(t)}, a_{j3}^{(t)}, a_{j4}^{(t)})$ in the allocation matrix $\mathfrak{T}^{(t)}$ of the solution candidate $\Psi^{(t)}$. Each logical route has the same probability to be chosen. We apply the following changes to these two selected logical routes:

1. **Case 1:** The sub-carriers assigned in the second-hop link of the two randomly chosen logical routes $a_{i4}^{(t)}$ and $a_{j4}^{(t)}$ are exchanged ($A \rightsquigarrow B$ means A is replaced by B):

$$\begin{aligned} l_u(a_{i1}^{(t)}, a_{i2}^{(t)}, a_{i3}^{(t)}, a_{i4}^{(t)}) &\rightsquigarrow l_u(a_{i1}^{(t)}, a_{i2}^{(t)}, a_{i3}^{(t)}, a_{j4}^{(t)}) \\ l_v(a_{j1}^{(t)}, a_{j2}^{(t)}, a_{j3}^{(t)}, a_{j4}^{(t)}) &\rightsquigarrow l_v(a_{j1}^{(t)}, a_{j2}^{(t)}, a_{j3}^{(t)}, a_{i4}^{(t)}). \end{aligned} \quad (5.10)$$

After the exchange of the sub-carriers, if the same sub-carrier is assigned in the first-hop and second-hop links of a modified logical route, we ensure that the WP of the logical route is a CP, if that is not the case, we replace the WP by the CP. If the sub-carriers are different and that the WP of the logical route is a CP, with equal probability, we either replace the sub-carrier in the first-hop link with that in the second-hop link, or we replace the CP with a WP.

2. **Case 2:** We exchange the sub-carriers assigned in the first-hop links of the two logical routes $a_{i3}^{(t)}$ and $a_{j3}^{(t)}$:

$$\begin{aligned} l_u(a_{i1}^{(t)}, a_{i2}^{(t)}, a_{i3}^{(t)}, a_{i4}^{(t)}) &\rightsquigarrow l_u(a_{i1}^{(t)}, a_{i2}^{(t)}, a_{j3}^{(t)}, a_{i4}^{(t)}) \\ l_v(a_{j1}^{(t)}, a_{j2}^{(t)}, a_{j3}^{(t)}, a_{j4}^{(t)}) &\rightsquigarrow l_v(a_{j1}^{(t)}, a_{j2}^{(t)}, a_{i3}^{(t)}, a_{j4}^{(t)}). \end{aligned}$$

Similarly as in the first case, we ensure that the new logical routes are partially valid based on the definition of a logical route. If the sub-carriers of a modified logical route are different and that the WP is the

CP, with equal probability, we either replace the CP with a WP, or we substitute the sub-carrier in the second-hop link with that of the first-hop link.

3. **Case 3:** We exchange the WPs of the two logical routes $a_{i2}^{(t)}$ and $a_{j2}^{(t)}$:

$$\begin{aligned} l_u(a_{i1}^{(t)}, a_{i2}^{(t)}, a_{i3}^{(t)}, a_{i4}^{(t)}) &\rightsquigarrow l_u(a_{i1}^{(t)}, a_{j2}^{(t)}, a_{i3}^{(t)}, a_{i4}^{(t)}) \\ l_v(a_{j1}^{(t)}, a_{j2}^{(t)}, a_{j3}^{(t)}, a_{j4}^{(t)}) &\rightsquigarrow l_v(a_{j1}^{(t)}, a_{i2}^{(t)}, a_{j3}^{(t)}, a_{j4}^{(t)}). \end{aligned}$$

After the exchange, if the WP of a modified logical route is the CP while the sub-carriers of the two hop links are different, we replace the sub-carrier of the second-hop link by that of the first-hop link. If the WP is not the CP and that the sub-carriers are the same, we replace the sub-carrier in the second-hop link of the modified logical route by the sub-carrier in the first-hop link of the selected logical route.

4. **Case 4:** We replace the WP $a_{i2}^{(t)}$ and $a_{j2}^{(t)}$ of each of the two chosen logical routes by one of their Neighbouring WP. This means that if WP₁ and WP₂ are Neighbouring WPs, location wise, and that WP₁ was assigned in the logical route before modification, after modification, WP₂ will be the one assigned in the modified logical route.

$$\begin{aligned} \text{Be } r \in \mathfrak{N}(a_{i2}^{(t)}), \quad l_u(a_{i1}^{(t)}, a_{i2}^{(t)}, a_{i3}^{(t)}, a_{i4}^{(t)}) &\rightsquigarrow l_u(a_{i1}^{(t)}, r, a_{i3}^{(t)}, a_{i4}^{(t)}); \\ \text{Be } w \in \mathfrak{N}(a_{j2}^{(t)}), \quad l_v(a_{j1}^{(t)}, a_{j2}^{(t)}, a_{j3}^{(t)}, a_{j4}^{(t)}) &\rightsquigarrow l_v(a_{j1}^{(t)}, w, a_{j3}^{(t)}, a_{j4}^{(t)}). \end{aligned}$$

After the changes, we make sure that the modified logical routes are partially valid based on the definition of a logical route, by modifying their allocated sub-carriers.

5. **Case 5:** For each of the selected logical routes, we replace their WPs $a_{i2}^{(t)}$ and $a_{j2}^{(t)}$ with those of their Neighbouring Logical Routes $a_{(i\pm 1)2}^{(t)}$ and $a_{(j\pm 1)2}^{(t)}$:

$$\begin{aligned} \text{Be } l_{u\pm 1}(a_{(i\pm 1)1}^{(t)}, a_{(i\pm 1)2}^{(t)}, a_{(i\pm 1)3}^{(t)}, a_{(i\pm 1)4}^{(t)}) &\in \mathfrak{N}(l_u(a_{i1}^{(t)}, a_{i2}^{(t)}, a_{i3}^{(t)}, a_{i4}^{(t)})), \\ l_u(a_{i1}^{(t)}, a_{i2}^{(t)}, a_{i3}^{(t)}, a_{i4}^{(t)}) &\rightsquigarrow l_u(a_{i1}^{(t)}, a_{(i\pm 1)2}^{(t)}, a_{i3}^{(t)}, a_{i4}^{(t)}); \\ \text{Be } l_{v\pm 1}(a_{(j\pm 1)1}^{(t)}, a_{(j\pm 1)2}^{(t)}, a_{(j\pm 1)3}^{(t)}, a_{(j\pm 1)4}^{(t)}) &\in \mathfrak{N}(l_v(a_{j1}^{(t)}, a_{j2}^{(t)}, a_{j3}^{(t)}, a_{j4}^{(t)})), \\ l_v(a_{j1}^{(t)}, a_{j2}^{(t)}, a_{j3}^{(t)}, a_{j4}^{(t)}) &\rightsquigarrow l_v(a_{j1}^{(t)}, a_{(j\pm 1)2}^{(t)}, a_{j3}^{(t)}, a_{j4}^{(t)}). \end{aligned}$$

We here again ensure that the modified logical route is a partially valid logical route based on the definition of a logical route, by either assigning a randomly selected sub-carrier to the two-hops, in case the new WP is the CP and that the previous WP was not the CP; or by assigning a randomly selected sub-carrier in the seond-hop link, in case the new WP is not the CP and that the previous WP was the CP.

6. **Case 6:** We exchange the sub-carrier in the second-hop link of one of the two selected logical routes by the that of the second-hop link of a neighbouring logical route.

$$\begin{aligned} \text{Be } l_{u\pm 1}(a_{(i\pm 1)1}^{(t)}, a_{(i\pm 1)2}^{(t)}, a_{(i\pm 1)3}^{(t)}, a_{(i\pm 1)4}^{(t)}) &\in \mathfrak{N}(l_u(a_{i1}^{(t)}, a_{i2}^{(t)}, a_{i3}^{(t)}, a_{i4}^{(t)})), \\ l_u(a_{i1}^{(t)}, a_{i2}^{(t)}, a_{i3}^{(t)}, a_{i4}^{(t)}) &\rightsquigarrow l_u(a_{i1}^{(t)}, a_{i2}^{(t)}, a_{i3}^{(t)}, a_{(i\pm 1)4}^{(t)}), \\ l_{u\pm 1}(a_{(i\pm 1)1}^{(t)}, a_{(i\pm 1)2}^{(t)}, a_{(i\pm 1)3}^{(t)}, a_{(i\pm 1)4}^{(t)}) &\rightsquigarrow l_{u\pm 1}(a_{(i\pm 1)1}^{(t)}, a_{(i\pm 1)2}^{(t)}, a_{(i\pm 1)3}^{(t)}, a_{i4}^{(t)}). \end{aligned}$$

To ensure that the modified logical routes are partially valid logical routes based on the definition of a logical route, we change the WP to CP if the sub-carriers in the two hop links are the same. If the sub-carriers are different, and that the WP is the CP, we either replace the sub-carrier in the first-hop link by that in the second-hop link, or replace the CP by a WP chosen randomly.

7. **Case 7:** We apply the same changes as in the sixth case to the other randomly selected logical route $l_v(a_{j1}^{(t)}, a_{j2}^{(t)}, a_{j3}^{(t)}, a_{j4}^{(t)})$.

$$\begin{aligned} \text{Be } l_{v\pm 1}(a_{(j\pm 1)1}^{(t)}, a_{(j\pm 1)2}^{(t)}, a_{(j\pm 1)3}^{(t)}, a_{(j\pm 1)4}^{(t)}) &\in \mathfrak{N}(l_v(a_{j1}^{(t)}, a_{j2}^{(t)}, a_{j3}^{(t)}, a_{j4}^{(t)})), \\ l_v(a_{j1}^{(t)}, a_{j2}^{(t)}, a_{j3}^{(t)}, a_{j4}^{(t)}) &\rightsquigarrow l_v(a_{j1}^{(t)}, a_{j2}^{(t)}, a_{j3}^{(t)}, a_{(j\pm 1)4}^{(t)}), \\ l_{v\pm 1}(a_{(j\pm 1)1}^{(t)}, a_{(j\pm 1)2}^{(t)}, a_{(j\pm 1)3}^{(t)}, a_{(j\pm 1)4}^{(t)}) &\rightsquigarrow l_{v\pm 1}(a_{(j\pm 1)1}^{(t)}, a_{(j\pm 1)2}^{(t)}, a_{(j\pm 1)3}^{(t)}, a_{j4}^{(t)}). \end{aligned}$$

Same modifications as in **Case 6** are applied to partially validate the modified logical routes.

8. **Case 8:** If there is a subset of sub-carriers which are not in-used $\mathcal{S}_{ni} = \{s_1, s_2, \dots, s_x, \dots\}$, we replace the second-hop links of the two selected logical routes by two sub-carriers, s_x and s_y , chosen randomly from that subset. Suppose that $\mathcal{S}_{ni} \neq \emptyset$:

$$\begin{aligned} s_y &\leftarrow \xi_{unif}(\mathcal{S}_{ni}), \quad l_u(a_{i1}^{(t)}, a_{i2}^{(t)}, a_{i3}^{(t)}, a_{i4}^{(t)}) \rightsquigarrow l_u(a_{i1}^{(t)}, a_{i2}^{(t)}, a_{i3}^{(t)}, s_y); \\ s_z &\leftarrow \xi_{unif}(\mathcal{S}_{ni}), \quad l_v(a_{j1}^{(t)}, a_{j2}^{(t)}, a_{j3}^{(t)}, a_{j4}^{(t)}) \rightsquigarrow l_v(a_{j1}^{(t)}, a_{j2}^{(t)}, a_{j3}^{(t)}, s_z). \end{aligned}$$

The sub-carriers can be the same if there is only one element in the subset. If the WP of the modified logical route was the CP, we either replace the CP by a WP of a neighbouring logical route or we replace the sub-carrier in the first-hop link by that of the second-hop link.

If all sub-carriers are in use, with equal probability, we either replace the WP of the first logical route by that of the second logical route, or by a WP_r chosen randomly:

$$l_u(a_{i1}^{(t)}, a_{i2}^{(t)}, a_{i3}^{(t)}, a_{i4}^{(t)}) \rightsquigarrow l_u(a_{i1}^{(t)}, a_{i2}^{(t)}, a_{i3}^{(t)}, a_{i4}^{(t)});$$

Or,

$$r \leftarrow \xi_{unif}(\mathcal{R}), \quad l_u(a_{i1}^{(t)}, a_{i2}^{(t)}, a_{i3}^{(t)}, a_{i4}^{(t)}) \rightsquigarrow l_u(a_{i1}^{(t)}, r, a_{i3}^{(t)}, a_{i4}^{(t)}).$$

For this last change we did not apply any control to partially validate the modified logical route. There was no particular reason for not doing so.

Once a solution candidate is selected for mutation, we decide to apply two of the above proposed modifications to the candidate. The changes above are selected with different probabilities depending on the total number of allocated logical routes ψ . If the total number of logical routes to be allocated is less than the number of sub-carriers $\psi < S$, the eight changes have equal probability to be selected. However, if the number of logical routes to be allocated equals the number of sub-carriers $\psi = S$, **Case 1** to **Case 5** are chosen with probability $\frac{1}{16}$ while **Case 6** to **Case 8** are selected with probability $\frac{1}{4}$. These probability values were chosen arbitrarily. The main objective is to assign a higher probability to **Case 6**, **Case 7** and **Case 8** so that they can be selected more often in a high sub-carrier reuse environment.

We have decided to increase the probability to select **Case 6** to **Case 8** compared to **Case 1** to **Case 5**, when $\psi = S$, to decrease the probability that the modified logical routes are invalid. When $\psi = S$, the probability for a modified logical to be invalid is very high because of high frequency reuse in a candidate.

In **Case 6** and **Case 7**, exchanges occur between neighbouring logical routes while in **Case 1** to **Case 5** they happen between two randomly selected logical routes. Two neighbouring logical routes have a higher probability to belong to the same MT than two randomly selected logical routes based on the structure of the allocation matrix $\mathfrak{T}^{(t)}$ (see Equation (5.1)).

Consider the set \mathcal{D}_m logical routes allocated to the m -th MT and located as illustrated in matrix $\mathfrak{T}^{(t)}$. If $l_e(\dots)$ is the e -th logical route in the set \mathcal{D}_m ($l_e(\dots) \in \mathcal{D}_m$) and $l_u(\dots)$ a neighbouring logical route of $l_e(\dots)$ ($l_u(\dots) \in \mathfrak{N}(l_e(\dots))$), the probability $p_r(l_u(\dots) \in \mathcal{D}_m)$ that $l_u(\dots)$ belongs to the set \mathcal{D}_m is given as:

$$p_r(l_u(\dots) \in \mathcal{D}_m) = \frac{D_m - 1}{D_m}. \quad (5.11)$$

If $l_e(\dots)$ and $l_u(\dots)$ are chosen randomly ($l_e(\dots) \leftarrow \xi_{\text{unif}}(\mathfrak{T}^{(t)})$ and $l_u(\dots) \leftarrow \xi_{\text{unif}}(\mathfrak{T}^{(t)})$) and that $l_e(\dots) \in \mathcal{D}_m$, the probability that $l_u(\dots) \in \mathcal{D}_m$ is given as:

$$p_r(l_u(\dots) \in \mathcal{D}_m) = \frac{D_m}{\psi}, \quad \text{with } \psi = D_1 + D_2 + \dots + D_m + \dots + D_M. \quad (5.12)$$

It can easily be shown that for $D_m > 1$ and $\psi > D_m$, $\frac{D_m - 1}{D_m} > \frac{D_m}{\psi}$. Hence, two neighbouring logical routes have a higher probability to belong to the same MT.

If two logical routes are allocated to the same MT and belong to the same WP, they remain valid after exchanging their sub-carriers in the first-hop links or in the second-hop links. However, if they do not belong to the same MT, which happens with high probability in case of two randomly selected logical

routes, exchanging their sub-carriers in the first-hop links or second-hop links has a non null probability which results in invalid logical routes.

In **Case 8** we try to assign a sub-carrier which is not in use. Hence, if there exist sub-carriers which are not in use, modified logical routes resulting from this case have a high probability to be valid because there is no sub-carrier reuse with the introduction of a new sub-carrier.

We could possibly derive other changes to apply as mutation. However, during the simulation process we have achieved enough performance with the following ones that we did not bother creating new ones. We understand this list of changes is not exhaustive. The mutation method is detailed in **Procedure Mutate**.

5.2.1.9 Crossover Method

The *Crossover* method is the reproduction method by which two candidates exchange part of their information to create two new offspring. The *Crossover* method that we have implemented is very simple. With equal probability, we either exchange one or two logical routes selected randomly from the two candidates. In order not to change the number of allocated logical routes per MT, we only exchange the WP and the sub-carriers when exchanging the logical routes between the candidates in the matrix $\mathfrak{T}^{(u)}$ associated to the candidate $\Psi^{(u)}$. Because of the sub-carrier reuse constraints, the modifications which can happen during crossover are limited to the two above. The different steps of the crossover method are detailed in **Procedure Crossover**.

5.2.1.10 Evolutionary Algorithm Core

The different methods previously described are connected to produce the set of the best candidates after G generations. At the end of the algorithm, the best candidates in the archive $Arch$ represent the optimal solutions found by the algorithm. The different steps are detailed in **Algorithm 8**.

5.2.2 Sub-Carrier Pair Allocation Scheme

A sub-carrier pair allocation scheme (SPA) was proposed in the literature for a two-hop network. We have decided to compare its performance with that of the evolutionary scheme as SPA was proposed as an optimal allocation scheme for two-hop networks. We have considered SPA because it is said to be an optimal scheme for two-hop systems when the sub-carriers in the two hops are different [41, 42]. Furthermore, its optimality does not depend on whether equal power allocation or optimal power allocation is considered [42].

We modify the SPA so to adapt it to multi-user allocation with sub-carrier reuse. In the modified version of SPA, the MTs are selected successively for sub-carrier-pair allocation. After allocation to an MT, the set of sub-carrier-pairs of the following MT is constructed using the constraints in Equa-

Procedure Mutate

Input: $\Psi^{(t)}$, S , $\mathfrak{T}^{(t)}$, and ψ
Output: New Offspring $\Psi_{\text{of}}^{(t)}$

```

begin
  for i = 1 : 2 do
    /* Choose randomly two logical routes */
     $l_u(a_{i1}^{(t)}, a_{i2}^{(t)}, a_{i3}^{(t)}, a_{i4}^{(t)}) \leftarrow \xi_{\text{unif}}(\mathfrak{T}^{(t)});$ 
     $l_v(a_{j1}^{(t)}, a_{j2}^{(t)}, a_{j3}^{(t)}, a_{j4}^{(t)}) \leftarrow \xi_{\text{unif}}(\mathfrak{T}^{(t)});$ 
    if  $\psi < S$  then
      | Choose change to apply with equal probability;
    end
    else
      | Choose cases Case 1 to Case 5 with probability  $\frac{1}{16}$ , and
      | cases Case 6 to Case 8 with probability  $\frac{1}{4}$ ;
    end
    switch  $x \leftarrow \xi_{\text{unif}}(\{1, 2, 3, \dots, 8\})$  do
      case  $x = 1$ 
        | Apply changes in Case 1;
      end
      case  $x = 2$ 
        | Apply changes in Case 2;
      end
      case  $x = 3$ 
        | Apply changes in Case 3;
      end
      case  $x = 4$ 
        | Apply changes in Case 4;
      end
      case  $x = 5$ 
        | Apply changes in Case 5;
      end
      case  $x = 6$ 
        | Apply changes in Case 6;
      end
      case  $x = 7$ 
        | Apply changes in Case 7;
      end
      case  $x = 8$ 
        | Apply changes in Case 8;
      end
    endsw
  end
end
```

Procedure Crossover

Input: $\Psi^{(t)}, \mathfrak{T}^{(t)}, \Psi^{(v)}, \mathfrak{T}^{(v)}$,

Output: New Offspring $\Psi_{\text{ofs}}^{(t)}$ and $\Psi_{\text{ofs}}^{(v)}$

begin

```

switch  $x \leftarrow \xi_{\text{unif}}(\{1, 2\})$  do
    case  $x = 1$ 
        /* Exchange one logical route between candidates
         */
         $i \leftarrow \xi_{\text{unif}}(\{1, 2, 3, \dots, \psi\})$ ;
         $l_e(a_{i1}^{(t)}, a_{i2}^{(t)}, a_{i3}^{(t)}, a_{i4}^{(t)}) \in \Psi^{(t)}$  and  $l_e(a_{i1}^{(v)}, a_{i2}^{(v)}, a_{i3}^{(v)}, a_{i4}^{(v)}) \in \Psi^{(v)}$ ;
         $l_e(a_{i1}^{(t)}, a_{i2}^{(t)}, a_{i3}^{(t)}, a_{i4}^{(t)}) \rightsquigarrow l_e(a_{i1}^{(t)}, a_{i2}^{(v)}, a_{i3}^{(v)}, a_{i4}^{(v)})$ ;
         $l_e(a_{i1}^{(v)}, a_{i2}^{(v)}, a_{i3}^{(v)}, a_{i4}^{(v)}) \rightsquigarrow l_e(a_{i1}^{(v)}, a_{i2}^{(t)}, a_{i3}^{(t)}, a_{i4}^{(t)})$ ;
    end
    case  $x = 2$ 
        /* Exchange two logical routes between candidates
         */
         $i \leftarrow \xi_{\text{unif}}(\{1, 2, 3, \dots, \psi\})$ ;
         $l_e(a_{i1}^{(t)}, a_{i2}^{(t)}, a_{i3}^{(t)}, a_{i4}^{(t)}) \rightsquigarrow l_e(a_{i1}^{(t)}, a_{i2}^{(v)}, a_{i3}^{(v)}, a_{i4}^{(v)})$ ;
         $l_e(a_{i1}^{(v)}, a_{i2}^{(v)}, a_{i3}^{(v)}, a_{i4}^{(v)}) \rightsquigarrow l_e(a_{i1}^{(v)}, a_{i2}^{(t)}, a_{i3}^{(t)}, a_{i4}^{(t)})$ ;
         $j \leftarrow \xi_{\text{unif}}(\{1, 2, 3, \dots, \psi\})$ ;
         $l_e(a_{j1}^{(t)}, a_{j2}^{(t)}, a_{j3}^{(t)}, a_{j4}^{(t)}) \rightsquigarrow l_e(a_{j1}^{(t)}, a_{j2}^{(v)}, a_{j3}^{(v)}, a_{j4}^{(v)})$ ;
         $l_e(a_{j1}^{(v)}, a_{j2}^{(v)}, a_{j3}^{(v)}, a_{j4}^{(v)}) \rightsquigarrow l_e(a_{j1}^{(v)}, a_{j2}^{(t)}, a_{j3}^{(t)}, a_{j4}^{(t)})$ ;
    end
endsw

```

end

Algorithm 8: Evolutionary Allocation Scheme (EAS)

Input: $\mathcal{M}, \mathcal{R}, \mathcal{S}, P, G, \varphi, U, T, \xi_{\text{unif}}()$

Output: Arch containing the best solution candidates

```

begin
     $g \leftarrow 0;$ 
    /* Create initial population */
     $\text{Pop} \leftarrow \text{create}(\mathcal{M}, \mathcal{R}, \mathcal{S}, P)$  using Procedure Create;
    while  $g < G$  do
        /* Evaluate population */
         $\text{Pop} \leftarrow \text{evaluate}(\text{Pop})$  using Procedure Evaluate;
        /* Assign fitness value and archive best candidates */
        /*
        */
         $\text{Pop}_{\text{fit}}, \text{Arch} \leftarrow \text{FitnessAssignArchive}(\text{Pop}, \text{Arch}, \varphi)$ 
        using Procedure FitAssignArchive;
        /* Select candidates for reproduction */
         $\text{Mate} \leftarrow \text{TournamentSelection}(\text{Pop}_{\text{fit}}, U, T)$ 
        using Procedure TournamentSelect;
        Increment  $g$ ;
        /* Reproduce to create new offspring */
         $\text{Pop} \leftarrow \text{Reproduce}(\text{Mate})$  using Procedure Reproduce;
    end
end

```

Algorithm 9: sub-carrier Pair Allocation Scheme (SPA)

Input: $\mathcal{M}, \mathcal{R}, \mathcal{S}$
Output: $\Psi^{(*)}$ best solution candidate

begin

foreach $r \in \mathcal{R}$ **do**

/* Sort sub-carriers in first-hop link based on SNR
 */
 $\mathcal{S} = \{\gamma_{WP_0-WP_r}(k_1) \geq \gamma_{WP_0-WP_r}(k_2) \geq \dots \geq \gamma_{WP_0-WP_r}(k_i) \geq \dots \geq \gamma_{WP_0-WP_r}(k_S)\};$
 /* Sort sub-carriers in second-hop link based on SNR
 */

foreach $m \in \mathcal{M}$ **do**

$\mathcal{S} = \{\gamma_{WP_r-MT_m}(k'_1) \geq \gamma_{WP_r-MT_m}(k'_2) \geq \dots \geq \gamma_{WP_r-MT_m}(k'_i) \geq \dots \geq \gamma_{WP_r-MT_m}(k'_S)\};$
 /* Pair sorted sub-carriers */
 $(\gamma_{WP_0-WP_r}(k_1), \gamma_{WP_r-MT_m}(k'_1));$
 $\vdots \quad \vdots;$
 $(\gamma_{WP_0-WP_r}(k_i), \gamma_{WP_r-MT_m}(k'_i));$
 $\vdots \quad \vdots;$
 $(\gamma_{WP_r-MT_m}(k_S), \gamma_{WP_r-MT_m}(k'_S));$
 If $k_i = k'_i$, exchange k'_i with k'_{i+1} ;
 $(\gamma_{WP_0-WP_r}(k_1), \gamma_{WP_r-MT_m}(k'_1)) \Rightarrow l_1^*(m, r, k_1, k'_1);$
 $(\gamma_{WP_0-WP_r}(k_i), \gamma_{WP_r-MT_m}(k'_i)) \Rightarrow l_e^*(m, r, k_i, k'_i);$
 $(\gamma_{WP_0-WP_r}(k_S), \gamma_{WP_r-MT_m}(k'_S)) \Rightarrow l_{D_r}^*(m, r, k_i, k'_S);$
 D_r is the number of sub-carrier pairs candidate in WP_r ;
 /* Evaluate capacity of sub-carrier pair */
 Evaluate SINR $\Gamma(l_e^*(m, r, k_i, k'_i))$ using Equation (2.15)
 on page 42;
 Evaluate $C(l_e^*(m, r, k_i, k'_i))$ using Equation (2.18)
 on page 42;
 /* Evaluate average capacity for this WP */
 Evaluate $C(m, r) = \frac{1}{D_r} \sum_{e=1}^{D_r} C(l_e^*(m, r, k_i, k'_i));$
 /* Select best WP_w based on average capacity */
 Select w so that $\forall z \in \mathcal{R}, C(m, w) \geq C(m, z)$;
 /* Allocate sub-carrier pair from best WP */
 $\mathcal{D}_m = \{l_1^*(m, w, k_1, k'_1), l_2^*(m, w, k_2, k'_2), \dots, l_{D_m}^*(m, w, k_i, k'_i)\};$
 If there is not enough sub-carrier pairs from WP_w choose
 from the next best WP;

end

end

end

tion (3.1)– (3.3) on page 51. The baseline approach of sub-carrier-pairs allocation to the m -th MT is as follows in **Algorithm 9**.

5.2.3 Simulation Assumptions and System Model

A single VC of a hexagonal shape has been considered. The radius of the VC is denoted by d_0 , and the distance between the CP and a WP by d . In a VC, all WPs are located at the same distance from the CP. The CP is located at the center of the VC.

We have defined the normalized transmission power as P_t/P_0 , where P_0 is the average transmission power for which the SNR at d_0 is 0dB, and P_t the total transmit power of the VC (see Equation (InterferenceSinceCell) on page 57). P_t/P_0 is equally distributed among all allocated logical routes in a VC. A 2-hop link logical route equally shared the allocated power between each link. We consider a path-loss exponent $\alpha = 4$, a standard deviation of the log-normally distributed shadowing loss $\sigma = 8$ dB, and $L = 8$ propagation paths independently distributed Rayleigh fading. The system bandwidth is divided into $S = 32$ sub-carriers; and 2 logical routes are allocated per MT.

5.2.4 Simulation Performance

In the simulations, we consider a single VC with $R = 7$ including the CP as illustrated in Figure 4.3 on page 90. The following parameter values have been used; for EAS, the initial population is set to $P = 800$, the number of candidates in the archive $\varphi = 300$, the number of generations $G = 1500$, and the number of mates $U = 1000$. As for SIS, $I = 500$ iterations have been simulated.

Figure 5.2 plots the ergodic channel capacity of the VCN based on the normalized transmission power for the different schemes EAS, modified-SPA, and SIS. A number of $M = 14$ MTs are uniformly located in the VC, and $D_m = 2$ logical routes or sub-carrier-pairs are allocated per MT. Figure 5.2 shows that the evolutionary scheme considerably outperforms the iterative and the modified-SPA schemes, in the interference dominant transmission power region. This is because the evolutionary scheme simultaneously allocates resources to MTs while the other schemes implement a successive allocation of resources to MTs. Hence, a better degree of route and frequency diversity can be achieved. According to Figure 5.2, the iterative scheme provides better ergodic capacity than the modified-SPA scheme. This is because, compared to the modified-SPA scheme, the iterative scheme can provide a better degree of route and frequency diversity by considering that the logical routes of an MT can be allocated from different WPs. In the modified-SPA, the sub-carrier-pairs of an MT are taken from the best WP.

Figure 5.3 shows the plots of the ergodic channel capacity of the evolutionary, and the iterative schemes (EAS, SIS) based on the number of generations and iterations when $P_t/P_0 = 20$ dB, $M = 10$ MTs, and $D_m = 3$ logical routes are

allocated per MT. The channel capacity of the modified-SPA scheme is also shown for comparison. The results show that even for a few generations or iterations, the evolutionary and the iterative schemes greatly outperform the modified-SPA scheme. It can also be noted that the iterative scheme saturates after $I = 150$ iterations while the capacity of the VCN can still be improved by 10% if the evolutionary scheme is applied until 600 generations. These results further corroborate the high performance of the evolutionary scheme compared to the other schemes.

Figure 5.4 represents the plots of the degree of fairness of the VCN for the different schemes (EAS, modified-SPA, and SIS) with $D_m = 2$ logical routes allocated per MT and $M = 14$ MTs. The degree of fairness is evaluated using the Jain's fairness index [45] defined in Equation (3.17) on page 75.

According to Figure 5.4, the evolutionary scheme achieves better degree of fairness than the other schemes in the interference dominant transmission power region, and the modified-SPA scheme performs the worst. In the interference dominant transmission power region, for the successive schemes, the channel capacity of the former MTs will degrade considerably as interference will be added from resource allocation to later MTs. This degradation will result in an unfairly shared resource between the MTs. As for the evolutionary scheme, since it considers the simultaneous allocation of the MTs, it can provide a more fair allocation of the resources to the MTs.

Figure 5.4 also shows that the other schemes slightly outperform the evolutionary scheme in the noise dominant transmission power region. These results suggest that, in the absence of intra-cell interference, successively allocating resources to MTs can slightly improve the degree of fairness compared to the simultaneous allocation. By successively assigning logical routes to MTs, the SIS and the modified-SPA maximize the capacity of each MT at each allocation. As for the evolutionary scheme, the maximization focuses more on a global scale. Therefore, in the noise dominant transmission power region, the channel capacity of the edge users in the evolutionary scheme is expected to be less than that of the edge users in the SIS and the modified-SPA. This disparity explains the reason why the successive schemes marginally provide a better degree of fairness than the evolutionary scheme in the noise dominant transmission power region.

Figure 5.5 plots the 1% and 10% outage channel capacity per MT of the VCN, represented respectively by the dash-dotted lines and the straight lines, for the different schemes with $D_m = 2$ logical routes allocated per MT and $M = 14$ MTs. The $x\%$ outage capacity per MT represents the highest channel capacity per MT which keeps the outage probability under $x\%$. The outage probability is defined as the probability that the required transmission rate of an MT exceeds the channel capacity of that MT. According to Fig. 5.5, compared to the other schemes, the evolutionary scheme can significantly increase the outage channel capacity in the interference dominant transmission power region. This is a consequence of the greater ergodic channel capacity observed in Figure 5.2. In the noise dominant transmission power region, all

the schemes perform almost the same.

The ergodic channel capacity of the VCN based on the number of MTs when the evolutionary, the iterative, and the modified-SPA schemes are applied is plotted in Figure 5.6. The straight lines, dashed dotted lines, and dotted lines represent the channel capacity when the normalized transmission power P_t/P_0 is 30dB, 10dB, and -10dB, respectively. Two logical routes are allocated per MT. Figure 5.6 shows that in the absence of intra-cell interference (noise dominant transmission power region – $P_t/P_0 = -10$ dB, low probability of sub-carrier reuse – from $M = 2$ to $M = 8$ MTs) the evolutionary, the iterative, and the modified-SPA schemes achieve almost the same performance. However, in the presence of intra-cell interference (interference dominant transmission power region – $P_t/P_0 = 10$ dB or 30dB, high probability of sub-carrier reuse – from $M = 8$ to $M = 16$ MTs) the evolutionary scheme outperforms the iterative and the modified-SPA schemes. The modified-SPA scheme presents the worst performance. The reason for this observation is the same as already explained in Figure 5.2. In the presence of intra-cell interference, simultaneously allocating logical routes to MTs yields better performance than successively assigning resources to MTs. It can also be noted, in the interference dominant transmission power region, the capacity of the modified-SPA scheme degrades as the number of MTs increases from $M = 8$ to $M = 16$ MTs. With $S = 32$ sub-carriers, the maximum number of 2-hop links logical routes which can be allocated without sub-carrier reuse is 16. Allocating more logical routes than this number will increase the probability of assigning logical routes with sub-carrier reuse. In this simulation, two logical routes are allocated per MT. Hence, increasing the number of MTs from $M = 8$ to $M = 16$ augments the probability of using logical routes with sub-carrier reuse. The performance of a scheme which does not incorporate any interference control during the assignment of logical routes will deteriorate as the number of MTs increases from $M = 8$ to $M = 16$ because of the added interference between the logical routes.

In the following simulations, we consider only EAS and SIS. Different number of WPs per VC have been considered. They are respectively 1 WP located at a distance d from the CP ($R = 2$ WPs), 2 WPs located at the edge of a line going through the center of the VC ($R = 3$ WPs), 3 WPs located at the edge of an equilateral triangle whose center is the CP ($R = 4$ WPs), 4 WPs located at the edge of a square whose center is the CP ($R = 5$ WPs), and 6 WPs located at the edge of a hexagon whose center is also the CP ($R = 7$ WPs).

Figure 5.7 plots the ergodic channel capacity of the VCN based on the normalized transmission power for different number of WPs per VC when EAS is applied. The case of $R = 1$ WP represents the SHN Figure 5.7 shows that as the number of WPs increases the ergodic channel capacity of the VCN augments. This augmentation is a consequence of the additional degree of route diversity created by the added WPs. It can be noticed that the improvement gained in the noise dominant transmission power region is more significant than that achieved in the interference dominant transmission power region.

This difference can be understood by the fact that, in the interference dominant transmission power region, the usage of WPs will increase the probability to select logical routes of 2-hop link and create more intra-cell interference in the VCN because of sub-carrier reuse. Therefore, to prevent intra-cell interference, the optimal solution provided by EAS will mainly be composed of logical routes of direct link which will create less intra-cell interference. As a consequence, adding more WPs will not generate any additional gain in a single cell environment in case of high transmission power.

The ergodic channel capacity based on the number of WPs when SIS and EAS are applied is plotted in Figure 5.8. The straight lines are those of EAS and the dashed dotted lines those of SIS. The different colors represent the different normalized transmission power used. Figure 5.8 shows that EAS achieves better ergodic channel capacity than SIS independently of the number of WPs and the transmission power. These results corroborate the fact that EAS can better solve the resource allocation problem in Equation (2.22) on page 43 than SIS, as already shown. According to Figure 5.8, for high transmission power, the channel capacity provided by SIS decreases as the number of WPs increases. This is because adding more WPs increases the probability of selecting logical routes of a 2-hop link which creates more intra-cell interference in the VCN, in the interference dominant transmission power region. Since SIS cannot avoid intra-cell interference as EAS, the capacity provided by SIS decreases as the number of WPs increases if high transmission power is considered.

Figure 5.9 plots the ergodic channel capacity of the VCN based on the distance ratio d/d_0 when SIS and EAS are applied. What was said previously regarding the colors and the lines remain the same in Figure 5.9. Based on Figure 5.9, an optimal distance ratio can be found in the interval 0.2~0.4 when EAS is applied. As for SIS, the optimal interval is the same if low transmission power is considered. However, in the case of high transmission power, no such optimal interval exists. To achieve higher channel capacity, the results suggest to increase the distance ratio. This is because in the interference dominant transmission power region, SHN ($R = 1$ WP) can provide higher capacity than SIS (see Figure 5.8). Since the more the WPs are distanced from the CP, the more the VCN tends to act like a single hop network, increasing the distance ratio will provide an augmentation of the capacity when SIS is applied with high transmission power.

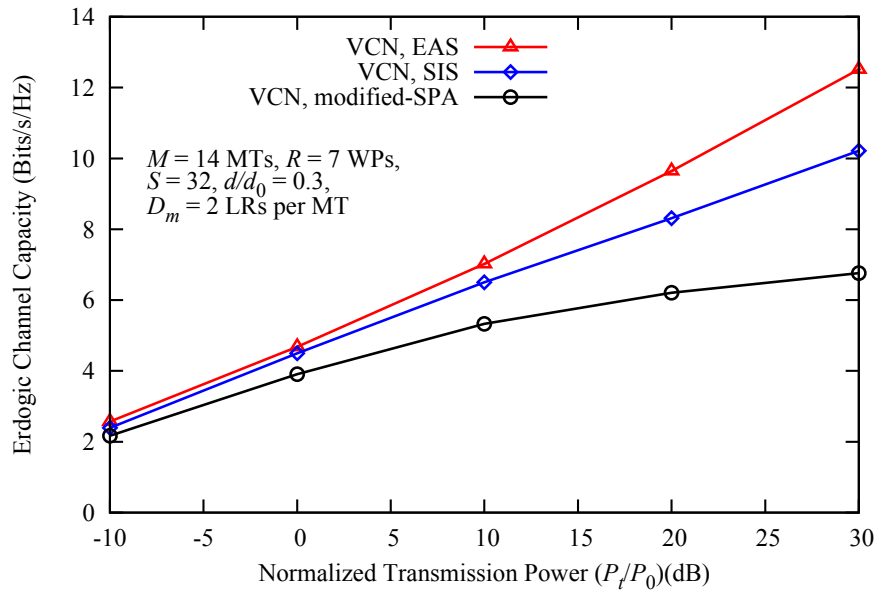


Figure 5.2: Ergodic capacity of EAS, modified-SPA, and SIS

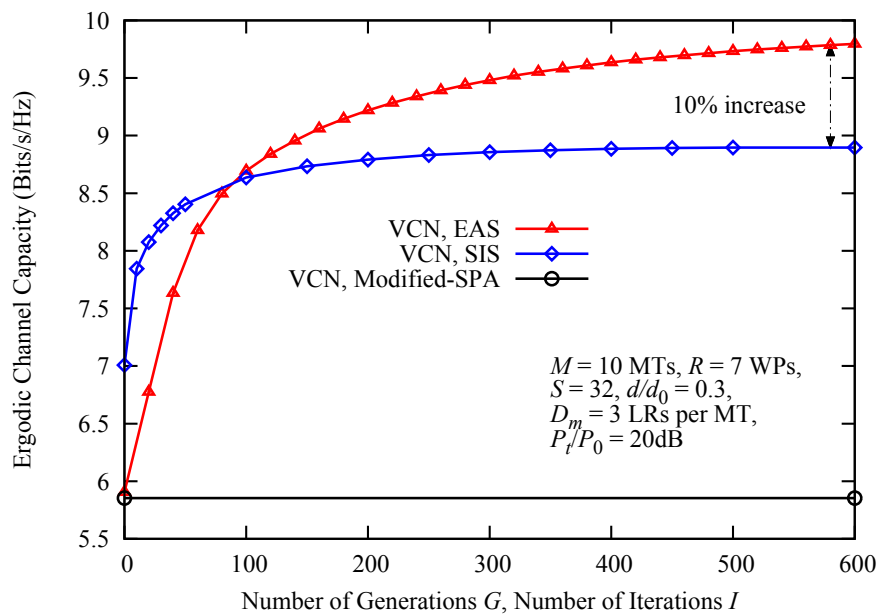


Figure 5.3: Convergence of EAS and SIS

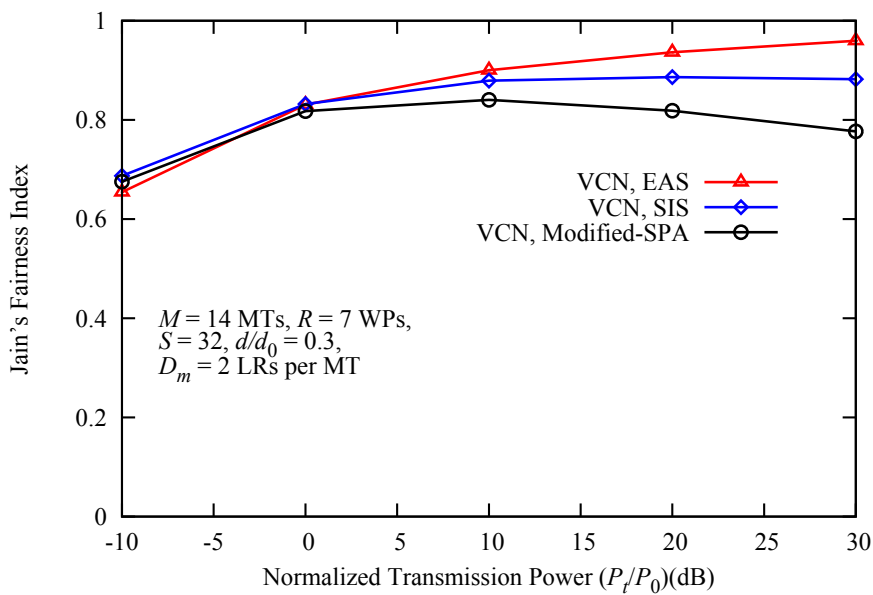


Figure 5.4: Jain's fairness index

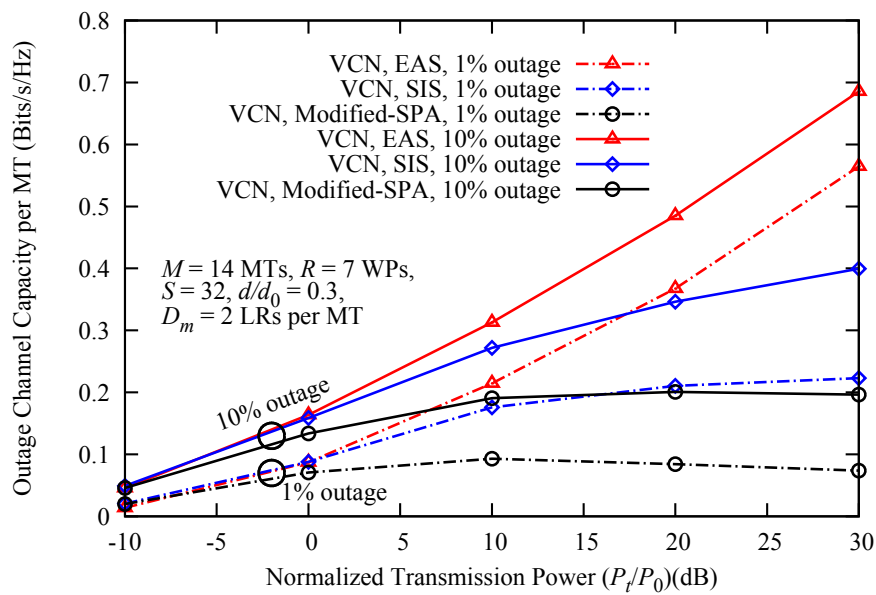


Figure 5.5: Outage channel capacity per MT

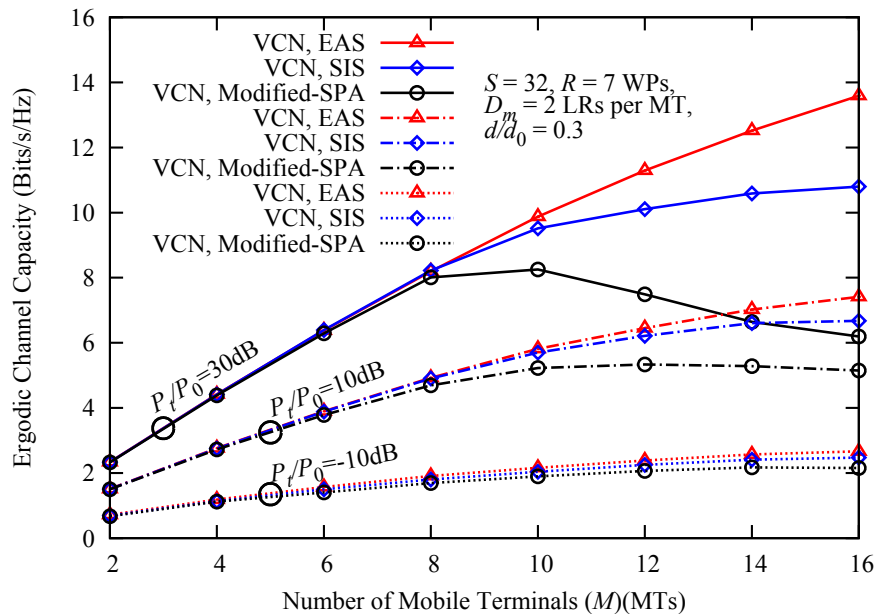


Figure 5.6: Ergodic channel capacity based on the number of MTs

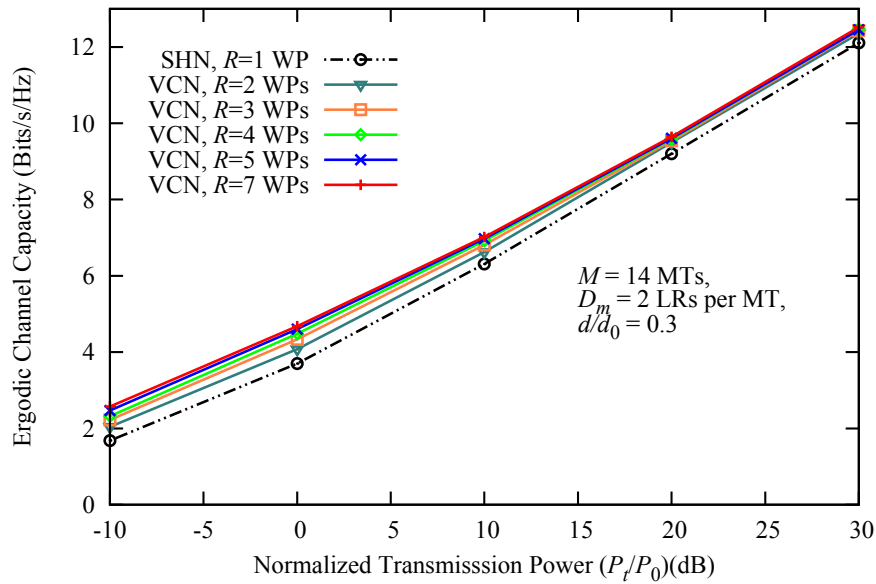


Figure 5.7: EAS Ergodic channel capacity different number of WPs

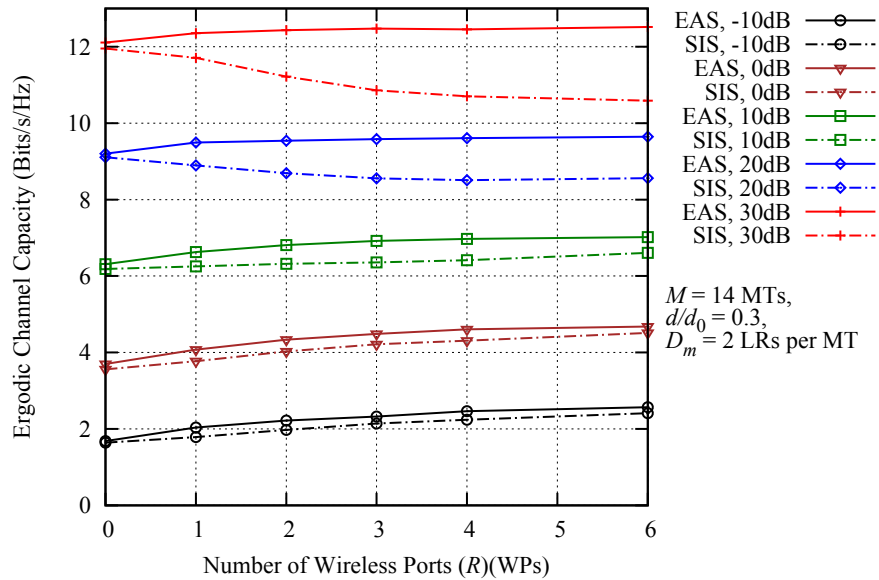
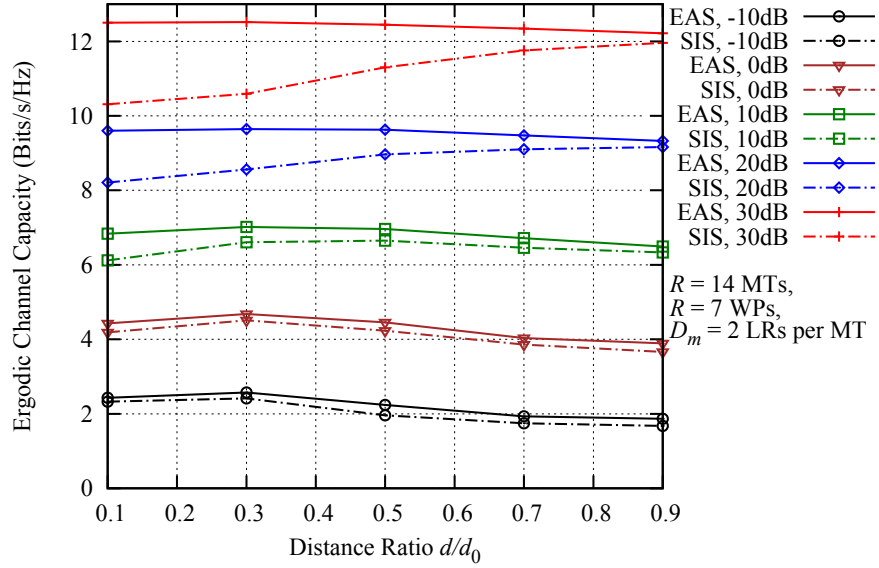


Figure 5.8: EAS, SIS Ergodic channel capacity based on the number of WPs

Figure 5.9: EAS, SIS Ergodic channel capacity based on the distance ratio d/d_0

5.3 Multi-cell Network

In this section, we study the performance of EAS in a multi-cell environment and compare its performance with that of the SIS.

5.3.1 System Model

We consider a multicell environment with a set \mathcal{V} of V VCs. A set \mathcal{R}_v of R_v WPs including the CP is distributed in the v -th VC. The channel bandwidth of the v -th VC is divided into a set \mathcal{S}_v of S_v orthogonal sub-carriers. A set \mathcal{M}_v of M_v MTs are located in the v -th VC. A set $\mathcal{D}_{m,v}$ of $D_{m,v}$ logical routes is to be allocated to the m -th MT ($MT_{m,v}$) in the v -th VC. The allocation problem is the same as defined in Equation (2.35) on page 47.

5.3.2 Evolutionary Allocation Scheme

We assume that there is no cooperation between the VCs. This means that the VCs do not share information regarding their allocated logical routes. Hence, we apply EAS separately in each VC.

We define a solution candidate as $\Psi_v^{(t)} = \{\mathcal{D}_{1,v}^{(t)}, \mathcal{D}_{2,v}^{(t)}, \dots, \mathcal{D}_{m,v}^{(t)}, \dots, \mathcal{D}_{M_v,v}^{(t)}\}$ where $\mathcal{D}_{m,v}^{(t)}$ denotes the set of logical routes allocated to $MT_{m,v}$ in the v -th VC. Similarly as in the single VC case, we define the allocation matrix $\mathfrak{T}_v^{(t)}$ associated to $\Psi_v^{(t)}$ as :

$$\mathfrak{T}_v^{(t)} = \begin{bmatrix} 1 & a_{12}^{(t)} & a_{13}^{(t)} & a_{14}^{(t)} \\ \vdots & \vdots & \vdots & \vdots \\ 1 & a_{D_{1,v},2}^{(t)} & a_{D_{1,v},3}^{(t)} & a_{D_{1,v},4}^{(t)} \\ 2 & a_{(D_{1,v}+1),2}^{(t)} & a_{(D_{1,v}+1),3}^{(t)} & a_{(D_{1,v}+1),4}^{(t)} \\ \vdots & \vdots & \vdots & \vdots \\ 2 & \vdots & \vdots & \vdots \\ \vdots & \vdots & \vdots & \vdots \\ M & \vdots & \vdots & \vdots \\ \vdots & \vdots & \vdots & \vdots \\ M & a_{\psi_v,2}^{(t)} & a_{\psi_v,3}^{(t)} & a_{\psi_v,4}^{(t)} \end{bmatrix}$$

with $0 \leq a_{i2}^{(t)} \leq R_v - 1$, $1 \leq a_{i3}^{(t)} \leq S_v$, $1 \leq a_{i4}^{(t)} \leq S_v$, $\forall i \in \mathbf{N}$, $1 \leq i \leq \psi_v$. (5.13)

The number of allocated logical routes in the v -th VC is noted as ψ_v . The allocation matrix $\mathfrak{T}_v^{(t)}$ has the same structure as defined in the single VC case.

Denote P_v the number of candidates in the initial population Pop_v , φ_v the number of candidates in the archive, and U_v the number of mates in the v -th VC. Besides the evaluation method in **Procedure Evaluate**, all the other

Procedure EvaluateMultiCell

Input: P_v , Pop_v , VC_v

Output: Pop_v : Population Evaluated

```

begin
    for  $t = 1 : P_v$  do
        /* Evaluate interference between logical routes */
        foreach  $l_e^*(v, m, r, k_i, k_j) \in \Psi_v^{(t)}$  and  $l_h(u, p, r', k_{i'}, k_{j'}) \in \Psi_u^{(t)}$ ,
             $\forall u \in \mathcal{V}$  do
                Evaluate interference using
                the Procedure InterferenceMultiCell on page 69;
            end
        Evaluate  $C(\Psi_v^{(t)})$  using Equation (2.34) on page 46;
    end
end

```

methods described above for a single VC can be applied in the v -th VC to find the set of best solution candidates of the resource allocation problem in Equation (2.35) on page 47.

As for the evaluation method, the objective function has to be changed since we consider a multi-cell environment. It has been modified as follows in **Procedure EvaluateMultiCell**.

The implementation of EAS in a multi-cell environment is detailed in **Algorithm 10**. **Algorithm 10** shows the different steps of EAS applied in the v -th VC.

5.3.3 Simulation Assumptions and System Model

We consider a multi-cell environment with $V = 19$ VCs as illustrated in Figure 3.12 on page 67. To reduce computational complexity we implement the wrap-around structure in Figure 3.13 on page 67. The distance D between the CPs of two neighbouring VCs is taken to be $D = d_0\sqrt{3}$, with d_0 being the radius of a VC.

We consider that each VC has the same number R of WPs, the same number of MTs $M = 7$ MTs and the same number of sub-carriers $S = 16$. The same number of logical routes $D_m = 2$ logical routes is allocated per MT in each VC.

In each VC, we consider a multipath frequency selective fading propagation channel with $L = 8$ propagation paths. The paths are considered to be independently distributed Rayleigh fading with uniformly distributed power delay profile. We assume the standard deviation of the log-normally distributed shadowing loss to be $\sigma = 8$ dB and a path-loss exponent $\alpha = 4$.

We assume the normalized total transmission power P_t/P_0 as defined in Equation (InterferenceMultiCell) on page 70 to be the same in all VCs. P_t/P_0 is equally shared among all allocated logical routes in a VC. A two hops logical route equally distributes its allocated power between the two links.

Algorithm 10: Evolutionary Allocation Scheme (EAS)

Input: $\mathcal{M}_v, \mathcal{R}_v, \mathcal{S}_v, P_v, G, \varphi_v, U_v, T, \xi_{\text{unif}}()$

Output: Arch_v containing the best solution candidates

```

begin
     $g \leftarrow 0;$ 
    /* Create initial population */
     $\text{Pop}_v \leftarrow \text{create}(\mathcal{M}_v, \mathcal{R}_v, \mathcal{S}_v, P_v)$  using Procedure Create;
    while  $g < G$  do
        /* Evaluate population */
         $\text{Pop}_v \leftarrow \text{evaluate}(\text{Pop}_v)$  using Procedure EvaluateMultiCell;
        /* Assign fitness value and archive best candidates
           */
         $\text{Pop}_{v\text{fit}}, \text{Arch}_v \leftarrow \text{FitnessAssignArchive}(\text{Pop}_v, \text{Arch}_v, \varphi_v)$ 
        using Procedure FitAssignArchive;
        /* Select candidates for reproduction */
         $\text{Mate}_v \leftarrow \text{TournamentSelection}(\text{Pop}_{v\text{fit}}, U_v, T)$ 
        using Procedure TournamentSelect;
        Increment  $g$ ;
        /* Reproduce to create new offspring */
         $\text{Pop}_v \leftarrow \text{Reproduce}(\text{Mate}_v)$  using Procedure Reproduce;
    end
end

```

During the simulation, we select a VC randomly and we apply EAS for one generation for the selected VC. While applying EAS for the selected VC, we assume that logical routes allocation has been completed for the other VCs. For the other VCs, their best candidate is considered as their best solution candidate. Inter-cell interference for the current VC is calculated using these best candidates.

For each VC we consider an initial population of $P = 800$ candidates, an archive of $\varphi = 300$ candidates, and a set of mates of $U = 1000$. The simulation is executed for $G = 19000$ generations so that each VC can be selected for an average of $G_{aver} = 1000$ generations.

5.3.4 Simulation Performance

We consider that $R = 7$ WPs including the CP are distributed in each VC (see Figure 4.3 on page 90). The WPs are distanced from the CP by a distance ratio $d/d_0 = 0.3$. Figure 5.10 shows the plots of the ergodic channel capacity of the VCN when EAS and SIS are applied in a multi-cell environment. For the SIS, we simulate $I = 50$ iterations. Based on Figure 5.10, we notice that EAS can provide better ergodic channel capacity than SIS in a multi-cell environment. These results corroborate the results obtained in a single cell scenario where EAS outperforms SIS.

In Figure 5.11, we plot the 10% outage channel capacity for EAS and SIS. It is observed that in the noise dominant transmission power region, SIS provides the same performance as EAS. However, in the interference dominant transmission power region, EAS outperforms SIS. The reasons are the same as already explained in the single cell environment. The performance of SIS degrades with interference since it is a successive allocation scheme while EAS can achieve optimality by simultaneously allocating logical routes to the MTs.

Figure 5.12 plots the Jain's fairness index for EAS and SIS. The Jain's fairness index is defined in Equation (3.17) on page 75. According to Figure 5.12, EAS and SIS can achieve almost the same fairness, independently of the transmission power, with SIS slightly outperforming EAS. These results suggest that the optimal solution, which maximizes the total channel capacity of a VC, loses in fairness. Though EAS is not more fair than SIS, it can at least provide almost the same fairness as SIS. Hence, EAS could be considered as a good candidate scheme to solve the allocation problem in Equation (2.35) on page 47.

To study the behaviour of EAS based on the distance ratio d/d_0 , in Figure 5.13 we plot the ergodic channel capacity of the VCN based on the distance ratio when EAS is applied in a multi-cell environment. We consider the VC layout in Figure 3.18 on page 74 with $R = 5$ including the CP. We observe that, similar to all previous results, an optimal distance ratio for the location of the WP can be found in the interval $0.2 \sim 0.4$.

To understand the results in Figure 5.13, we plot the probability that a two-hop link logical route will be allocated based on the distance ratio d/d_0

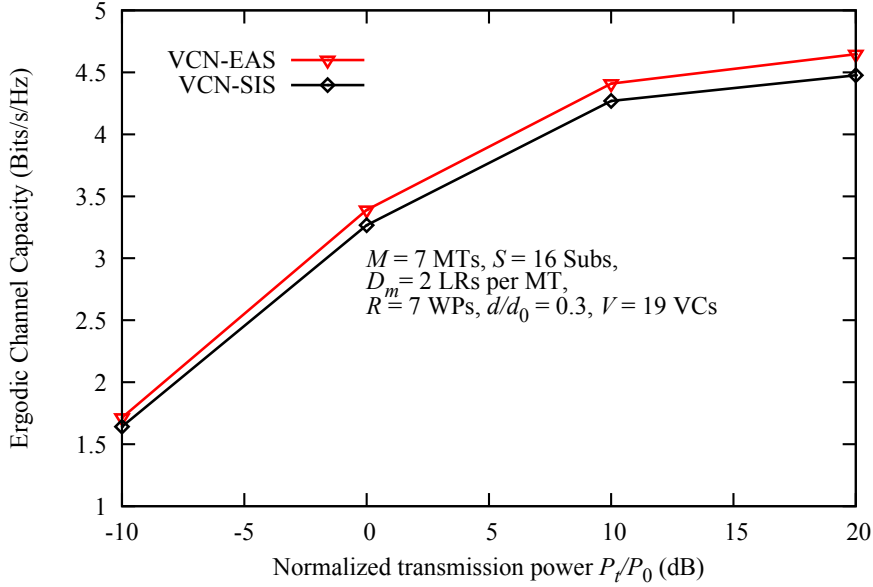


Figure 5.10: Ergodic channel capacity of EAS and SIS

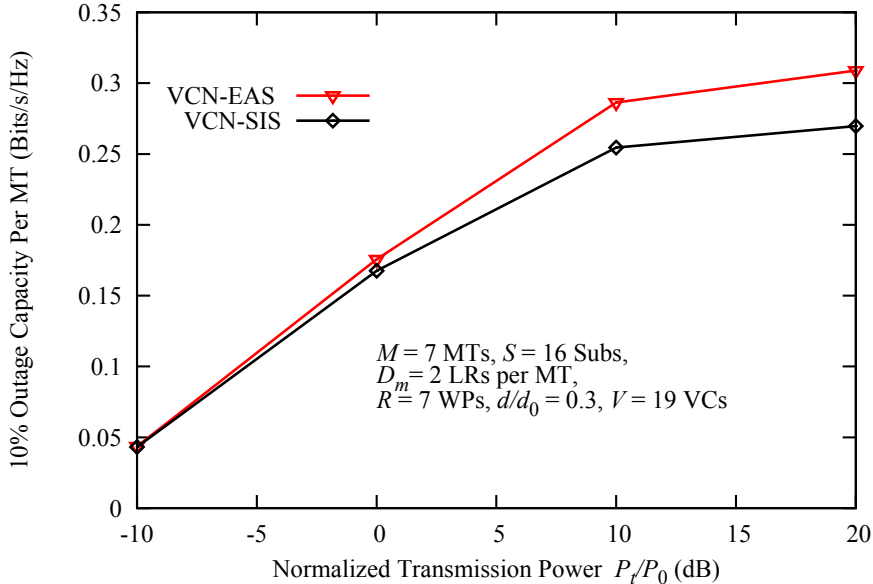


Figure 5.11: Outage channel capacity of EAS, and SIS

in Figure 5.14. The understanding is that in a two-hop network where a direct link can be chosen, a two-hop link route will be selected only if that two-hop link route provides better capacity than the direct link. Our objective is to place the WPs in a location where they can be selected to provide higher capacity than the direct link. Figure 5.14 shows that WPs located at a distance ratio in the interval $0.2 \sim 0.4$ have a higher probability of being selected.

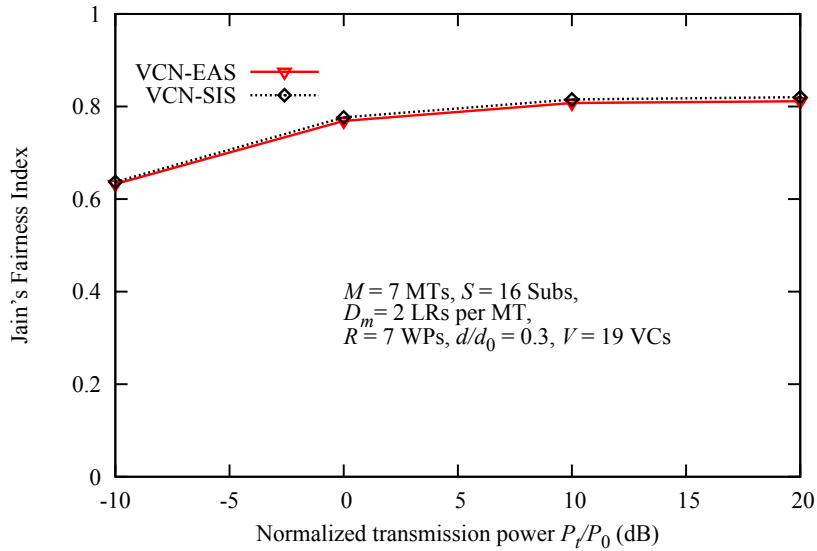


Figure 5.12: Jain's fairness index of EAS, and SIS

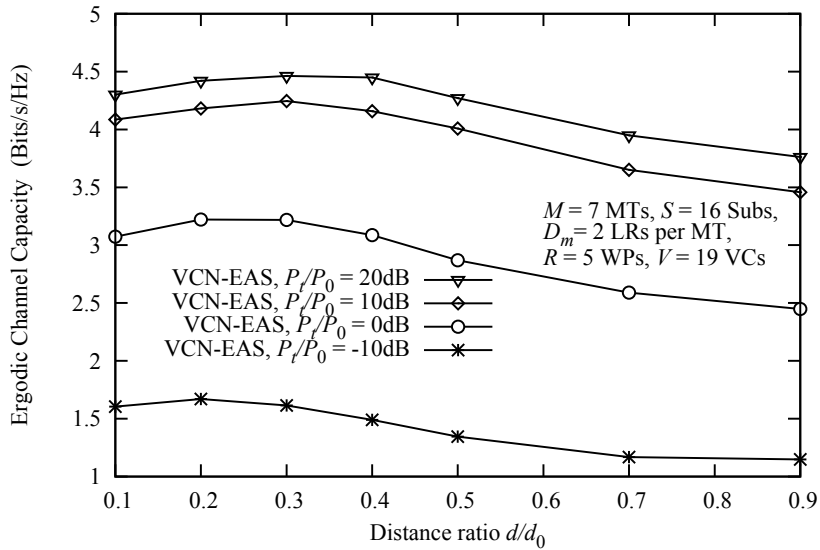


Figure 5.13: Ergodic channel capacity based on distance ratio of EAS

Hence we conclude that placing the WPs at a distance ratio in the interval $0.2 \sim 0.4$ can ensure higher ergodic channel capacity.

So far we have been studying the optimal distance ratio using ergodic channel capacity. Ergodic channel capacity is an average metric and does not provide enough detail on how the total capacity is shared among the MTs. Hence, in order to have a better understanding on where to place the WPs to optimize the capacity per MT, we plot respectively in Figure 5.15 and Figure 5.16 the outage channel capacity per MT and the Jain's fairness index

based on the distance ratio d/d_0 . We notice that the assumption that an optimal distance ratio lies in the interval $0.2 \sim 0.4$ still remains valid. However, Figure 5.15 and Figure 5.16 suggest that a distance ratio closer to 0.4 will be more beneficial to the MTs when fairness is accounted for. Based on Figure 5.15 and Figure 5.16, higher degrees of fairness and outage channel capacity per MT can be obtained when the distance ratio is closer to 0.4.

In Figure 5.17 and Figure 5.18, we plot respectively the ergodic channel capacity and the 10% outage channel capacity per MT based on the number of WPs. We observe that increasing the number of WPs can help improve the performance of the system. These results can be understood by the fact that adding new WP helps increase the degree of route diversity in the network. The increased performance of the system is a direct consequence of the increased degree of route diversity.

We have not determined what could be an optimal number of WPs. However, we have found that as we increase the number of WPs, the additional gain obtained by adding a new WP is decreasing. These results are plotted in Figure 5.19. Figure 5.19 plots the percentage of increased capacity for different transmission power based on the number of WPs added. In Figure 5.19, we observe that, regardless of the transmission power, the increased capacity gained by adding a third WP is less than that obtained when adding the second WP; and similarly the increased capacity provided by the addition of a second WP is less than that provided by adding the first WP. These results suggest that we cannot infinitely increase the capacity of the system by just increasing the number of WPs.

In Figure 5.20, we plot the ergodic channel capacity of the VCN based on the number M of MTs. We observe that the ergodic channel capacity increases with the number of MTs. This increase is a direct consequence of multi-user diversity provided by OFDMA.

Figure 5.21 plots the 10% outage channel capacity per MT based on the number M of MTs. According to Figure 5.21, the outage capacity per MT decreases as the number of MT increases. This is a trivial result as the total capacity has to be shared with more MTs. Hence, the capacity per MT decreases.

The Jain's fairness index based on the number M of MTs is plotted in Figure 5.22. We remark that the fairness of the system decreases with the number of MTs.

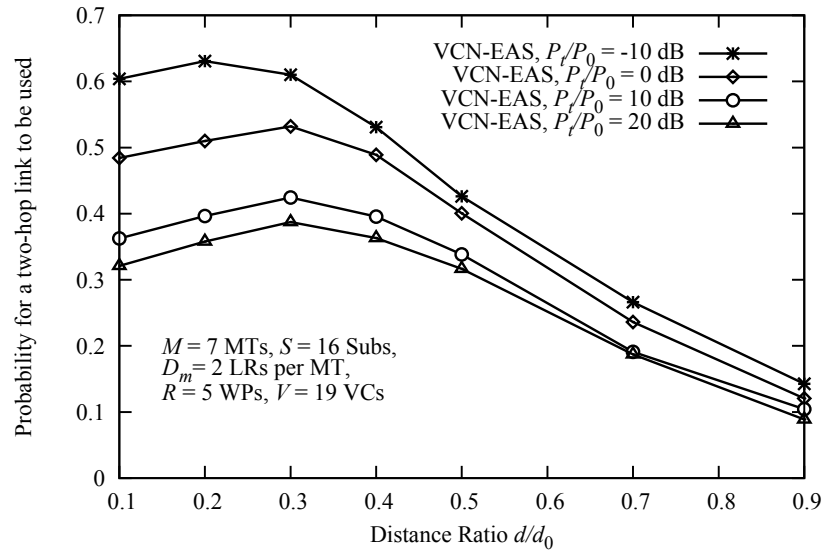


Figure 5.14: Probability for a two hops link to be selected

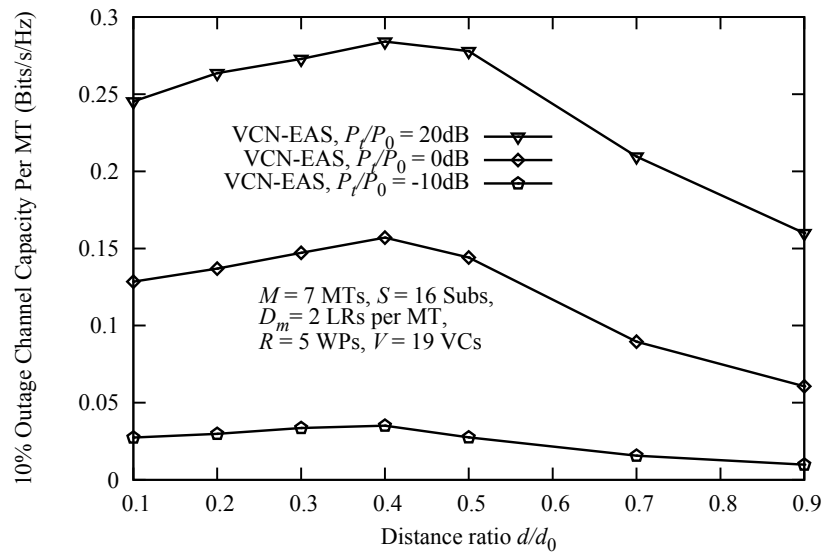


Figure 5.15: Outage channel capacity based on distance ratio of EAS

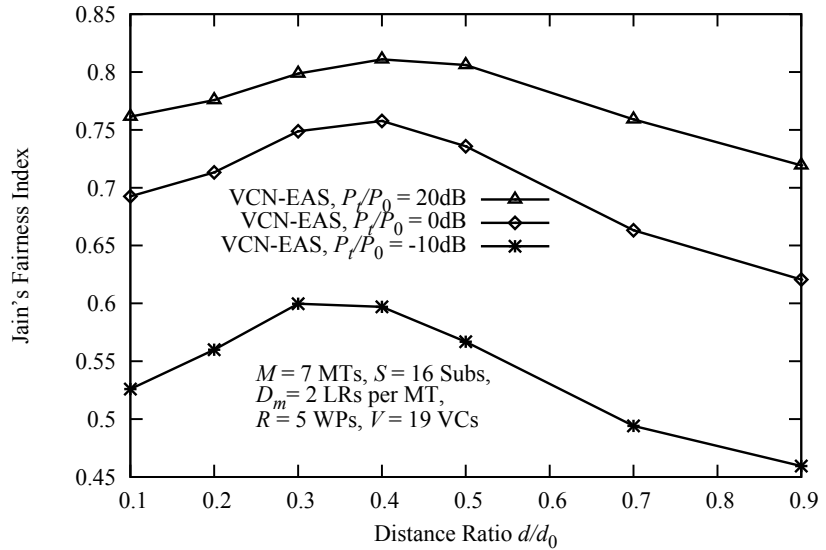


Figure 5.16: Jain's fairness index based on distance ratio of EAS

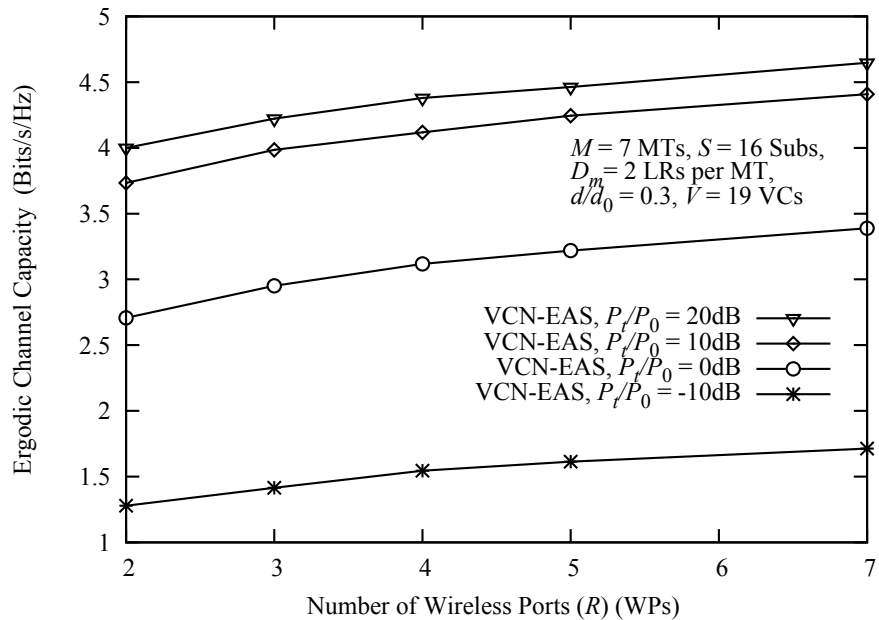


Figure 5.17: Ergodic channel capacity based on the number of WPs

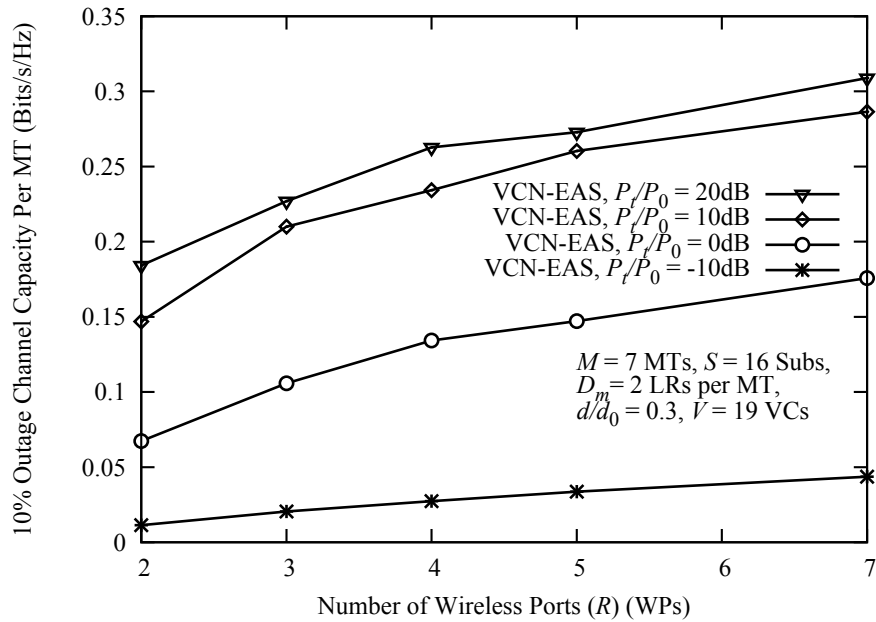


Figure 5.18: Outage channel capacity based on the number of WPs

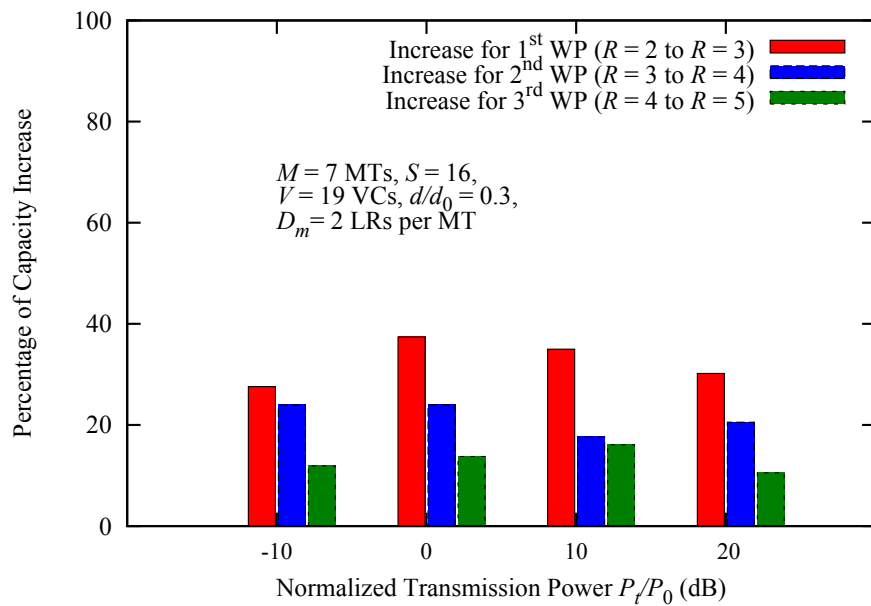


Figure 5.19: Percentage of increased capacity when adding a WP

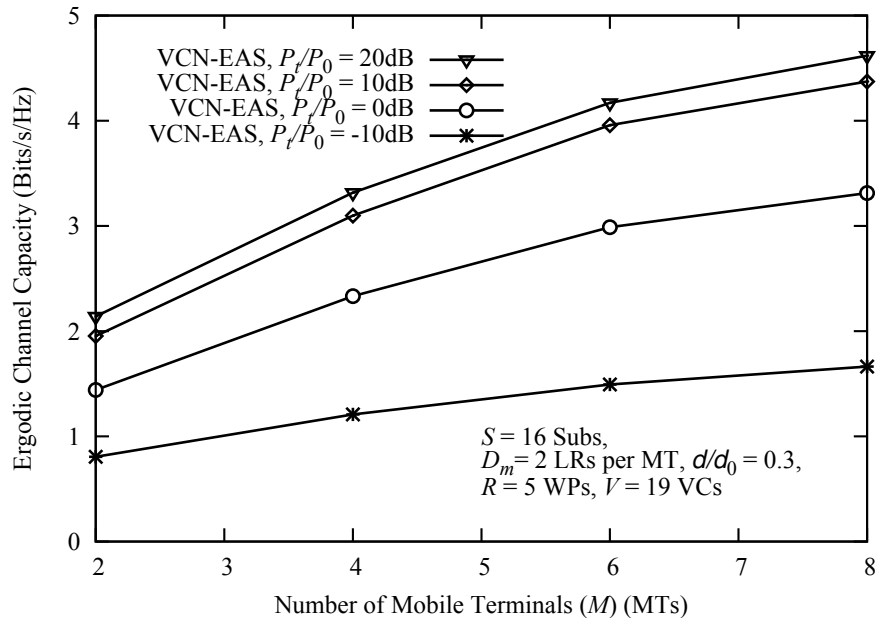
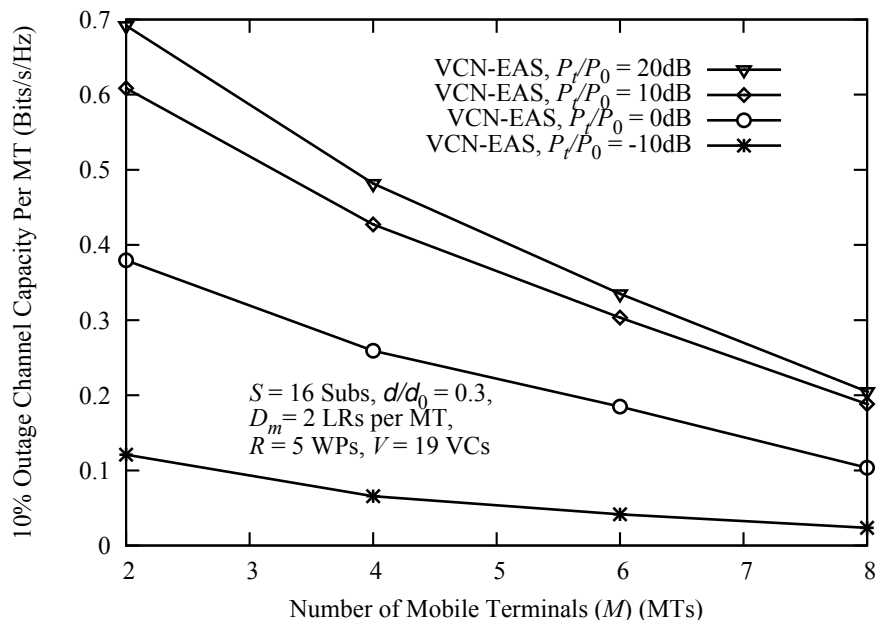


Figure 5.20: Ergodic channel capacity based on the number of MTs



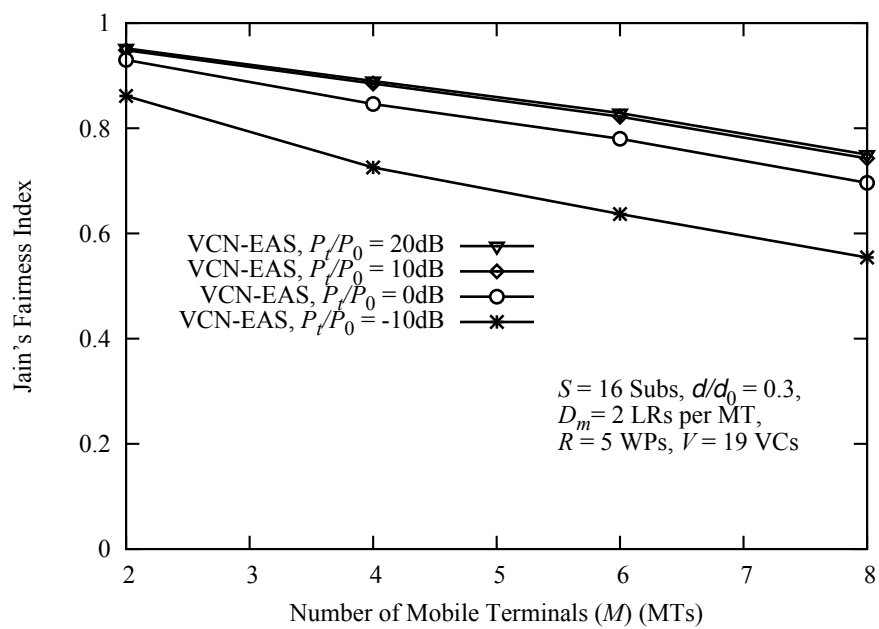


Figure 5.22: Jain's fairness index based on the number of MTs

5.4 EAS Performance Comparison With Optimal Scheme

To evaluate the performance of EAS compared with the optimal exhaustive allocation scheme, we consider a single VC with 3 WPs located as shown in Figure 3.24 on page 80. The system bandwidth is divided into $S = 8$ orthogonal sub-carriers. $M = 2$ MTs are generated randomly in the VC. $D_m = 4$ logical routes are allocated per MT.

In Figure 5.23, we plot the ergodic channel capacity of EAS compared with that of SIS, SAS, and the optimal exhaustive allocation scheme. For the EAS, the same parameter values have been used, initial population $P = 800$ candidates, $G = 1500$ generations, $U = 1000$ mates, and $\varphi = 300$ candidates. For SIS, $I = 500$ iterations have been simulated. According to Figure 5.23, EAS can provide the same ergodic channel capacity as the optimal exhaustive allocation scheme. As for SIS and SAS, their performance is less than that of the optimal scheme. This is because EAS is able to avoid local optimal solution and find global optimal solutions by considering the simultaneous allocation of logical routes to MTs. SAS and SIS cannot provide optimal solutions because they are successive schemes. These results prove that EAS can be considered as an optimal allocation scheme to solve the resource allocation problem in Equation (2.22) on page 43.

Figure 5.24 shows the plots of the 1% and 10% outage channel capacity of the EAS, SIS and the optimal exhaustive scheme. Figure 5.24 again corroborates the results in Figure 5.23. In the interference dominant transmission power region, EAS approximates very well the performance of the optimal exhaustive scheme. SIS does not provide such performance. We notice a slight difference between EAS and the exhaustive scheme in the interference dominant transmission power region for 1% outage channel capacity. These results suggest that our resource allocation problem might have many global solutions and EAS does not always reach the best global solution. If we consider the noise dominant transmission power region, in Figure 5.24 we observe that SIS achieves the same performance as EAS and the optimal exhaustive scheme. This can be understood by the fact that in the absence of interference, SIS can be considered as an optimal allocation scheme. These results only support all the previous results we have encountered so far where SIS and EAS achieve almost the same performance in the noise dominant transmission power region.

In Figure 5.25, we compare the computational complexity of the three algorithms. We plot the CPU Time in second (s) of each algorithm based on the normalized transmission power. The CPU Time is defined as the running time of an algorithm to solve the resource allocation problem in Equation (2.22) on page 43. We observe that the evolutionary scheme requires far less computational time than the optimal exhaustive allocation scheme. We hence conclude that EAS can achieve almost similar performance as the optimal ex-

haustive scheme while reducing considerably the computational complexity.

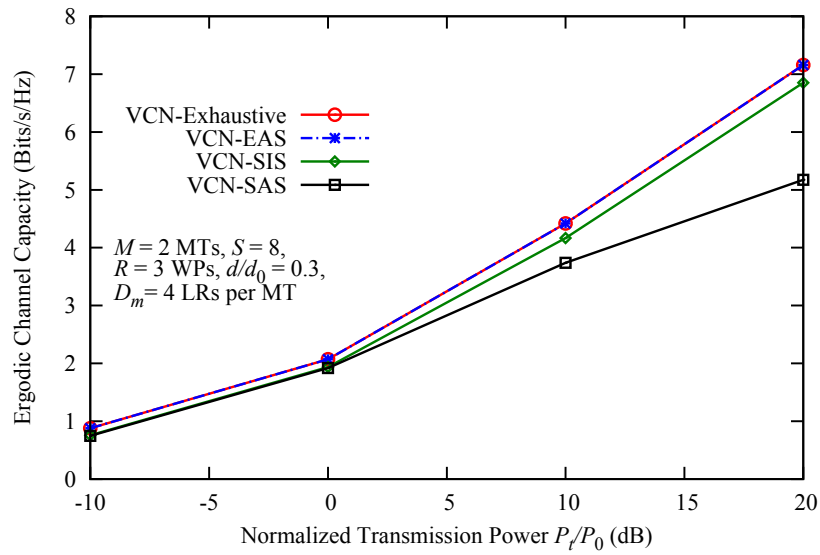


Figure 5.23: Ergodic channel capacity of EAS, SIS, SAS, and exhaustive scheme

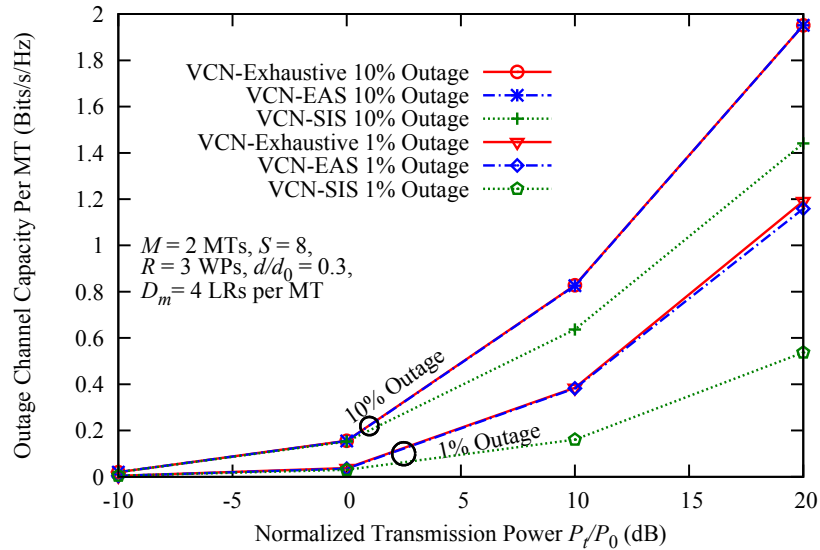


Figure 5.24: Outage channel capacity of EAS, SIS and exhaustive scheme

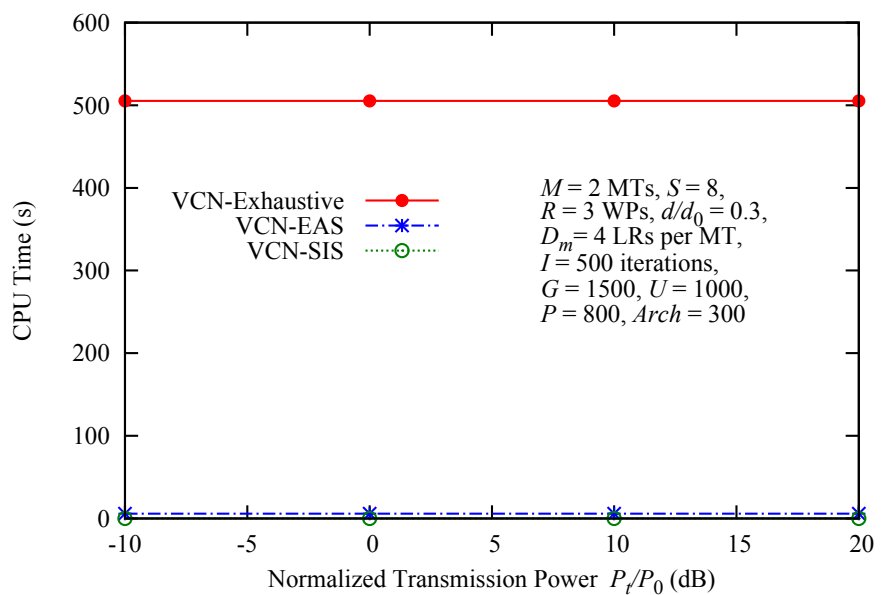


Figure 5.25: Computational complexity of EAS, SIS and exhaustive scheme

5.5 Summary

In this chapter, we proposed an evolutionary allocation scheme (EAS) to approximate the optimal solution of the resource allocation problems in Equation (2.22) on page 43 and in Equation (2.35) on page 47. We showed by computer simulation that the EAS can optimally approximate the optimal solution. The simulation results corroborated that EAS can provide better performance than the SAS and the SIS proposed in the previous chapters.

CHAPTER 6

Conclusion

This chapter concludes the thesis. We also discuss some future work related to this thesis.

6.1 Conclusion

In order to accommodate the increasing demand of high data transmission in wireless networks, a new network paradigm is necessary. Wireless multi-hop networks have been proposed by many researchers as a new network architecture to satisfy that increase of data transmission without increasing the transmitted power. Among the different multi-hop network architectures proposed, there exists a virtual cellular network (VCN) in which the base station is named as central port and the relay stations as wireless ports. As a transition step in the implementation of multi-hop networks, a two-hop VCN can be considered to increase the data transmission rate.

Though multi-hop networks can increase the data transmission rate without increasing the transmission power, they also present many challenges. A common challenge is resource allocation to multiple users. In a two-hop VCN where OFDMA is applied, resources can be considered as routes (WPs), and sub-carriers in first-hop and second-hop links. The problem of joint route and sub-carrier allocation to multiple users in a multi-cell environment, where a sub-carrier can be reused simultaneously in multiple links within a cell, was not yet solved in the literature.

6.1.1 Chapter 2

In Chapter 2, we formulated the problem of route and sub-carrier allocation to multiple mobile terminals using the concept of logical routes. We modelled the resource allocation problem for both single cell and multi-cell environments. We defined the different constraints that have to be respected for a sub-carrier to be reused simultaneously in multiple links.

We derived the numerical expressions to calculate the signal-to-interference-plus-noise power ratio of a logical route in both single cell and multi-cell environments. The total channel capacity for a virtual cell was derived for single cell and multi-cell networks in a multi-user environment.

The resource allocation problem was formulated as an optimization allocation problem where the channel capacity of a VC is considered as the objective function. Different sub-carrier reuse constraints were defined for the optimization allocation problem in both single cell and multi-cell environments.

6.1.2 Chapter 3

The optimal solution of the joint route and sub-carrier allocation problem requires an exhaustive search which may not be applied in a practical system. To reduce computational complexity, we proposed a successive allocation scheme (SAS) in Chapter 3. The successive allocation scheme considers the successive allocation of the logical routes to the MTs.

Firstly, we proposed the SAS in a single cell environment. We studied the performance in a single cell and showed that SAS can increase the ergodic channel capacity in the noise dominant transmission power region when compared to the current single hop network (SHN). Using SAS, we showed by computer simulation that the ergodic channel capacity and the degree of fairness of the VCN are superior to those of the conventional SHN for low transmission power. We also acknowledged that as the distance ratio increases, the channel capacity of the VCN approximates that of the SHN. Furthermore, if we consider low transmission power, the optimal distance ratio d/d_0 for the location of the WPs can be found in the interval $0.2 \sim 0.3$. We also remarked that the ergodic channel capacity of the VCN remains better than that of the SHN as the number of MTs increases for low transmission power.

Secondly, we modified the SAS to apply it in a multi-cell environment and study its performance. We evaluated the ergodic channel capacity and the outage capacity per MT of the VCN, in the presence of inter-cell interference, and compared the results to those of the SHN. The simulation results showed that the VCN can provide better outage capacity per MT and greater ergodic channel capacity than the SHN, even for high transmission power, in a multi-cell environment. As the number of MTs increases, the ergodic channel capacity of the VCN still remains greater than that of the SHN. Furthermore, the VCN presents a better degree of fairness than the SHN. We also showed that increasing the number of WPs R from 4 to 7 in the VCs can further enhance the ergodic channel capacity of the VCN if the WPs are placed at a well chosen distance from the CP. The optimal distance ratio d/d_0 to place the WPs can be found in the interval $0.2 \sim 0.4$; and it depends neither on the number of WPs in the VCs nor on the normalized transmission power. We also noticed that, if a frequency reuse factor of 1 is applied, the ergodic channel capacity degrades considerably.

Considering a single cell with $R = 3$ WPs and $M = 2$ MTs, we compared the performance of SAS with that of the optimal exhaustive scheme. Though SAS could approximate the performance of the exhaustive scheme in the noise interference dominant transmission power region, its performance degrades

considerably in the interference dominant transmission power region. These results suggest that SAS cannot be considered as an optimal scheme because it is not resilient to intra-cell and inter-cell interference.

6.1.3 Chapter 4

The performance of the SAS proposed in Chapter 3 degrades with interference. In Chapter 4, considering a single cell environment, we proposed the sequential (SIS) and the random (RIS) iterative schemes to enhance the channel capacity of the VCN in the interference dominant transmission power region. The SIS considers the reallocation of the logical routes taking the MTs in a sequential order. As for the RIS, the MTs are selected randomly for logical routes reallocation. Using computer simulations, we showed that high improvement can be achieved if SIS and RIS are applied in a single cell environment. We also noticed that the SIS converges faster than the RIS.

In addition to SIS and RIS, we investigated the permutational (PIS) and permutational combined (PCIS) iterative schemes. The PIS generates multiple random permutations of the MTs; and logical route allocation is performed using SAS for each of these permutations. The PCIS is a combined algorithm where SIS is applied as the allocation scheme for each permutation of the PIS. PICS been a combined version of PIS provides better performance than PIS and SIS. However, PCIS is not a practical allocation scheme since it requires complete deallocation of the MTs in order to be implemented. Hence, the PCIS was used to evaluate the performance of the SIS. The simulation results showed that the performance of the SIS approaches that of the PCIS. Since the SIS presents less computational complexity and was more practical than the PCIS, we have retained the SIS as the best iterative scheme to replace SAS.

The SIS was modified so that it could be applied in a multi-cell environment. We showed that, compared to SAS, with using the SIS, considerable improvement of the ergodic and outage channel capacity of the VCN can be achieved in the interference dominant transmission power region, with low complexity cost.

Compared to the conventional single hop network, we also showed that the performance gained in the VCN when SIS is applied is higher than that obtained in the SHN. Furthermore, the simulation results corroborated that adding more WPs per VC can increase the outage channel capacity and boost the degree of fairness of the VCN.

Using the same single cell layout with $R = 3$ WPs and $M = 2$ MTs as in Chapter 3, we compared the performance of the SIS with that of the SAS and the optimal exhaustive allocation scheme. We showed that SIS can improve the ergodic channel capacity of the VCN in the interference dominant transmission power region compared to SAS. However, the performance of the SIS compared to the optimal exhaustive scheme could still be improved.

6.1.4 Chapter 5

SIS as a successive scheme could not approximate the optimal exhaustive allocation scheme. In Chapter 5, we proposed an evolutionary allocation scheme (EAS) to approximate the optimal exhaustive allocation scheme.

EAS is based on the evolution theory where population candidates go through many evolutionary methods to provide better candidates. We modelled the resource allocation problem as an evolutionary allocation problem. We defined and implemented the following evolutionary methods for our resource allocation problem: Creation, Evaluation, Fitness Assignment, Archiving, Validation, Tournament Selection, Mutation, Crossover, and Reproduction. These methods were combined to provide the best solution candidate for our resource allocation in a single cell.

Considering a single cell, we compared the performance of the EAS with that of the SIS and a modified sub-carrier pair allocation scheme. Simulation results corroborated that, compared to the SIS and a modified-subcarrier pair allocation scheme, by simultaneously allocating resources to MTs, EAS can improve the ergodic channel capacity of the VCN in the presence of intra-cell interference.

The evaluation method of the EAS was modified so that EAS could be applied in a multi-cell environment. We showed that in a multi-cell environment, EAS outperforms SIS in the interference dominant transmission power region. We also studied the performance of the EAS based on the number of WPs and location of the WPs. We showed that similar to other schemes, for the EAS, an optimal distance ratio for the location of the WPs could be found in the interval $0.2 \sim 0.4$. The performance of the VCN increases with the number of WPs. However, the achievable gain obtained when adding a new WP decreases as we increase the number of WPs.

To compare the performance of the EAS with that of the optimal exhaustive allocation scheme, we considered the same system layout of $R = 3$ WPs and $M = 2$ MTs as in Chapter 3 and Chapter 4. We compared the performance of the EAS with that of the SAS, the SIS and the exhaustive scheme. We showed that EAS outperforms both SAS and SIS. Furthermore, EAS could provide almost the same performance as the optimal exhaustive scheme for low level of complexity. Hence, we concluded that EAS should be considered as the optimal allocation scheme for the resource allocation problems defined in Chapter 2.

6.2 Future Work

In our work, we considered that the CP has the channel station information (CSI) of all links inside a virtual cell. The simulations were conducted based on that assumption. It is our understanding that providing the CSI to the CP will create overhead in the system. Furthermore, simulation results corroborated that adding more WPs per VC can increase the outage channel capacity

and boost the degree of fairness of the VCN. Adding more WPs in the VCN will increase the signalling overhead in the network. The added signalling overhead will impact the achievable channel capacity of the network. Further studies could focus on the reduction of signalling overhead in the VCN.

We have not taken into account the quality of service in our system. In mobile cellular network, some applications require real-time transmission with limited delay while others are more flexible with it comes to transmission delay. Therefore, when allocating resources the quality of service should be considered in order to satisfy those customers with transmission delay constraints. Allocation resources which take into account the quality of service in two-hop networks are required in future work.

In our work, we have used the ergodic capacity as the performance metric. Though the ergodic capacity gives a good understanding of the performance of a scheme, the throughput of a system is another good performance metric which can provide further detail in the performance of a cellular system. Scheduling should be considered in future studies to evaluate the throughput of the network.

In this study, we have not applied any transmit power control. Interference between the logical routes can be mitigated if transmit power control is performed. Hence, future work can focus on studying optimal transmit power control in the VCN.

In mobile cellular networks, data transmission occurs in two ways: uplink and downlink transmission. In this thesis, we have only considered resource allocation for the downlink transmission. Future studies can focus on resource allocation algorithms for the uplink.

We have considered in this thesis that the CP allocates resources to all nodes in a VC. This scheme is referred to as a centralized allocation scheme. A decentralized resource allocation scheme can be considered as an interesting research topic also.

Glossary

- AWGN** additive white Gaussian noise.
- BS** base station.
- CDMA** code division multiple access scheme.
- CMOS** complementary metal oxide semiconductor.
- CN** core network.
- CP** central port.
- FFT** fast Fourier transform.
- FRN** fixed relay network.
- GSM** Global System for Mobile Communications.
- IFFT** inverse Fast Fourier transform.
- MRN** mobile relay network.
- MT** mobile terminal.
- NP-hard** non-deterministic polynomial-time hard.
- OFDM** orthogonal frequency division multiplexing.
- OFDMA** orthogonal frequency division multiple access.
- QPSK** quadrature phase shift keying.
- RIS** random iterative allocation scheme.
- SAS** successive allocation scheme.
- SHN** single hop network.
- SINR** signal-to-interference-plus-noise power ratio.
- SIS** sequential iterative allocation scheme.
- SNR** signal-to-noise power ratio.
- TDMA** time division multiple access.
- VC** virtual cell.
- VCN** virtual cellular network.
- WP** wireless port.

Journal Publications and Conferences

- [1] G. J. Paraison and E. Kudoh, “A sequential iterative resource allocation scheme for a 2-hop OFDMA virtual cellular network,” *Conditional Acceptance at IEICE Trans. Commun.*, 2015.
- [2] G. J. Paraison and E. Kudoh, “Study of multi-cell interference in a 2-hop OFDMA virtual cellular network,” *IEICE Trans. Commun.*, vol. E96-B, pp. 3163–3171, Dec. 2013.
- [3] G. J. Paraison and E. Kudoh, “Study of a multiuser resource allocation scheme a 2-hop OFDMA virtual cellular network,” *IEICE Trans. Commun.*, vol. E96-B, pp. 2112–2118, Aug. 2013.
- [4] G. J. Paraison and E. Kudoh, “Performance analysis of an evolutionary allocation scheme for a 2-hop virtual cellular network,” in *Proc. IEEE Asia Pacif. Wirel. Commun. Symp. (APWCS 2014)*, (Kenting, Taiwan), Aug. 2014.
- [5] G. J. Paraison and E. Kudoh, “Study of an iterative resource allocation algorithm for a 2-hop OFDMA virtual cellular network,” in *Proc. IEEE Veh. Technol. Conf. (VTC-Fall 2013)*, (Las-Vegas, USA), Sept. 2013.
- [6] G. J. Paraison and E. Kudoh, “Study of the degree of fairness for a parallel relay 2-hop OFDMA virtual cellular networkk,” in *Proc. IEEE Veh. Technol. Conf. (VTC-Fall 2012)*, (Quebec, Canada), Sept. 2012.
- [7] G. J. Paraison and E. Kudoh, “Study of multicell interference in a 2-hop OFDMA virtual cellular network,” in *Proc. IEEE Asia Pacif. Wirel. Commun. Symp. (APWCS 2012)*, (Kyoto, Japan), Aug. 2012.
- [8] G. J. Paraison and E. Kudoh, “Resource allocation with interference for a parallel realy 2-hop OFDMA virtual cellular network,” in *Proc. IEEE Asia Pacif. Wirel. Commun. Symp. (APWCS 2011)*, (Singapore), Aug. 2011.
- [9] G. J. Paraison and E. Kudoh, “Outage capacity of a 2-hop OFDMA virtual cellular network using genetic resource allocation scheme,” in *Proc. IEICE General Conference*, (Niigata, Japan), Mar. 2014.
- [10] G. J. Paraison and E. Kudoh, “Resource allocation for a 2-hop OFDMA virtual cellular network based on genetic algorithm,” in *Proc. IEICE Society Conference*, (Kyushu, Japan), Sept. 2013.
- [11] G. J. Paraison and E. Kudoh, “Iterative resource allocation scheme for a two-hop OFDMA virtual cellular network,” in *Proc. IEICE General Conference*, (Gifu, Japan), Mar. 2013.

- [12] G. J. Paraison and E. Kudoh, "Multi-user throughput analysis of a 2-hop OFDMA virtual cellular network," in *Proc. IEICE General Conference*, (Okayama, Japan), Mar. 2012.
- [13] G. J. Paraison and E. Kudoh, "Study of the distance ratio for the location of wireless ports in a 2-hop OFDMA virtual cellular network," in *Proc. IEICE Society Conference*, (Hokkaido, Japan), Sept. 2011.

Bibliography

- [1] J. G. Proakis and M. Salehi, *Digital Communications*. McGraw-Hill, fifth ed., Nov. 2007.
- [2] C. E. Shannon, “A mathematical theory of communication,” *The Bell Syst. Tech. Journal*, vol. 27, pp. 379–423, July 1948.
- [3] D. Gilstrap, “Ericsson mobility report,” tech. rep., Ericsson, Nov. 2012.
- [4] Cisco, “Cisco visual networking index: Global mobile data traffic forecast update, 20132018,” tech. rep., Cisco, Feb. 2014.
- [5] T. Jasny, “New approaches in the new chapter of telecommunications,” *IEEE Commun. Mag.*, vol. 49, pp. 20–22, Oct. 2011.
- [6] T. S. Rappaport, R. M. S. Shu, Z. Hang, Y. Azar, K. Wang, G. N. Wong, J. K. Schulz, M. Samimi, and F. Gutierrez, “Millimeter wave mobile communications for 5g cellular: it will work!,” *IEEE Access*, vol. 1, pp. 335–349, May 2013.
- [7] W. Hong, K. H. Baek, Y. Lee, Y. Kim, and S. T. Ko, “Study and prototyping of practically large-scale mmwave antenna systems for 5g cellular devices,” *IEEE Trans. Commun.*, vol. 52, pp. 63–69, Sept. 2014.
- [8] J. N. Laneman and G. Wornell, “Energy-efficient antenna sharing and relaying for wireless networks,” in *Proc. IEEE Wirel. Commun. Net. Conf.*, (pp. 7–12), Aug. 2002.
- [9] A. Sedoris, E. Erkip, and B. Aazhang, “User cooperation diversity part i: System description,” *IEEE Trans. Commun.*, vol. 51, pp. 1927–1938, Nov. 2003.
- [10] A. Sendoris, E. Erkip, and B. Aazhang, “user cooperation diversitypart ii: Implementation aspects and performance analysis,” *IEEE Trans. Commun.*, vol. 51, pp. 1939–1948, Nov. 2003.
- [11] S. W. Peter and R. W. H. Jr., “The future of WiMAX: multihop relaying with IEEE 802.16j,” *IEEE Commun. Mag.*, vol. 47, pp. 104–111, Jan. 2009.
- [12] J. Boyer, D. D. Falconer, and H. Yanikomeroglu, “Multihop diversity in wireless relaying channels,” *IEEE Trans. Commun.*, vol. 52, pp. 1820–1830, Oct. 2004.

- [13] L. Piazzo, "A practical algorithm for power minimisation in wireless networks by means of multi-hop and load partitioning," *IEEE Trans. Commun.*, vol. 56, pp. 270–278, Feb. 2008.
- [14] J. N. Laneman, D. C. Tse, and G. W. Wornell, "Cooperative diversity in wireless networks: efficient protocols and outage behavior," *IEEE Trans. Inf. Theory*, vol. 50, pp. 3062–3080, Dec. 2004.
- [15] E. Kudoh and F. Adachi, "Distributed dynamic channel assignment for multi-hop DS-CDMA virtual cellular network," *IEICE Trans. Commun.*, vol. 88-B, pp. 2525–2531, June 2005.
- [16] E. Kudoh and F. Adachi, "Power and frequency efficiency wireless multi-hop virtual cellular concept," *IEICE Trans. Commun.*, vol. 88-B, pp. 1613–1621, Apr. 2005.
- [17] B. Hamdaoui, T. Alshammari, and M. Guizani, "Exploiting 4g mobile user cooperation for energy conservation: challenges and opportunities," *IEEE Trans. Commun.*, vol. 20, pp. 62–67, Oct. 2013.
- [18] T. Ojanpera and R. Prasad, "An overview of third-generation wireless personal communications: a european perspective," *IEEE Personal Commun. Mag.*, vol. 5, pp. 59–65, Dec. 1998.
- [19] M. Rahman and H. Yanikomeroglu, "Qos provisioning in the absence of ARQ in cellular fixed relay networks through inter-cell coordination," in *Proc. IEEE Global Telecom. Conf.*, (pp. 1–5), Nov. 2006.
- [20] P. Li, M. Rong, T. Liu, and D. Yu, "Interference modeling and analysis in two-hop cellular network with fixed relays in FDD mode," in *Proc. IEEE Int. Conf. Wirel. Commun. Net. Mob. Comp. (WiCOM '05)*, (pp. 427–451), Sept. 2005.
- [21] M. A. and I. Syed and H. Yanikomeroglu, "On the performance of TDMA-based multi-hop fixed cellular networks with respect to available frequency channels," *IET Commun.*, vol. 2, pp. 1196–1204, Oct. 2008.
- [22] I. Chih-Lin, C. A. Webb, H. C. Huang, S. Brink, S. Nanda, and R. D. Gitlin, "Is-95 enhancements for multimedia services," *The Bell Syst. Tech. Journal*, vol. 1, no. 2, pp. 60–87, 1996.
- [23] A. Radwan and H. S. Hassanein, "On the capacity of multi-hop CDMA cellular networks," in *Proc. IEEE Symp. Comp. Commun. Conf.*, (pp. 409–414), July 2007.
- [24] L. S. E. Alami, E. Kudoh, and F. Adachi, "On-demand channel assignment using channel segregation for uplink DS-CDMA multi-hop virtual cellular network," in *Proc. IEEE Veh. Technol. Conf. (VTC-Spring 2006)*, (Melbourne, Australia), pp. pp. 713–717, May 2006.

- [25] H. Viswanathan and S. Mukherjee, "Performance of cellular networks with relays and centralized scheduling," *IEEE Trans. Commun.*, vol. 4, pp. 2318–2328, Sept. 2005.
- [26] G. Berardinelli, L. A. R. de Termino, S. Frattasi, M. I. Rahman, , and P. Mogenson, "OFDMA vs. SC-FDMA: performance comparison in local area imt-a scenarios," *IEEE Trans. Commun.*, vol. 15, pp. 64–72, Oct. 2008.
- [27] H. Li and H. Liu, "An analysis of uplink OFDMA optimality," *IEEE Trans. Wireless Commun.*, vol. 6, pp. 2972–2983, Aug. 2007.
- [28] C. M. Yen, C. J. Chang, and L. Wang, "A utility bassed TMCR scheduling scheme for downlink multiuser MIMO-OFDMA systems," *IEEE Trans. Veh. Technol.*, vol. 50, pp. 4105–4115, Oct. 2010.
- [29] A. Nosratinia, T. E. Hunter, and A. Hedayat, "Cooperative communication in wireless network," *IEEE Commun. Mag.*, vol. 42, pp. 74–80, Oct. 2004.
- [30] M. Moretti and A. Todini, "A resource allocator for the uplink of multi cell OFDMA systems," *IEEE Trans. Wireless Commun.*, vol. 6, pp. 2807–2812, Aug. 2007.
- [31] C. Bae and D.-H. Cho, "Fairness-aware adaptive resource allocation scheme in multihop OFDMA systems," *IEEE Commun. Lett.*, vol. 11, pp. 134–136, Feb. 2007.
- [32] J. Shi, G. Yu, Z. Zhang, and P. Qui, "Resource allocation in OFDM based multihop wireless network," in *Proc. IEEE Veh. Technol. Conf. (VTC-Spring 2006)*, (Melbourne, Australia), May 2006.
- [33] R. Kwak and J. M. Cioffi, "Resource-allocation for OFDMA multi-hop relaying downlink system," in *Proc. IEEE Global Telecom. Conf.*, (pp. 3225–3229), Nov. 2007.
- [34] C. Jeong and H. Kim, "Radio resource allocation in OFDMA multihop cellular cooperative networks," in *Proc. IEEE Pers. Indoor and Mob. Radio Commun. Conf. (PIMRC 2008)*, (Cannes, France), Sept. 2008.
- [35] E. Dahlman, S. Parkvall, and J. Skold, *4G LTE/LTE-Advanced for mobile broadband*. Oxford: Elsevier, 2011.
- [36] W. Forum, "Mobile wimax -part i: A technical overview and performance evaluation." White paper, Aug. 2006.
- [37] M. Liang, H. Fan, Y. F. Wang, and D. C. Yang, "Power-based routing for two-hop ofdma cellular networks with fixed relay stations," in *Proc. IEEE Int. Conf. Wirel. Commun. Net. Mob. Comp. (WiCOM '08)*, (Dalian, China), June 2008.

- [38] C. K. Lo, S. vishwanath, and R. W. Heath, "Relay subset selection in wireless networks using partial decode-and-forward transmission," *IEEE Trans. Veh. Technol.*, vol. 58, pp. 692–704, Feb. 2009.
- [39] W. S. Jeon, S. S. Jeong, and D. G. Jeong, "Efficient resource allocation for OFDMA-based two-hop relay systems," *IEEE Trans. Veh. Technol.*, vol. 60, pp. 2378–2383, June 2011.
- [40] Y. Hua, Q. Zhang, and Z. Niu, "Resource allocation in multi-cell OFDMA-based relay networks," in *Proc. IEEE Infocom'10*, (San Diego, USA), Mar. 2010.
- [41] I. Hammerstrom and A. Wittneben, "Power allocation schemes for amplify-and-forward MIMO-OFDM relay links," *IEEE Trans. Commun.*, vol. 6, pp. 2798–2802, Aug. 2007.
- [42] Y. Li, W. Wang, J. Kong, and M. Peng, "Subcarrier pairing for amplify-and-forward and decode-and-forward OFDM relay links," *IEEE Commun. Lett.*, vol. 13, pp. 209–211, Apr. 2009.
- [43] O. Oyman, "Opportunistic scheduling and spectrum reuse in relay-based cellular OFDMA networks," in *Proc. IEEE Global Telecom. Conf.*, (pp. 3699–3703), Nov. 2007.
- [44] H. Ishida, E. Kudoh, and F. Adachi, "Channel capacity of parallel relaying 2-hop OFDMA virtual cellular network," in *Proc. IEEE Veh. Technol. Conf. (VTC-Fall 2009)*, (Anchorage, Canada), Sept. 2009.
- [45] R. K. Jain, D. W. Chiu, and W. R. Hawe, *A Quantitative measure of fairness and discrimination for resource allocation in shared computer system*. Hudson, MA: Digital Equip. Corp., 1984.
- [46] K. S. Hindi, H. Yang, and K. Flesza, "An evolutionary algorithm for resource-constrained project scheduling," *IEEE Trans. Evol. Comput.*, vol. 6, pp. 512–518, Oct. 2002.
- [47] J. Liu, W. Zhong, and L. Jiao, "A multiagent evolutionary algorithm for combinatorial optimization problems," *IEEE Trans. Syst., Man, Cybern. B*, vol. 40, pp. 229–240, Feb. 2010.